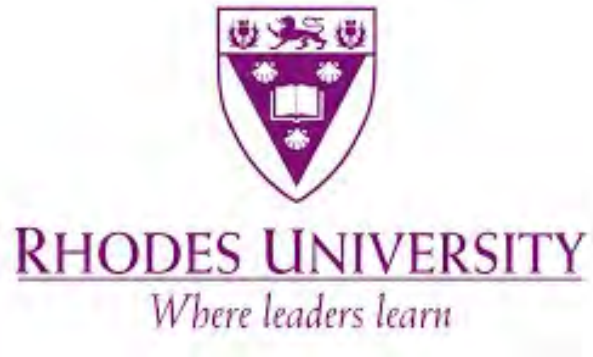

Evaluation of an NADPH-Dependent Assay for Inhibition Screening of *Salmonella enterica* DOXP Reductoisomerase for Identification of Novel Drug Hit Compounds

Dissertation submitted in the fulfilment of the requirements for the degree of

Master of Science in Biochemistry

Department of Biochemistry and Microbiology
Rhodes University

by

Khanyisile Ngcongco
ORCid number: 0000-0003-3340-5170

January 2020

ABSTRACT

Invasive non-typhoidal *Salmonella*, caused by the intracellular pathogen *Salmonella enterica*, has emerged as a major cause of bloodstream infections. It remains a neglected infection responsible for many deaths in Africa, as it fails to receive the level of support that is given to most better-known infections. There are currently no vaccines against invasive non-typhoidal *Salmonella*. First-line antibiotics have been used for treatment, however, the rise in the resistance of the bacteria against these antibiotics has made treatment of invasive salmonellosis into a clinical problem. Therefore, the discovery of new compounds for the development of antibiotic drugs is required. Central metabolic pathways can be a useful source for identifying drug targets and among these is the non-mevalonate pathway, one of the pathways used for the biosynthesis of isoprenoid precursors. The second step of the non-mevalonate pathway involves the NADPH-dependent reduction of 1-deoxy-D-xylulose 5-phosphate (DOXP) into 2-*C*-methyl-$_D$-erythritol 4-phosphate (MEP). 1-Deoxy-D-xylulose 5-phosphate (DOXP) reductoisomerase plays a vital role in the catalysis of this reaction and requires NADPH and divalent metal cations as co-factors for its activity. In this investigation recombinant DOXP reductoisomerase from *Salmonella enterica*, *Plasmodium falciparum* and *Mycobacterium tuberculosis* were biochemically characterized as potential targets for developing drugs that could be used as treatment of the disease. The expression and nickel-chelate affinity purification of *S. enterica* DOXP reductoisomerase in a fully functional native state was successfully achieved. However, the expression and purification of *P. falciparum* DXR and *M. tuberculosis* DXR was unsuccessful due to the formation of insoluble inclusion bodies. Although alternative purification strategies were explored, including dialysis and slow dilution, these proteins remained insoluble, making their functional analysis not possible.

An NADPH-dependent enzyme assay was used to determine the activity of *S. enterica* DXR. This assay monitors the reduction of DOXP to MEP by measuring the absorbance at 340 nm, which reflects the concentration of NADPH. An alternative assay, resazurin reduction, which monitors the NADPH-dependent reduction of resazurin to resorufin, was explored for detecting enzyme activity. The recombinant *S. enterica* DOXP reductoisomerase had a specific activity of 0.126 ± 0.0014 μmol/min/mg protein and a K_m and V_{max} of 881 μM and 0.249 μmol/min/mg respectively. FR900098, a derivative of fosmidomycin, is a well-known inhibitor of DXR, however, the sensitivity of *S. enterica* DXR towards FR900098 has not yet been reported. The NADPH-

dependent enzyme and resazurin reduction assays were used to determine whether FR900098 has enzyme inhibitory effects against *S. enterica* DXR. Upon confirming that FR900098 is able to inhibit *S. enterica* DXR, FR900098 was used as a control compound in the screening of novel compounds. The *S.* enterica DXR enzyme was screened for inhibition by the collection of compounds from the Pathogen Box. Compounds that exhibited the desired inhibitory activity, referred to as 'hits' were selected for further investigation. These hits were confirmed using the NADPH-dependent enzyme assay, resulting in the identification of two different DXR inhibitor compounds, MMV002816, also known as diethylcarbamazine, and MMV228911. The inhibitory concentration (IC_{50}) values of FR900098, MMV002816 and MMV228911 against *S. enterica* DXR were 1.038 μM, 2.173 μM and 6.861 μM respectively. The binding mode of these compounds to *S. enterica* DXR could lead to the discovery of novel druggable sites on the enzyme and stimulate the development of new antibiotics that can be used for treating *Salmonella* infections.

Table of Contents

List of Figures

List of Tables

Symbols and Abbreviations

%	Percentage
$(His)_6$	6 x histidine tag
±	Standard deviation
3-D	Three dimensional
AGE	Agarose gel electrophoresis
Abs_x	Absorbance at x nm
bp	Base pairs
BSA	Bovine serum albumin
CD-ME	4-(cytidine 5'-diphospho)-2-*C*-methyl-$_D$-erythritol
cm	Centimetres
DMAP	4-dimethylaminopyridine
DNA	Deoxyribonucleic acid
DOXP	1-deoxy-$_D$-xylulose-5-phosphate
DXR	DOXP reductoisomerase
E. coli	*Escherichia coli*
g	Gram
HIV	Human Immunodeficiency Virus
Hz	Hertz
IPP	Isopentenyl diphosphate units
IPTG	Isopropyl-β-D-thiogalactopyranoside
kb	Kilobase
kbp	Kilo base pairs
kDa	Kilodalton
K_m	Concentration of substrate that leads to half-maximal velocity
L	Litre
M	Molar
MECDP	2-*C*-methyl-$_D$-eryhtritol-2,4-cyclodiphosphate
MEP	2-*C*-methyl-$_D$-erythritol 4-phosphate
min	Minutes

ml	Millilitre
mm	Millimetres
mM	Millimolar
mmol	Millimoles
mol	Moles
mRNA	Messenger ribonucleic acid
MVA	Mevalonate
NADH	Nicotinamide adenine dinucleotide (reduced form)
NADPH	Nicotinamide adenine dinucleotide phosphate (reduced form)
Ni	Nickel
ºC	Degree Celsius
P. falciparum	*Plasmodium falciparum*
pH	- log [H]
RNA	Ribonucleic acid
rpm	Revolution per minute
S. enterica	*Salmonella enterica*
SeDXR	*S. enterica* DOXP reductoisomerase
S. cerevisiae	*Saccharomyces cerevisiae*
SDS	Sodium dodecyl sulphate
SDS-PAGE	Sodium dodecyl sulphate polyacrylamide gel electrophoresis
tRNA	Transfer ribonucleic acid
V	Volts
V_{max}	Maximum initial velocity or rate of a reaction
v/v	Volume/volume
w/v	Weight/volume
α	Alpha
β	Beta
ε	Extinction coefficient
λ	Lambda
μ	Micro
μg	Microgram

µl	Microlitre
µM	Micromolar
µmol	Micromoles

Acknowledgements

I would like to thank my supervisor Professor Heinrich Hoppe for his guidance, patience, advice and support. I am grateful for the help that you have provided over the course of this research project. I would like to thank my parents, Thandeka and Sandile Ngcongco, my sister Nokuthula, for their love and support through what seemed like a never-ending process, for cheering me up, motivating me and constantly reminding me that I can do it.

I would like to the thank the present and past members of Lab 301, for their help and good times in the lab. To Apelele Ntlantsana, thank you for always being there, for being my motivator, for being the serious one with words of wisdom, for not accepting defeat and for being a constant reminder that there is a light at the end of the tunnel.

To my friends, Nosipho Hlalukana and Akhona Ngqinambi, thank you for being my cheerleaders, your love, support and advice has carried me throughout this degree. Thank you for crazy yet wonderful times in the midst of success and failure of experiments. I thank God for giving me friends like you, words cannot begin to describe how grateful I am for our friendship and I will miss us being referred to as the “Three Musketeers”.

I would like to thank the National Research Foundation (NRF) for funding, providing financial support for my studies.

A lot went in for this research project, blood, sweat, tears and coffee. Through it all God has been faithful, and I am grateful for His presence, for giving me strength and courage and for having His hand over me.

CHAPTER 1: LITERATURE REVIEW

1.1. INVASIVE NON-TYPHOIDAL SALMONELLA

1.1.1. The Burden of Invasive Non-Typhoidal *Salmonella*

Salmonellae are gram-negative facultative anaerobes that cause human diseases that are divided into a small number of human-restricted invasive typhoidal serotypes such as *Salmonella enterica* var Typhi (S Typhi) and *Salmonella enterica* var Paratyphi A (S Paratyphi A) and thousands of non-typhoidal *Salmonella* serotypes (Feasey *et al*., 2012; Tennant *et al*., 2016). The latter serotypes have been known to cause non-typhoidal *Salmonella* disease which manifests in immunocompetent hosts as a mild, self-limiting gastroenteris, whereas other serotypes cause the invasive non-typhoidal *Salmonella* disease which presented as a febrile bacteremia (Haselbeck *et al*., 2017). Invasive non-typhoidal *Salmonella* has emerged as one of major bloodstream infections and if left untreated can be fatal (Gordon, 2011; Haselbeck *et al*., 2017).

Invasive non-typhoidal *Salmonella* remains a neglected infection that is responsible for a large number of deaths in Africa and it fails to receive the level of support of infectious diseases that are better-known in Africa such as HIV, malaria and tuberculosis (Gordon, 2011; MacLennan and Levine, 2013). Invasive non-typhoidal *Salmonella* has been reported to be responsible for up to 39% of blood infections acquired in Sub-Saharan Africa with an average Case Fatality Rate (CFR) of 19% (Uche *et al*., 2017). Invasive non-typhoidal *Salmonella* infections have been estimated to have caused approximately 3.4 million cases and over 600 000 deaths annually (Kariuki *et al*., 2016). A mortality rate of 20-30% in vulnerable children under the age of 5 years is caused by invasive non-typhoidal *Salmonella* (Kariuki *et al*., 2016). Given the high morbidity and mortality rate caused by the invasive non-typhoidal *Salmonella* disease, it is important that effective treatment, control and prevention strategies are developed (Uche *et al*., 2017).

Immunosuppressed individuals and young children are more susceptible to invasive non-typhoidal *Salmonella* compared to healthy individuals, hence host risk factors of the disease are infants and young children, individuals with HIV, malaria, malnutrition and anemia (Crump *et al*., 2015;

Haselbeck *et al*., 2015). It was discovered that diagnosis of invasive non-typhoidal *Salmonella* is difficult due to its clinical presentation being nonspecific because validated biomarkers of nontyphoidal *Salmonella* or rapid diagnostic serological tools are not available (Tennant *et al*., 2016; Gilchrist and MacLennan, 2019). Better diagnostic tests are required to improve management and surveillance of the disease (Manore *et al*., 2018).

1.1.2. The Invasion of *Salmonella*

The relevance of invasive non-typhoidal *Salmonella* as pathogens arise when they infiltrate and colonize the bloodstream, thereby progressing to disease (Mobegi *et al*., 2014). *Salmonella* interacts with the receptors on host cell membranes using a variety of mechanisms to enter phagocytic and non-phagocytic cells, after the bacteria is engulfed in the host cell, a membrane compartment called the vacuole encases it (Velge *et al*., 2012; Eng *et al*., 2015). Normally, when foreign bacterial body is present, the host cell immune response is activated, resulting in fusion of lysosomes and digesting enzymes to be secreted causing degradation of the foreign bacteria, however, other bacterial effector proteins are injected into the vacuole as *Salmonella* uses the type III secretion system (Eng *et al*., 2015; Hanson-Wester *et al*., 2015). This type III secretion system is a virulence mechanism that most gram-negative bacteria use to promote invasion of host cells. The injected effector proteins alter the compartment structure of the vacuole, blocking the fusion of lysosomes (Hanson-Wester *et al*., 2015). The bacteria override existing signaling pathways in these cells, altering gene expression and protein function, this enables the bacteria to invade epithelial cells and allows *salmonella* to survive and replicate in host cells (Al kraiem *et al*., 2018).

Non-typhoidal *Salmonella* causing gastroenteritis is mainly transmitted to humans by the ingestion of animal food products from infected animals, produce contaminated with animal waste, contaminated water, direct contact with infected animals and their environment (Kariuki *et al*., 2006; Uche *et al*., 2017). The source and mode of transmission of invasive non-typhoidal *salmonella* remains unknown, however, an important route of infection of the disease is human to human transmission (Kingsley *et al*., 2009).

1.2. VACCINES AND ANTIBACTERIAL DRUGS

1.2.1. Vaccines for *Salmonella*

There are currently no vaccines available for treating invasive non-typhoidal *Salmonella* directly. In *Salmonella* vaccine development, a variety of strategies are investigated, these include conjugate vaccines, live attenuated vaccines, vesicle-based vaccines, inactivated vaccines, DNA vaccines and subunit vaccines (Clem, 2011; Micoli *et al*., 2018). In the case of conjugate vaccines, a T cell-dependent antibody response is induced by polysaccharides, such as Vi and O-antigen surface polysaccharides, that are covalently linked to a carrier protein, the polysaccharides are then converted from T-independent to T-dependent antigens (Maclennan *et al*., 2014; Micoli *et al*., 2018). These vaccines aim to produce specific anti O-antigen antibodies which target the O-antigen moiety of *Salmonella* lipopolysaccharide (LPS), mediating killing of bacteria and conferring protection against infection (Micoli *et al*., 2018). The application of this approach has been successful in encapsulated bacteria such as *Hemophilus influenzae* b, meningococcus and pneumococcus (Maclennan *et al*., 2014). Although *S. typhi* is the only encapsulated serovar among the rest of the *Salmonella* serovars causing invasive *Salmonella* disease, evidence from animal studies has been found to support the development of conjugate vaccines against the other serovars (Maclennan *et al*., 2014). The serovars' lipopolysaccharide O-antigens are conjugated to carrier proteins (Maclennan *et al*., 2014).

Live attenuated vaccines have the ability to induce cell-mediated and mucosal responses (Zhi *et al*., 2019). These usually contain versions of the original pathogenic agent that have been laboratory weakened, they induce strong cellular and antibody responses, they have been found to elicit excellent T-cell responses (Clem, 2011; Zhi *et al*. 2019). These vaccines contain living microorganisms which produce the actual disease, it has been found that it is easier to create live attenuated vaccines with viruses instead of bacteria, due to the presence of fewer genes in viruses compared to bacteria (Clem, 2011). *Salmonella*-specific T cell responses required for clearing the residual infection are elicited by live attenuated vaccines (Kantele *et al*., 2012). Multiple *Salmonella* antigens are delivered to the immune system, this increases the chances of induction of a broad coverage across *Salmonella* serovars (Maclennan *et al*., 2014). A live attenuated vaccine

that has been developed through non-specific chemical mutagenesis is the Ty21a vaccine, although it is derived from expression of the Vi antigen by *S. Typhi* Ty2 strain Ty21a does not express the Vi antigen, therefore an immune response to this antigen is not attributed to the vaccine (Kantele *et al*., 2013). This vaccine has great potential in inducing T cell immunity and cross-protection against non-*Typhi* serovars (Maclennan *et al.*, 2014). Studies suggest that Ty21a acts primarily through humoral immune responses that it creates instead of through cell-mediated immunity (Maclennan *et al*., 2014). Evidence suggests that this vaccine could potentially be used against invasive non-typhoidal *Salmonella* serovars and *S. enteritidis* serovars due to the high B cell response that is directed against the O-antigen (Maclennan *et al*., 2014).

Vesicle-based vaccine strategies include generalized modules for membrane antigens (GMMA) technology and native outer membrane vesicles (NOMVs) which can be used as delivery vehicles for the *Salmonella* LPS O-antigen to the immune system (Micoli *et al*., 2018; Schager *et al*., 2018). These are microvesicles that consist of bulges of plasma membrane of cells, referred to as blebs, that are produced and released by gram-negative bacteria (Schager *et al*., 2018; Stentz *et al*., 2018). The protein-based vaccine development strategy uses recombinant or purified proteins, such as flagellin and porins OmpC, F and D, which are able to induce antibody and a T cell response (MacLennan *et al*., 2014). Some of the proteins, OmpC and F, have been successful in inducing long lasting responses in mice, and found to be safe and immunogenic (MacLennan *et al*., 2014). However, preserving the conformation of the proteins is an issue, as a result of this antibodies with poor function are induced (MacLennan *et al*., 2014).

In inactivated vaccines, pathogenic agents are destroyed with chemicals, heat or radiation (Clem, 2011). The microorganism is inactivated so that the vaccine can be more stable (Clem, 2011). Immunity has to be maintained, this is due to the weak immune responses produced by the vaccines, therefore booster shots are required along with the vaccine (Clem, 2011). DNA vaccines use the pathogenic agent or components of the pathogenic agent to induce adaptive immune responses, the pathogenic agent is modified so that it does not cause harm or disease in the host (Hobernik and Bros, 2018; WHO, 2019). Vaccine delivery is by intramuscular, intradermal and subcutaneous injections, which transfect keratinocytes, myocytes and antigens presenting cells (APC) found near the injection side as well (Hobernik and Bros, 2018). Once these vaccines have

been internalized, the DNA is translocated to the nucleus for transcription then translated in the cytoplasm producing antigens which induce immune responses (Clem, 2011; Hobernik and Bros, 2018). Subunit vaccines consist of purified antigen instead of whole microorganism, these purified antigens are transported by different carriers (Vartak and Sucheck, 2016). These antigens elicit a T-cell dependent adaptive immune response and the immune response is based on the antigen used (Vartak and Sucheck, 2016). With the advancement of molecular biology, new and much better vaccines against *Salmonella* are being investigated and designed, and these will potentially make a great impact on global health (Maclennan *et al*., 2014).

1.2.2. Antibiotics Available for Treating *Salmonella*

Antibiotics or antimicrobial agents are natural or synthetic substances that have inhibitory effects on the growth of microorganisms or have the ability to kill microorganisms (Onwuezobe *et al*., 2012). The mechanism of action of the antibiotic determines whether it will be clinically useful for treating an infection (Onwuezobe *et al*., 2012). Broad spectrum agents such as ampicillin, amoxycillin, chloramphenicol, tetracycline, and cotrimoxazole have been used for treating *Salmonella* infections, however, it was discovered that these agents lack substantial intracellular activity (Sirinavin and Garner, 1999; Kariuki *et al*., 2016). These agents were replaced by the extended-spectrum fluoroquinolones such as norfloxacin, ofloxacin, fleroxacin, ciprofloxacin, and extended-spectrum cephalosporins such as cefuroxime, cefamandole, cefotaxime, ceftriaxone, (Kariuki *et al*., 2016; Shahbaz, 2017).

Fluoroquinolones are potent, broad spectrum antibiotics that belong to the quinolone family and are commonly used for treating resistant infections since the late 1980s (Redgrave *et al*., 2014). These compounds play a role in the inhibition of bacterial type II topoisomerases, which are essential for key processes such as DNA replication (Redgrave *et al*., 2014). Cephalosporins belong to the β-lactam family and resemble the structure of penicillin and have been used for treating respiratory tract infections (RTI), skin infections and urinary tract infections (UTI) (Shahbaz, 2017). These antibiotics target penicillin binding proteins which play an important role in the cell wall synthesis process, causing bacterial lysis and cell death (Macheboeuf *et al*., 2006;

Shahbaz, 2017). These antibiotics have been used for treating *Salmonella* infections, as they inhibit key processes in the bacteria.

1.2.3. Antimicrobial Resistance

More frequent hospitalizations, complicated and prolonged illnesses, failure of treatment and higher risk of invasive disease are a result of antimicrobial resistance (Maka and Popowska, 2016). Antimicrobial resistance in invasive non-typhoidal *Salmonella* serotypes is considered as a global problem, as the rates of resistance to traditional agents are increasing and this has turned the treatment of invasive salmonellosis into a clinical problem (Chen *et al*., 2013). Multidrug-resistant (MDR) non-typhoidal isolates are closely related to the increasing morbidity compared to strains that are antibiotic sensitive, that are very important with regards to the health and safety concern in humans and animals (Kariuki *et al*., 2016).

The resistance against antibiotics such as ampicillin, chloramphenicol and trimethoprim/sulfamethoxazole are common in invasive non-typhoidal *Salmonella* (Lunguya *et al*., 2013). Treating invasive non-typhoidal *Salmonella* increasingly relies on fluoroquinolones such as ciprofloxacin or cephalosporins such as cefotaxime (Lunguya *et al*., 2013). However, the decreased susceptibility to fluoroquinolones and the resistance of non-typhoidal *Salmonella* isolates to these antibiotics is a growing problem, with the resistance of *Salmonella enterica* to ciprofloxacin resulting in treatment failure (Kariuki *et al*., 2016). Extended-spectrum beta-lactamases has threatened cephalosporins as an option that can be used for treatment (Lunguya *et al*., 2013). These extended-spectrum beta-lactamases are enzymes that are produced by bacteria, that are resistant to cephalosporin antibiotics (Lunguya *et al*., 2013). The rapid drug resistance to existing antimicrobial drugs in bacteria has created the need for the prediction of novel targets and leads which have been derived from original compounds that have improved activity against a validated target (Qidwai *et al*., 2014).

The indiscriminate use of antibiotics is linked to the development of antimicrobial resistance of pathogens, which are capable of being resistant to a whole drug class due to a variety of antibiotics belonging to the same drug class (WHO, 2015). One of the factors that has contributed towards

the resistance of pathogens is the inappropriate consumption of antibiotics, causing the selection and spread of resistant bacteria (Blázquez, 2003). Antimicrobial resistance is spread by mutations or the acquirement of resistance genes, which takes place due to the actions of mobile genetic elements (Collignon *et al*., 2018). These elements may assist and allow intracellular DNA mobility whereby there is transfer of the resistance genes from chromosome to plasmid or between plasmids (Partridge *et al*., 2018). However, it has been found that antimicrobial resistance can also be spread via vectors such as humans, insects, agriculture and water (Collignon *et al*., 2018).

Table 1: Mechanism of action and resistance of the different classes of antimicrobial drugs.

Drug Class	Target and Mode of Action	Resistance	Example	Reference
Fluoroquinolones	Inhibit bacterial topoisomerase enzymes	Mutations in the quinolone-resistance-determining regions (QRDRs) on chromosomal genes encoding topoisomerases	Ciprofloxacin Ofloxacin Nalidixic acid	Cuypers *et al*. (2018)
Beta-Lactams	Inhibit the peptidoglycan layer of bacterial cell wall	Overproduction of beta-lactamases that degrade beta-lactams	Cefotaxime Ceftriaxone Cefixime	Al kraiem *et al*. (2018)
Sulfonamides	Inhibit dihydropteroate synthase	Mutations in the dihydropteroate synthase gene	Trimethoprim Sulfamethoxazole	Sköld (2000)
Aminoglycosides	Inhibit polypeptide synthesis	Removal of drug from bacterial cell by increased efflux Mutations in the ribosomal subunit interfering with binding	Gentamicin Tobramycin Amikacin	Doi *et al*. (2016)
Tetracyclines	Inhibit polypeptide synthesis	Altering ribosomes to prevent binding Increased efflux to remove of drug from bacterial cell	Chlortetracycline Oxytetracycline Minocycline	Speer *et al*. (1992)

Phenicols	Inhibit polypeptide synthesis	Enzymatic inactivation by acetylation of drug Mutations in the target site Removal of the drug in the bacterial cell by efflux	Chloramphenicol Florfenicol	Fernández *et al*. (2012)

1.3. THE DRUG TARGET DOXP REDUCTOISOMERASE (DXR)

1.3.1. Identifying Novel Drug Targets

With the rapid rise in the resistance of pathogens to first-line antimicrobials, the discovery of new drug targets is required to provide global healthcare management of invasive non-typhoidal *Salmonella* (Mobegi *et al*., 2014). Existing antimicrobials have been found to target a limited number of cellular functions including cell wall synthesis, DNA replication, transcription and translation (Gerdes *et al*., 2002). Unexplored cellular functions can be identified as potential drug targets, therefore a greater understanding of related biological processes in pathogens and their hosts is required (Gerdes *et al*., 2002). Drug targets are biomolecules that are involved in signaling or metabolic pathways specific to a disease process, and these biomolecules play crucial roles in the progression of the disease (Mandal *et al*., 2009). Disease progression occurs by communication of these biomolecules by protein-protein interactions or protein-nucleic acid interactions resulting in the propagation of signaling processes or alteration of metabolic processes (Mandal *et al*., 2009). The biological functions performed by these biomolecules can be modulated, which can be achieved by (i) the inhibition of the drug target function using small molecules that competitively bind to the active site within the drug target, or (ii) the inhibition of bimolecular interactions between biomolecules using small molecules as a way of preventing cross talks between the biomolecules, or (iii) activation of the biomolecules that are functionally regulated in some diseases (Fuller *et al*., 2009; Mandal *et al*., 2009).

The identification of these drug targets is an essential part in the drug discovery process and most drug targets have been found to be proteins (Bull and Doig, 2015). For a protein to qualify as a desirable drug target, its traits should include essentiality, druggability, assayability, and specificity or selectivity. The essentiality of a protein can be used to evaluate whether it is a suitable potential drug target. The target must play an essential role in the growth, replication and survival in the host, therefore the protein must be encoded by genes that are essential or crucial for the life stages of the pathogen (Sakharkar *et al*., 2004). These genes are usually involved in metabolic and

signaling pathways, and they may be located within protein-protein interaction networks (Ji *et al*., 2019). These genes should not be homologous to human genes and those present in the host gut commensal microbiota to avoid antibiotic killing of this microbiota which could have detrimental effects on human nutrition, health and physiology (Mobegi *et al.*, 2014). For a protein to be considered as druggable, it should contain sites that will enable binding of small drug-like molecules favouring interaction between the protein and the molecule (Bull and Doig, 2015). This interaction allows potential inhibitors to have access to the protein, thus changing the conformation of the protein and as a result inhibiting the function or activity of the protein.

Researchers should be able to detect protein activity using assays, as this will allow screening strategies to be used for the screening of compound libraries directly against a drug target (Hughes *et al*., 2011; Neelapu *et al*., 2013). These assays can determine or identify compounds that have the desired effect or mechanism of action against the target of interest (Hughes *et al*., 2011). Potential antimicrobial drugs must have specificity or selectivity towards crucial proteins which are of great importance to the pathogen's growth and survival, so that these antimicrobial drugs can have inhibitory effects on targets without causing harm to the host (Shanmugham and Pan, 2013). To avoid unwanted host-drug interactions, antimicrobial drug candidates should be based on the criteria of selectivity or specificity for drug targets (Shanmugham and Pan, 2013).

More biological cellular processes are being explored for identifying drug targets. Investigations being done include studies in pathogen-host interactions to fully understand how pathogens are able to grow and survive in hosts using metabolic processes (Passalacqua *et al*., 2016). Advanced genome-based technology has become an attractive approach in identifying drug targets using genome sequences of bacteria (Oany *et al*., 2018). This technology has access to host and pathogen genome sequence information making it easier to find drug targets in pathogens (Oany *et al*., 2018).

Although more drug targets are being discovered, there is a challenge in the development of lead molecules and effective drugs (small molecules possessing desired properties) (Mandal *et al*., 2009). The availability of 3D X-ray or NMR structures of biomolecules, docking tools and computer aided methodologies has significantly increased drug discovery (Mandal *et al*., 2009).

There are currently about 57 558 3D structures that are held by the Protein Data Bank (PDB), but even with this high number of available structures there continues to be stumbling blocks in the development of drugs (Mandal *et al*., 2009). Some drug targets have more than one structure bound to different molecules, and the 3D structures of many other targets remain unknown (Mandal *et al*., 2009). These problems associated with currently available drugs which have been developed on the basis of the sole approach of structure guided drug design require an improved approach of rational drug design (Mandal *et al*., 2009).

Almost all current drugs have been designed to directly bind to the primary active (orthosteric) sites of their targets either by inhibiting or modulating the function of the target (Grover, 2013; Abdel-Magid, 2015). A drug binds to the active site of a biomolecule such as an enzyme to prevent the binding of substrates to the site, and as a result the function of the enzyme is inhibited (Abdel-Magid, 2015). Similarly, an agonist or antagonist bind to the orthosteric site of receptors causing activation or deactivation of the functions of the receptors (Abdel-Magid, 2015). The most successful drugs on the market are designed with this approach, although these drugs target diseases with high degrees of specificity and affinity, side effects have been found to occur due to the similarity of many enzymes or receptors with related functions (Abdel-Magid, 2015). A new approach for drug design is based on binding of the drugs to secondary binding sites known as allosteric sites instead of orthosteric sites (Grover, 2013). This has emerged as an attractive approach because of the possibility of finding unique allosteric sites and as a result more specific targets (Grover, 2013).

It is important that drug action occurs at the desired site, and the ideal drug should exhibit minimum side effects. These are usually caused by interaction of the drug with biological molecules other than the one that the drug has been targeted for in treating the disease (Grover, 2015). Therefore, binding of the drug only to its desired site of action is very important (Grover, 2015).

1.3.2. Targeting Metabolic Pathways

Current antimicrobial drugs work by inhibiting a variety of cellular processes including DNA replication, protein synthesis and cell wall synthesis. However, due to the rise in antibiotic resistance there is a great interest in investigating alternative essential cellular processes, such as bacterial central metabolic pathways, as drug target platforms for new antimicrobial drugs (Murima *et al*., 2014). Virulence factors dictate microbial pathogenicity. These factors play a role in establishing the infection at a given site and through metabolic pathways which are required for growth (Brown *et al*., 2008). The host microenvironment is exploited by the pathogen and is considered as a growth medium for the pathogen to grow and multiply causing disease (Brown *et al*., 2008). An essential part of innate immunity is the ability to restrict access of pathogens to nutrients, however, pathogens overcome this defence by reprogramming their metabolic network. As a result there is a balance of biosynthetic processes with enough ATP biogenesis to support growth and survival of the pathogen (Murimo *et al*., 2014). These altered metabolic pathways are of great importance for the survival of the pathogen *in vivo* and represent an appealing space for exploring potential antimicrobial drug targets (Murimo *et al*., 2014).

Historically, there have been limitations with using central metabolism for exploring antimicrobial drug targets, such as possible lack of selectivity due to most metabolic enzymes being conserved from bacteria to human, making it unattractive for antimicrobial development. It is important to remember that conserved cellular processes are also targeted by most clinically used antibiotics (Murimo *et al*., 2014). The understanding of the regulation of the flux of nutrients into pathways that play an important role in biosynthesis and energy metabolism under good growth conditions will aid in successful targeting of central metabolism (Murimo *et al*., 2014).

Table 2: Different metabolic pathways and their roles/functions

Metabolic Pathway	Role/Function	Reference
Amino acid Biosynthesis	Produces precursors used for synthesis of metabolites with important functions in growth and biological processes of organisms	Bromke (2013)
Fatty Acid Biosynthesis	Produces fatty acid components of phospholipids Important for membrane structure	Parsons and Rock (2011) Wright and Reynolds (2007)
Folate Biosynthetic Pathway	Production of folate, a dietary requirement for cells	Bertacine Dias *et al*. (2018)
Isoprenoid Biosynthetic Pathway	Produced isoprenoid precursors responsible for growth and survival of the organism	Qidwai *et al*. (2014) Zhao *et al.* (2013)
NAD biosynthetic pathway	Synthesis of cofactors required for energy metabolism, redox balance and activity of NAD-dependent enzymes and signaling reactions	Dölle *et al*. (2013) Boshoff *et al*. (2008).

A number of metabolic pathways of pathogens have been discovered for the development of antimicrobial drugs to overcome some infections. Among these metabolic pathways is isoprenoid biosynthesis which can occur via two pathways, namely the mevalonate pathway (MVA pathway) and the non-mevalonate pathway (MEP pathway) (Zhao *et al.*, 2013; Qidwai *et al*., 2014). These pathways lead to the synthesis of isoprenoid precursors which are important for the growth and survival of organisms (Qidwai *et al*., 2014). Isoprenoid precursors are a diverse group of natural products which include cholesterol, bile acids, dolichol, prenylated proteins and different plant terpenoids (Qidwai *et al*., 2014). All isoprenoid precursors are derived from isopentyl diphosphate (IPP), which is a five-carbon precursor, or its isomer dimethylallyl diphosphate (DMAPP) (Zhao *et al.*, 2013). More than 35 000 isoprenoid precursors have been identified to date in the bacteria, archaea and eukaryotic domains and they have important biological functions including hormone based signaling, protein degradation and the regulation of transcription (Heuston *et al.*, 2012).

The mevalonate pathway is responsible for producing isoprenoid precursors in fungi, plant cytoplasm, most eukaryotes, archaea and some eubacteria (Miziorko, 2011). This pathway consists of six enzymatic steps resulting in the biosynthesis of IPP and DMAPP. The initial step involves the condensation of acetyl-CoA to acetoacetyl-CoA, which is then converted into 3-hydroxy-3-methylglutaryl CoA (HMG-CoA) (Heuston *et al.*, 2012; Zhao *et al.*, 2013). HMG-CoA is reduced to mevalonate, followed by two phosphorylation steps resulting in the production of mevalonate-5-diphosphate (Mevalonate-PP), which is converted into the isoprenoid precursors IPP and DMAPP as shown in Figure 1 (Zhao *et al.*, 2013). The alternative pathway referred to as the non-mevalonate pathway (MEP pathway) consists of a series of seven enzymatic steps that also lead to the production of IPP and DMAPP. It has been found that many other organisms including eubacteria, apicomplexan parasites, algae and chloroplasts in higher plants use the MEP pathway for isoprenoid biosynthesis (Hunter, 2007).

The initial step of the non-mevalonate pathway is the condensation of pyruvate and glyceraldehyde 3-phosphate to form 1-deoxy-D-xylulose 5-phosphate (DOXP), catalyzed by the thiamine diphosphate-dependent DXP synthase (Kuzuyama *et al.*, 2000). The second step is the conversion of DOXP to 2-*C*-methyl-$_{D}$-erythritol 4-phosphate (MEP) catalyzed by 1-deoxy-D-xylulose 5-phosphate reductoisomerase (DXP reductoisomerase or DXR) (Kuzuyama *et al.*, 2000). MEP is

coupled with cytidine 5'-triphosphate (CTP) in the reaction catalyzed by CDP-ME synthase to form methylerythritol cytidyl diphosphate (CDP-ME) (Zhao *et al.*, 2013). CDP-ME is phosphorylated by an ATP-dependent 4-diphosphocytidyl-2-*C*-methyl-$_D$-erythritol kinase (CDP-MEP kinase) producing 4-diphosphocytidyl-2-*C*-methyl-$_D$-erythritol (CDP-MEP) which is then cyclized to 2-C-methyl-D-erythritol-2,4-cyclodiphosphate (MEcPP) (Zhao *et al.*, 2013). MEcPP is converted to 4-hydroxy-3-methyl-butenyl 1-diphosphate (HMBPP) and the final step of the pathway is the conversion of HMBPP to form both IPP and DMAPP (Zhao *et al.*, 2013).

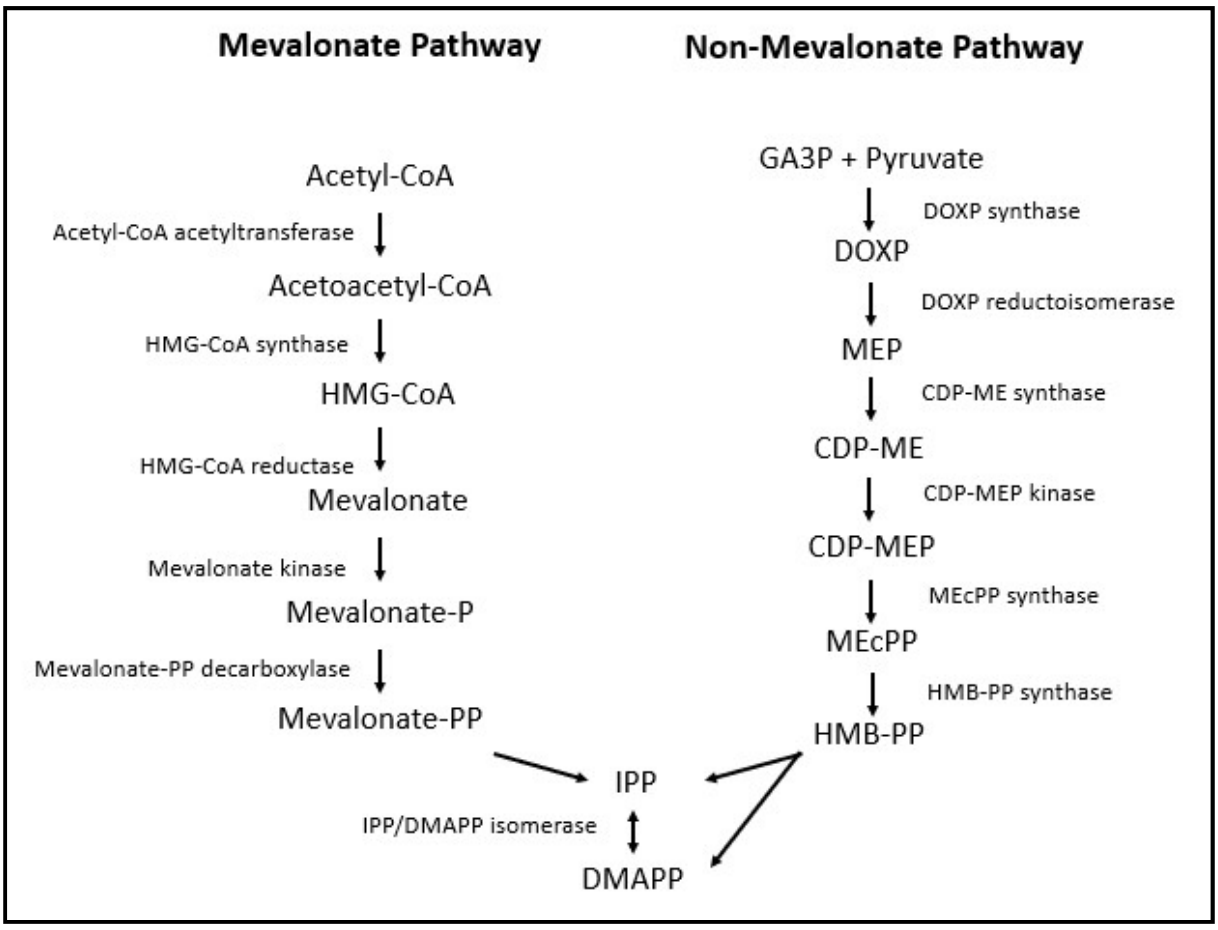

Figure 1: Isoprenoid biosynthesis via the mevalonate and non-mevalonate pathway.
The enzymatic steps of the mevalonate and non-mevalonate pathways are shown above (adapted from Heuston *et al*. (2012)), each pathway leading to the production of the isoprenoid precursors IPP and DMAPP.

The non-mevalonate pathway is heterologous from the mevalonate pathway and contains different intermediates and enzymes (Murkin *et al*., 2014). Human pathogens rely only this pathway for

isoprenoid biosynthesis Along with the distinctiveness from the MEP pathway, this make the enzymes of this pathway attractive targets for drug development while avoiding toxicity to humans (Zhao *et al*., 2013; Murkin *et al*., 2014). The enzymes of the MEP pathway are referred to as metabolic chokepoints, meaning that they consume a specific substrate or generate a specific product and other enzymes cannot compensate for their function (Yeh *et al*, 2004; Heuston *et al.*, 2012). This is another reason why the enzymes of the MEP pathway are considered as good targets for drug design (Kuzuyama *et al.*, 2000).

1.3.3. The Catalytic Mechanism of DOXP Reductoisomerase

The enzymes of the non-mevalonate pathway have become potential targets for novel drug development for several bacterial and pathogens including malaria (Kuzuyama *et al*., 2000). The second step of this pathway is the intramolecular rearrangement of 1-deoxy-D-xylulose 5-phosphate (DOXP) to 2-C-methyl-$_D$-erythritol 4-phosphate (MEP), mediated by DOXP reductoisomerase (DXR) (Reuter *et al*., 2002). The rearrangement of DOXP was assumed to give 2-*C*-methylerythrose 4-phosphate, a hypothetical rearrangement intermediate by a reduction reaction (Takahashi *et al*., 1998). Although this rearrangement is not fully understood, Munos *et al*. (2009) proposed that an α-ketol rearrangement mechanism and a retroaldol/aldol mechanism may be involved. In the α-ketol rearrangement mechanism, the C-3 hydroxyl group of DOXP gets deprotonated, followed by a 1,2(C4-to-C2)-migration forming the intermediate methylerythrose phosphate which gets reduced by NADPH into MEP (Munos *et al*., 2009). In the retroaldol/aldol mechanism, the C3-C4 bond of DOXP is cleaved by DOXP reductoisomerase in a retroaldol manner generating a three-carbon and two-carbon phosphate bimolecular intermediate (Munos *et al*., 2009). These are then combined by the formation of a new C-C bond by an aldol reaction, producing the intermediate methylerythrose phosphate followed by the reduction of the intermediate to MEP by NADPH (Munos *et al*., 2009).

A large number of enzymes solely consist of protein. However some contain a non-protein component, referred to as a cofactor, which is required for the enzyme's catalytic activity (Robinson, 2015). A cofactor can be another organic molecule (in this case it will be called a coenzyme) or an inorganic molecule, which is usually a metal ion including iron, manganese,

cobalt, copper or zinc. DOXP reductoisomerase activity also requires cofactors such as divalent metal cations for example Mg^{2+}, Mn^{2+}, Co^{2+} etc. (Murkin *et al*., 2014; Robinson, 2015). The conversion of DOXP to MEP is NADPH-dependent. NADPH is considered as a co-substrate, as it gets consumed in the reaction along with the substrate DOXP (Munos *et al*., 2009; Murkin *et al*., 2014).

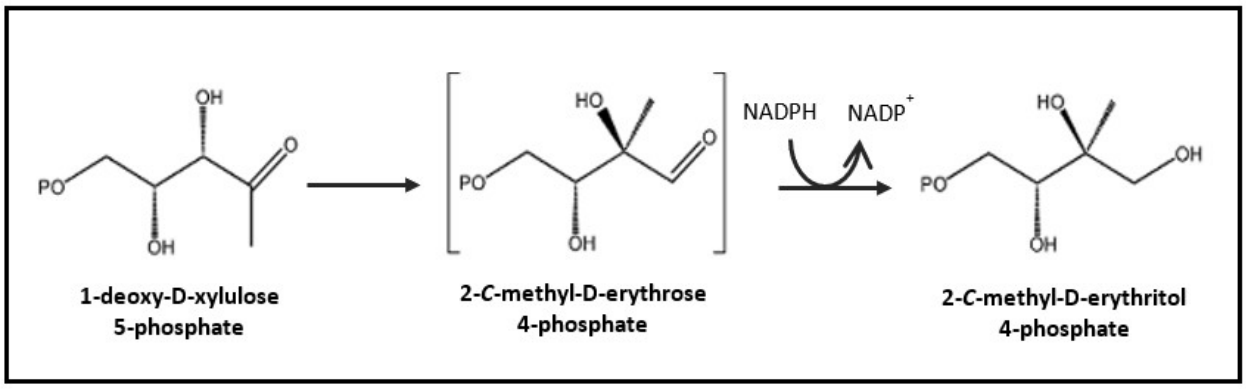

Figure 2: Reaction of the conversion of 1-deoxy-D-xylulose 5-phosphate (DOXP) to 2-C-methyl-D-erythritol 4-phosphate (MEP).
The above reaction (adapted from McKenney et al., 2012) illustrates the conversion of DOXP into MEP with the intermediate 2-C-erythrose 4-phosphate. The reaction is catalysed by the enzyme DOXP reductoisomerase (DXR) in the presence NADPH which is then oxidized into $NADP^+$.

1.3.4. Structural Characterization of DOXP Reductoisomerase

X-ray crystallography, solution NMR and molecular dynamics have been used to determine the structure and complexes of DOXP reductoisomerase (DXR) (Steinbacher *et al.*, 2003). These structures reveal that known DOXP reductoisomerases exist as homodimers, each subunit with a molecular weight of 39-45 kDa (Steinbacher *et al.*, 2003). The monomeric structure of DXR contains three domains, the NADPH-binding N-terminal responsible for the binding of NADPH, central catalytic domain responsible for metal and substrate binding, and C-terminal α-helical domain (Yajima *et al*., 2007; Takenoya *et al*., 2010; Umeda *et al*., 2011). The active site of DXR consists of three regions that the substrate binds to. These regions include a positively charged site that the phosphate moiety of the substrate binds to, a hydrophobic pocket that interacts with the

backbone of the substrate and the amphipathic region where the hydroxamate moiety binds (Williams and McCammon, 2009). The binding site of the divalent metal ion is formed by a cluster of conserved acidic residues, Asp151,Glu153 and Glu222, (Williams and McCammon, 2009). The NADPH cofactor plays an essential role in the tight binding of the substrate or inhibitor as the nicotinamide ring contributes to the formation of hydrophobic binding pocket (Williams and McCammon, 2009).

The crystal structure of DXR from numerous organisms such as *E. coli*, *M. tuberculosis*, *P. falciparum*, *Zymamonas mobilis* and *thermotoga maritima* have been reported (Reuter *et al*., 2002; Yajima *et al*., 2002; Ricagno *et al*., 2004; Mac Sweeney *et al*., 2005; Yajima *et al*., 2007; Takenoya *et al*., 2010; Umeda *et al*., 2010; Jansson *et al*., 2013). The crystal structure of DXR with or without cofactors and/or substrates/inhibitors has provided structural information required for understanding the enzyme's mode of action and a starting point for designing effective drugs (Reuter *et al*., 2002; Yajima *et al*., 2007). These structures include: *E. coli* DXR present in an apo form (Reuter *et al*., 2002); *E. coli* DXR complexed with NADPH and a sulphate ion (Yajima *et al*., 2002); *Z. mobilis* DXR complexed with NADPH (Ricagno *et al*., 2004); *E. coli* DXR in a ternary complex with NADPH and the DOXP substrate (Mac Sweeney *et al*., 2005); *E. coli* DXR in a ternary complex with NADPH and fosmidomycin (Mac Sweeney *et al*., 2005); *T. maritima* DXR complexed with and without fosmidomycin (Takenoya *et al*., 2010); *P. falciparum* DXR complexed to NADPH (Umeda *et al*., 2010); *M. tuberculosis* DXR as an apoenzyme in ternary complexes with NADPH and fosmidomycin (Jansson *et al*., 2013); *M. tuberculosis* DXR as an apoenzyme in ternary complexes with NADPH and FR900098 (Jansson *et al*., 2013). However, Yajima *et al*. (2007) reported the first crystal structure of DXR from *E. coli* in a quaternary complex with Mg^{2+}, NADPH and fosmidomycin.

1.3.5. Inhibitors of DOXP Reductoisomerase

Initial database searches were done to identify antibiotics that had activity against *Escherichia coli* and *Bacillus subtilis*, in order to identify potential inhibitors of DXR (Kuzuyama *et al.*, 1998). From such searches, the inhibitor fosmidomycin (FR-31564) was identified as being a possible

inhibitor of DXR (Kuzuyama *et al*., 1998). Fosmidomycin is a natural product isolated from the actinobacterium *Streptomyces lavendulae* and its acetyl derivative, FR900098, which differs from fosmidomycin by an addition of a methyl group, was isolated from *Streptomyces rubellomurinus* (McKenney *et al*., 2012; Wiesner *et al*., 2016). These compounds were originally identified as spheroplast-inducing antibacterials that inhibit most Gram-negative and some Gram-positive bacteria (Mac Sweeney *et al*., 2005). The compounds work by blocking the non-mevalonate pathway by binding to the substrate binding site in the active site of DXR, thereby inhibiting the action of DXR and blocking the synthesis of isoprenoid precursors (Jansson *et al*., 2013).

A study conducted by Jomaa and colleagues provided evidence that fosmidomycin and FR900098 are two drugs that suppressed the *in vitro* growth of multidrug resistant *P. falciparum* strains(Jomaa *et al.*, 1999). It was suggested that the compounds could inhibit DOXP reductoisomerase from the malaria parasite in a dose-dependent manner and cured mice that were infected with the rodent malaria parasite *P. vinckei* (Jomaa *et al.*, 1999). Therefore, these can be effective in the chemotherapy of malaria (Kuzuyama *et al*., 2000). However, FR900098 has been found to have twice the activity of fosmidomycin against the malaria parasite *in vivo* and *in vitro* (McKenney *et al*., 2012). A structural analysis of *P. falciparum* DXR bound to FR900098 showed that the van der Waals contact with the side chain of tryptophan residue formed by the additional methyl group of FR900098 may explain why FR900098 is found to be more active than fosmidomycin (Umeda *et al*., 2011). The hydroxamate moiety (bearing functional group RCNR') chelating with a divalent metal cation (Mn^{2+}, Mg^{2+}, or Co^{2+}) and a phosphonate group that is negatively charged are the two functional groups that are important for the binding efficacy and inhibition of DXR by fosmidomycin and FR900098 (McKenney *et al*., 2012).

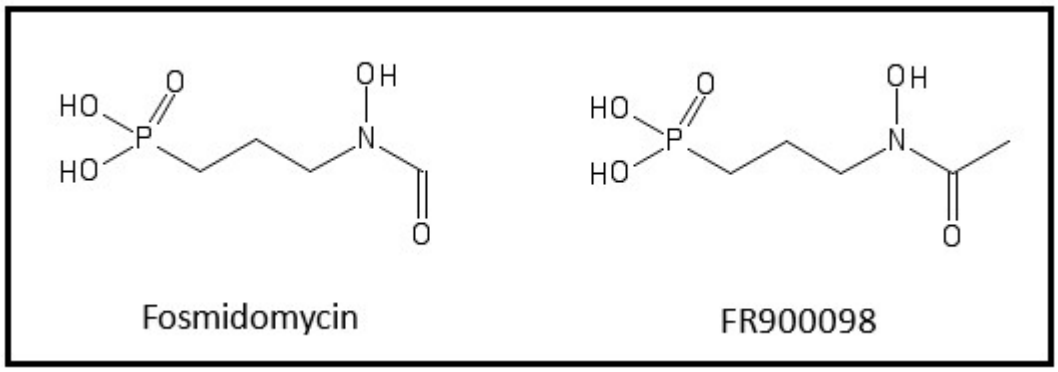

Figure 3: The chemical structures of fosmidomycin and FR900098.
The structures above, adapted from Wiesner *et al*. (2016), represent the well known inhibitors of DOXP reductoisomerase, fosmidomycin and FR900098, responsible for inhibiting the conversion of DOXP to MEP in the second step of the non-mevalonate pathway.

Confirmation of the antibacterial activity of fosmidomycin was done in a pilot phase II trial of patients with acute urinary infections and minor adverse effects were reported (Wiesner *et al*., 2016). The clinical development of fosmidomycin as an antibacterial agent was discontinued due to probable reasons such as its lower efficacy compared to other antibiotics that were being developed, the lack of activity against bacteria such as streptococci and staphylococci and the development of resistance (Wiesner *et al*., 2016). However, the molecular target of fosmidomycin was discovered resulting in the renewed interest in fosmidomycin as a potential antimalarial drug (Missinou *et al*., 2002). Fosmidomycin reverted to clinical phase II studies and oral treatment resulted in the reduction of parasitemia in patients with acute *P. falciparum* malaria (Lell *et al*., 2003).

Fosmidomycin gets actively transported into cells by a glycerol-3-phosphate transporter (GIpT). This poses a problem with pathogens that lack GIpT proteins, making fosmidomycin less effective against diseases caused by these pathogens (Jansson *et al*., 2013). *M. tuberculosis* is one of several pathogens that lack GIpT proteins. Although fosmidomycin has been reported to display inhibition against *M. tuberculosis* DXR, this inhibitor does not have an effect on whole cells of the bacteria as it is too polar, making it unable to penetrate the thick cell wall (McKenney *et al*., 2012). This causes resistance of *M. tuberculosis* to fosmidomycin, as it is unable to get intracellular access,

however, some studies have proved that compounds that increase solubility can be used in conjunction with fosmidomycin as an alternative for treatment (Brown and Parish, 2008).

Wiesner *et al*. (2016) reported that the combination of clindamycin with fosmidomycin has emerged for the treatment of malaria. Clindamycin is known for having antimalarial activity, however, the sole use of it for *falciparum* malaria is not recommended due to its slow onset of action, which poses a danger to individuals requiring fast clearance of the parasite (Lell and Kremsner, 2002). Therefore, taking advantage of its antimalarial potential will require combining it with a fast-acting drug (Lell and Kremsner, 2002). High cure rates were achieved with longer treatment durations with the fosmidomycin-clindamycin combination in Gabon and Thailand, but lower cure rates were observed in children younger than 3 years of age (Na-Bangchang *et al*., 2007; Wiesner *et al*., 2016). Although, the cure rates observed for this group were lower, suggesting a lower efficacy of the drug combination which may be reflect inadequate formulation, further clinical development was advocated for (Wiesner *et al*., 2016).

FR900098 was found to be twice as active as fosmidomycin against malaria parasites. In addition, it has a higher affinity for DXR (Jomaa *et al*., 1999; Wiesner *et al*., 2016). This is due to the van der Waals contact formed between the methyl group of FR900098 and the side chain of a tryptophan residue which was observed in a study where the structure of *P. falciparum* DXR bound to FR900098 was analysed (McKenney *et al*., 2012). Wiesner *et al*. (2016) studied the acute toxicity and genotoxicity of FR900098 in rats to assess whether the inhibitor can be used to form the basis for further antimicrobial drug development. No toxicity or substance related deaths or significant adverse effects in the rats used were observed in the study (Wiesner *et al*., 2016). These toxicity studies are of great importance as they are able to determine whether an inhibitor displaying the desired *in vitro* activity is not harmful or toxic to human cells and that it can be used for further drug development programs which include clinical trials.

1.4. PROBLEM STATEMENT

Invasive non-typhoidal *Salmonella* is the leading cause of bacterial bloodstream infections in sub-Saharan Africa (Gordon, 2011). The rates of antibiotic resistance of invasive non-typhoidal *Salmonella* are increasing and the treatment of invasive Salmonellosis is a dilemma, therefore the discovery of new compounds for the development of antibiotic drugs is required (Chen *et al*., 2013). Despite the non-mevalonate (MEP) pathway being regarded as an attractive drug target for antimicrobial drug discovery, there are no published reports describing the properties of *Salmonella enterica* DOXP reductoisomerase or if FR900098 can inhibit the enzyme.

1.5. HYPOTHESIS

Inhibition screening of the *Salmonella enterica* DOXP reductoisomerase enzyme can be used in high through-put screening assays to identify potential new drug compounds.

1.6. AIMS AND OBJECTIVES

The aim of this project is to develop a *Salmonella enterica* DOXP Reductoisomerase enzyme assay and screen for compounds that could potentially form basis for developing new broad-spectrum antibiotics that can be used for treating salmonellosis.

The aim was achieved under the following objectives:

- Optimise the heterologous expression of *Salmonella enterica*, *Plasmodium falciparum* and *Mycobacterium tuberculosis* 1-deoxy-D-xylulose 5-phosphate reductoisomerase in small scale *Escherichia coli* cultures.
- Purify recombinant *Salmonella enterica*, *Plasmodium falciparum* and *Mycobacterium tuberculosis* 1-deoxy-D-xylulose 5-phosphate reductoisomerase by IMAC affinity chromatography from large scale *Escherichia coli* cultures.

- Develop an assay for detecting the activity of *Salmonella enterica* 1-deoxy-D-xylulose 5-phosphate reductoisomerase.
- Determine the kinetic parameters of *Salmonella enterica* 1-deoxy-D-xylulose 5-phosphate reductoisomerase.
- Screen for novel compounds from the Pathogen Box library for potent inhibitors of *Salmonella enterica* 1-deoxy-D-xylulose 5-phosphate reductoisomerase)

CHAPTER 2: HETEROLOGOUS PRODUCTION AND PURIFICATION OF THE DOXP REDUCTOISOMERASE TARGET ENZYME

2.1. INTRODUCTION

The expression of proteins of interest is done in both academic and industrial laboratories whereby their structures, functions and potential therapeutic uses are investigated (Cabrita and Bottomly, 2004). These investigations involve processes such as cloning of target genes and heterologous expression of the protein of interest with the utilization of specific host expression systems (Cabrita and Bottomly, 2004). There are several hosts that can be used for the production of recombinant proteins - these include bacteria, yeast, insect, plant and animal cells (Kaur *et al*., 2017).

Studies show that the utilization of *E. coli* as an expression host for recombinant proteins is popular due to its cost-effectiveness, rapid growth making mutant selection easy and producing high density cultures for improved yields, efficient transformation with foreign DNA, and recombinant protein expression at high rates (Rosano and Ceccarelli, 2014; Kaur *et al*., 2017). Although *E. coli* has these advantages making it a dominant expression host for recombinant proteins, its use has some limitations such as lack of secretion systems which aid in efficiently releasing proteins into the growth medium, limited ability to facilitate the extensive formation of disulfide bonds, decreased protein stability due to its inability to do post-translational modifications, increased immunogenicity, leaky expression when tight regulation of expression is required and is associated with different expression systems found in this organism and the production of insoluble inclusion bodies due to frequent deposition of the expressed protein (Cabrita and Bottomly, 2004; Chen, 2012; Kaur *et al*., 2017).

Codon bias is one of the factors that affect the levels of recombinant proteins produced (Gustafsson *et al*., 2004; Menzella, 2011). Codon bias occurs when there is a significant difference in the frequency of occurrence of synonymous codons in foreign coding DNA compared to the host genome. As a result, low abundance tRNAs are depleted causing the misincorporation of amino

acids directly affecting protein expression levels (Gustafsson *et al*., 2004; Rosano and Ceccarelli, 2014). Strategies for solving this issue include synthesizing codon optimized genes for proteins using suitable codons for the host cell without alteration of the amino acid sequence (Inouye *et al*., 2015). Recent research shows that the application of codon optimization of heterologous protein genes can achieve optimum protein expression of proteins in different host cells which include bacteria, fungi, plants and animals (Inouye *et al*., 2015).

Extracellular proteins are secreted out of the cell, however *E. coli* expression results in intracellular proteins and some methods must be applied to break down the cells so that crude protein can be obtained (Mondal and Gupta, 2006). These include physical methods such as osmotic shock or freezing and thawing, mechanical methods such as ultrasonication, homogenization and bead mills, and a combination of chemical and enzymatic methods such as treatment with different solvents, detergents, and enzymes (Vallejo and Rinas, 2004; Mondal and Gupta, 2006).

The formation of inclusion bodies is a stumbling block in protein expression and purification. Batas and Chaudhuri (1996) suggest that high level of expression may lead to incomplete protein folding (possibly due to oversaturation of the chaperone machinery required to assist formation of the mature protein conformation). Unfolded protein molecules have solvent exposed hydrophobic cores and as a result, interactions can occur between the hydrophobic regions of the different polypeptide chains forming an aggregate. Altering the growth conditions is one of the solutions for decreasing the formation of inclusion bodies. These include changing the growth temperature, the concentration of the inducer used and induction time (Yamaguchi and Miyazaki, 2014). Other methods have been developed for dealing with inclusion bodies after expression that require extensive processing including isolation of the inclusion bodies from cells, solubilization using chaotropic agents or detergents, refolding by buffer exchange, e.g. dilution into refolding buffer and purification to obtain soluble proteins (De Bernadez Clark, 2001; Singh *et al*., 2015). If the proteins of interest are expressed in an insoluble form, after the inclusion bodies are isolated, they are suspended in buffers containing high concentrations of chaotropic agents such as guanidine chloride and urea or detergents such as sarkosyl that will solubilize the misfolded proteins (inclusion bodies) (Patra *et al*., 2000). The process of refolding recombinant proteins from solubilized inclusion bodies begins with the dilution of the fully unfolded protein solution into a

refolding buffer in which the protein refolds (Burgess, 2009). Refolding of this protein results in a biologically active protein with a native-like structure (Yamaguchi and Miyazaki, 2014). Techniques for refolding proteins include the conventional dialysis and dilution methods, chromatography, zeolite absorbing systems and natural GroEL-GroES chaperone systems (Yamaguchi and Miyazaki, 2014). The subsequent step in recovering proteins from insoluble bodies or from crude lysates of bacteria expressing the protein in soluble form is protein purification.

A widely used separation technique for protein purification is immobilized-metal affinity chromatography (IMAC). This technique uses the coordination chemistry of metal ions immobilized on solid chromatographic supports with bound chelating compounds serving as affinity ligands for different proteins (Gaberc-Porekar and Menart, 2001). The benefits of using IMAC include ligand stability, high protein loading, easy regeneration, cost-effectiveness and applicability under denaturing conditions (Gaberc-Porekar and Menart, 2001). IMAC is based on the binding of a transition metal ion such as Co^{2+}, Ni^{2+}, Cu^{2+}, Zn^{2+} to chromatographic matrices, which efficiently retain peptides that contain a sequence of consecutive histidine residues, and specific amino acid side chains (Bornhorst and Falke, 2000). The most commonly used IMAC column matrix consists of Ni^{2+} chelated by nitrilotriacetic acid (NTA) attached to agarose beads. An amino acid that displays a very strong attraction to the immobilized metal ion matrices is histidine. This is due to the coordination bonds formed by the electron donor groups on the imidazole ring of the histidine with the immobilized transition metal (Bornhorst and Falke, 2000). Recombinant proteins are therefore typically engineered to contain an oligohistidine (typically 6 residues) tag at the N- or C-terminus to facilitate selective binding of the protein to a Ni^{2+}-NTA matrix. After the matrix material has undergone a washing step, the peptides or proteins containing sequences of histidine residues can be eluted and this elution process is made by the adjustment of the column buffer's pH, addition of EDTA to strip the Ni^{2+} from the NTA-agarose matrix or, most commonly, by the addition of excess free imidazole to the column buffer to outcompete the binding of the oligohistidine tag to the column (Bornhorst and Falke, 2000).

Once a protein is purified as a soluble protein, its activity can be assessed by conducting preliminary functional assays, e.g. enzyme activity assays in the case of metabolic enzymes.

Enzymes that produce or consume NADPH/NADH as a co-factor are convenient because, in their reduced form, these nucleotides absorb light at 340 nm and the enzyme reaction can be monitored by absorbance spectroscopy. This is the case with DOXP reductoisomerase. The NADPH-dependent enzyme assay has been developed to monitor the reduction of DOXP to MEP by measuring the absorbance at 340 nm, which reflects the change in concentration of NADPH. This assay is based on an intramolecular rearrangement and reduction reaction carried out by DOXP reductoisomerase in the second step of the non-mevalonate pathway (whereby DOXP is converted to MEP, in the presence of NADPH) (Yajima *et al*., 2007; Zhao *et al*., 2013). A decrease in the levels of NADPH is expected due to the consumption of NADPH in the reaction as it is a co-substrate. To explore alternative novel methods for measuring NADPH concentration decrease due to DOXP reductoisomerase activity, a fluorescence-based enzyme assay, the resazurin reduction assay, was explored in this study. This assay can be used for monitoring the NADPH-dependent reduction of resazurin to resorufin.

Resazurin (also known as Alamar Blue) is a widely used cell viability indicator that has applications in cell viability assays, proliferation assays, cytotoxicity assays and drug susceptibility assays (Borra *et al*., 2009; Osaka and Hefty, 2013). These assays are important tools in determining whether compounds that could be of clinical importance in order to pursue these compounds as potential leads in drug development. The principle behind the use of resazurin is that it is converted to resorufin (a pink fluorescent product, with an excitation wavelength of 560 nm and an emission wavelength of 590 nm) by the reducing environment found in live, metabolically intact cells. Its usefulness is enhanced by the fact that it is inexpensive and cell viability assays are straightforward – the resazurin is simply added to cell cultures in microtiter plates and, after a suitable incubation period, resorufin absorbance or fluorescence is directly measured in a plate reader. It can also be used with a wide variety of cells, including mammalian cells (Al-Nasiry *et al.*, 2007), bacteria (Martin *et al.*, 2003), yeast or fungi (Repp *et al.*, 2007), and parasites (Veale and Hoppe, 2018). It has reported that the concentration of NADPH present in a biochemical assay can be quantified by coupling an NADPH-dependent enzyme to resazurin (Hall *et al*., 2016). This suggests that resazurin could be used to detect the activity of any enzyme that consumes or produces NADPH or NADH and could be a useful substitute method if the reaction contains additional components or compounds that absorb at 340 nm.

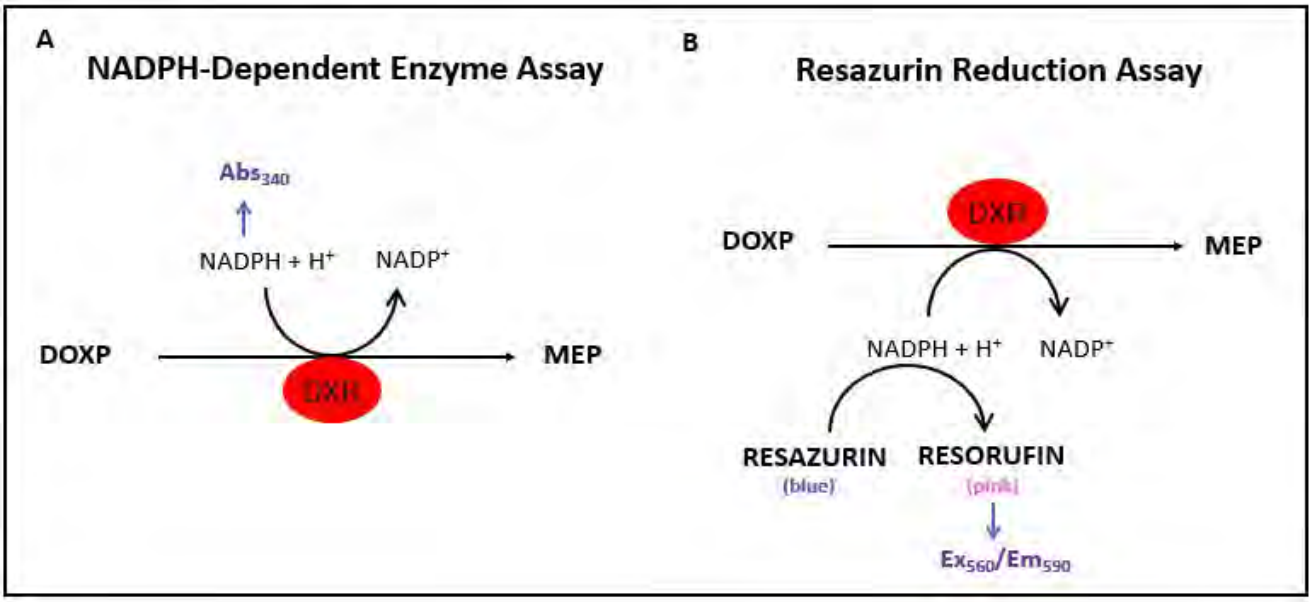

Figure 4: Diagrams of the (A) NADPH-Dependent Enzyme Assay and (B) Resazurin Reduction Assay.

(A) DOXP is converted to MEP in the presence of DOXP reductoisomerase (DXR) and NADPH. The absorbance of NADPH is measured at 340 nm. (B) Resazurin (blue coloured reagent) is reduced to resorufin (pink coloured product) in the presence NADPH. The fluorescence of resorufin is measured at excitation and emission wavelengths of 560 nm and 590 nm respectively.

In this study, the NADPH-dependent enzyme assay and resazurin reduction assay was used for analyzing the function of *S. enterica* DOXP reductoisomerase and confirming its soluble, functional expression and purification from *E. coli*. The purified recombinant enzyme was expected to lower the levels of NADPH in the reaction, as NADPH is a co-substrate and gets consumed in order to form MEP and $NADP^+$. Thus, in the presence of the functional enzyme, NADPH gets used up in an accelerated rate compared to reactions where there is no functional enzyme. These assays could also be used for determining potential inhibitors of *S. enterica* DOXP reductoisomerase.

This section aimed to:

- Transform competent T7 Express lysY *Escherichia coli* cells with pET28a(+) plasmid containing the coding sequences of *Salmonella enterica* and *Mycobacterium tuberculosis* 1-deoxy-D-xylulose 5-phosphate reductoisomerase.
- Optimise the heterologous expression of *Salmonella enterica*, *Plasmodium falciparum* and *Mycobacterium tuberculosis* 1-deoxy-D-xylulose 5-phosphate reductoisomerase. in small scale *Escherichia coli* cultures.
- Purify *Salmonella enterica*, *Plasmodium falciparum* and *Mycobacterium tuberculosis* DXR by IMAC affinity chromatography from large scale *Escherichia coli* cultures.
- Establish an assay for detecting the activity of *Salmonella enterica* 1-deoxy-D-xylulose 5-phosphate reductoisomerase.
- Determine the kinetic parameters of *Salmonella enterica* 1-deoxy-D-xylulose 5-phosphate reductoisomerase.

2.2. EXPERIMENTAL PROCEDURES

2.2.1. Preparation of Transformed of *E. coli* Stocks

The *S. enterica* (subspecies enterica, serovar Typhimurium, strain LT2 - NCBI reference NP_459225.1), and *M. tuberculosis* (GenBank AJP81541.1) DXR coding sequences were codon-optimized for *E. coli* expression, synthesized and subcloned into the *Nhe*I and *Xho*I restriction sites of the pET28a(+) expression plasmid by GenScript (Hong Kong). *E. coli* XL-1 Blue stocks containing the *P. falciparum* DXR coding sequence cloned into pQE30 was previously prepared by J. L. Goble (Goble *et al*., 2013) and donated for this study.

2.2.1.1. Transformation

A frozen stock of XL-10 gold competent *E. coli* cells (Stratagene) was thawed on ice and 0.5 µl of the pET-28a(+) plasmid (containing the coding sequence of DXR cloned into the *Nhe*I/*Xho*I sites) was added to a 50 µl aliquot of the competent cells, briefly mixed and incubated on ice for 30 minutes. The cells were heat-shocked at 42.5°C for 60 seconds and incubated on ice for 5 minutes. Luria broth (Invitrogen) was added to the cells and incubated at 37°C for 1 hour. The cells were centrifuged (3100 *g*, 3 minutes), 200 µl of the supernatant discarded, the pellet resuspended and 50 µl of the resuspended pellet plated on a Luria-agar plate containing 50 µg/ml kanamycin (Kanamycin sulfate; Sigma-Aldrich). The plate was incubated overnight at 37°C. Frozen stocks of the transformed XL-10 gold *E. coli* cells containing the expression plasmids were prepared by inoculating a colony picked from the plate containing transformed bacteria into 5 ml Luria broth with kanamycin (50 µg/ml) and incubating overnight at 37°C with shaking. Glycerol stocks were prepared by mixing 150 µl sterile glycerol with 850 µl overnight culture and the stocks were stored at -80°C.

2.2.1.2. Plasmid Miniprep Preparation by Alkaline Lysis

Plasmid minipreps were prepared by scraping frozen glycerol stocks of the transformed XL-10 gold *E. coli* cells, adding the scraping to 3 ml Luria broth and kanamycin (50 µg/ml) and culturing overnight. The bacteria were pelleted (3100 *g*, 3 min), the Luria broth was discarded and the pellet was resuspended in GTE buffer (30 mM glucose, 25 mM Tris, 10 mM EDTA, 10 µg/ml RNase, pH 8.0). NaOH/SDS lysis solution (0.2 N NaOH, 1% (w/v) SDS) was added and the suspension incubated for 1-2 minutes. Potassium acetate solution (5 M) was added to the suspension and the precipitate pelleted (16 900 *g*, 5 min). The supernatant was transferred into a new microcentrifuge tube, the plasmid DNA was precipitated by adding 2 volumes absolute ethanol with brief mixing and the plasmid DNA was pelleted (16 900 *g*, 6 min). The supernatant was discarded, and the pellet was washed in 70% (v/v) ethanol and pelleted (16 900 *g*, 3 minutes). The supernatant was discarded, and the DNA pellet was dried on a heating block at 37°C. The pellet was dissolved in molecular biology grade water and the alkaline lysis miniprep was stored at -20°C.

2.2.1.3. Restriction Digestion

The restriction digest was conducted by mixing 10 µl of the plasmid miniprep, 5 units of both the restriction enzymes *Xho*I and *Nhe*I (New England Biolabs), 11.5 µl water and 2.5 µl 10x restriction digest buffer. The sample was incubated at 37°C for an hour and stored at -20°C. Before agarose gel electrophoresis analysis, samples were mixed with sample buffer to obtain a final concentration of 5% (v/v) glycerol, 0.042 % (w/w) bromophenol blue in TBE buffer (100 mM Tris, 100 mM boric acid, 2 mM EDTA).

2.2.1.4. Agarose Gel Electrophoresis Analysis

TBE buffer (100 mM Tris, 100 mM boric acid, 2 mM EDTA) was added to agarose (0.8% (w/v) and the suspension was heated in a microwave oven. Ethidium bromide (Sigma-Aldrich) (1.2 µg/ml) was added and the gel was poured into a gel casting tray fitted with a comb. The gel was left to solidify for 20-30 minutes. The gel was submerged in TBE buffer in the gel buffer tank. The samples were loaded into the agarose gel submerged in 1X TBE buffer and run alongside a 1 kb

DNA ladder (Promega) at 80 V for 45-50 minutes. The restriction digestions were visualized and photographed under UV light using a ChemiDoc™ XRS$^+$ gel documentation system (Bio-Rad).

2.2.2. Expression of 1-Deoxy-D-xylulose 5-phosphate Reductoisomerase

2.2.2.1. Small-Scale Protein Expression

Competent T7 Express LysY *E. coli* cells (New England Biolabs) were transformed with the pET-28a plasmids containing the DXR coding sequences and glycerol stocks of these cells were prepared as per the transformation procedure. An overnight culture was prepared by placing a scraping of transformed T7 Express LysY *E. coli* cells from the glycerol stock into a McCartney bottle containing 5 ml LB broth with kanamycin (50 µg/ml) and incubated at 37°C overnight with shaking (150-180 rpm). Aliquots (400 µl) of the overnight starting culture were added to two McCartney bottles containing 8 ml Luria broth with kanamycin (50 µg/ml). The cultures were incubated with shaking at 37°C until an OD_{600} reading (using a UVmini-1240 UV-Vis Spectrophotometer; Shimadzu) of 0.4-0.6 was reached. IPTG (Isopropyl β-D-1-thiogalactopyranoside; Sigma-Aldrich) (1 mM) was added to one of the cultures to induce protein expression, while the other culture was an uninduced control (no IPTG was added to it) and both cultures were incubated further for 3 hours at 37°C. The bacteria were pelleted by centrifugation (JA-20 rotor, 5 000 *g*, 10 minutes, 4°C) using an Avanti® J-E centrifuge (Beckman Coulter) and the pellets were frozen (-20°C) overnight. The frozen pellets were thawed on ice and resuspended in wash buffer (50 mM Tris-HCl pH 8.0). Lysozyme (Lysozyme from chicken egg white; Sigma-Aldrich) (10 mg/ml) was added to the suspensions and incubated on ice for 30 minutes. The bacteria were lysed by two cycles (60 Amps) of probe sonication (Vibra-Cell™ sonicator; Sonics & Materials Inc) at 60 Hz for 45 seconds separated by a 1 minute rest on ice, and the cell lysate was centrifuged (JA-20 rotor, 14 000 g, 10 minutes, 4°C). The soluble and insoluble fractions were separated and collected. The insoluble pellet fractions were resuspended in wash buffer to a volume equal to the soluble supernatant fraction and both fractions stored at -20°C.

2.2.2.2. SDS-PAGE Analysis

Protein expression was confirmed by SDS-PAGE analysis. A discontinuous SDS-PAGE was run on a 12% acrylamide gel, using an adaption of the method described by Laemmli (1970). The gel was made up of a 12% (w/v) resolving gel [4 ml 30% (w/v) acrylamide, 2.5 ml lower gel buffer (1.5 M Tris-HCl, 0.4% (w/v) SDS, pH 8.8), 3.5 ml water, 35 µl 10% (w/v) ammonium persulfate (Sigma-Aldrich) and 7 µl TEMED (N,N,N',N'-Tetramethylethylenediamine; Sigma-Aldrich)] and a 4% stacking gel [0.7 ml 30% (w/v) acrylamide, 1.25 ml stacking gel buffer (0.5 M Tris-HCl, 0.4% (w/v) SDS, pH 6.8), water, 25 µl 10% (w/v) ammonium persulfate and 6 µl TEMED]. The soluble and insoluble samples were mixed with 4X SDS sample buffer (10 ml stacking buffer, 8 ml glycerol, 0.8 g SDS, 0.8 ml 2-mercaptoethanol, 0.2 mg bromophenol blue, 1.2 ml water) in a 3:1 sample to sample buffer ratio and heated in boiling water for 5 minutes. The 4 samples – induced soluble, induced insoluble, uninduced soluble and uninduced insoluble fractions - were run on the SDS- PAGE gel alongside 5 µl protein standard (Color Prestained Protein Standard, broad-range, New England Biolabs) in SDS running buffer (25 mM Tris-HCl, 0.2 M glycine, 3.5 mM SDS) at 120 V constant voltage for 1.5 hours. The gel was stained with Coomassie stain (45 % (v/v) water, 45% (v/v) methanol, 10% (v/v) acetic acid, 0.25% (w/v) Coomassie Brilliant Blue R-250) overnight at room temperature with gentle shaking (Enduro™ Minimix). The gel was destained with destain solution (44% (v/v) water, 45% (v/v) methanol, 11% (v/v) acetic acid) at room temperature with gentle shaking. The destain solution was changed every 15 minutes until the protein bands were visible. The gel was photographed using the ChemiDoc™ XRS$^+$ gel documentation system (Bio-Rad).

2.2.2.3. Western Blotting

Proteins resolved on a polyacrylamide gel were transferred onto an Amersham Hybond™ ECL nitrocellulose blotting membrane at 90 V for 1 hour while submerged in a transblot buffer (25 mM Tris, 192 mM Glycine, 20% (v/v) methanol in water). The membrane was washed in water, stained for 5 minutes with Ponceau S stain (0.1% (w/v) Ponceau S, 1% (v/v) glacial acetic acid in water) and rinsed in Ponceau S destain (1% (v/v) glacial acetic acid in water) until clear. For detection of His-tagged proteins, the blot was blocked in 20 ml incubation buffer (0.1% (v/v) Tween-20, 1%

(w/v) BSA, 10 mM imidazole in TBS) overnight at 4°C. The blot was probed with a 1:5000 dilution of HisDetector Nickel-HRP (SeraCare) for 1 hour at ambient temperature. The blot was washed in three volumes of wash buffer (0.1% (v/v) Tween-20, 10 mM imidazole in TBS), covered in TMB membrane peroxidase substrate (SeraCare) and rinsed in water after bands became visible on the blot.

2.2.3. Purification of the recombinant 1-Deoxy-D-xylulose 5-phosphate reductoisomerase (DXR)

2.2.3.1. Large-Scale Protein Expression

An overnight starter culture was prepared by placing a scraping of transformed T7 Express LysY *E. coli* cells from the glycerol stock into a McCartney bottle containing 5 ml Luria broth with kanamycin (50 µg/ml) and incubated at 37°C overnight with shaking (150-180 rpm). A 5 ml aliquot of the overnight culture was added to 250 ml Luria broth containing kanamycin (50 µg/ml) and grown until an OD_{600} reading of 0.5-0.9 was reached, followed by a 3-hour incubation with IPTG (1 mM) induction at 37°C with shaking. The cells were pelleted (JA-14 rotor, 5000 g, 10 minutes, 4°C) using an Avanti® J-E Centrifuge (Beckman Coulter) and the pellet was washed with equilibration buffer (50 mM Tris-HCl, 20 mM imidazole, pH 8.0). Centrifugation was repeated and the pellet was stored at -20°C until purification.

2.2.3.2. Ni-NTA Column Purification

The bacterial pellet was resuspended in column equilibration buffer and lysozyme (2 mg/ml) was added, then incubated on ice for 30 minutes. The bacteria were lysed by two cycles (60 Amps) of probe sonication at 60 Hz for 1 minute each with 1 minute rest on ice, and centrifuged (JA-14 rotor, 14 000 g, 30 minutes, 4°C) to obtain a soluble bacterial lysate. The cell lysate was pre-cleared through a 0.45 µM syringe filter, followed by a 0.2 µM syringe filter. A 130 µl aliquot of the cell lysate was collected and stored on ice for SDS-PAGE analysis. The storage buffer was

drained from a column containing nickel-NTA agarose resin and the column (Ni-NTA fast start kit, Qiagen) was rinsed with filter-sterilized dH_2O and conditioned with equilibration buffer (50 mM Tris-HCl, 20 mM imidazole, pH 8.0). The filtered bacterial supernatant was loaded into the column, a 130 µl aliquot of the flow-through was collected and stored on ice for SDS-PAGE analysis. The column was washed twice with 5 ml equilibration buffer and a 130 µl aliquot from each wash was collected and stored on ice. A 3 ml volume of elution buffer (50 mM Tris-HCl, 500 mM Imidazole, pH 8.0) was used to elute the protein and 130 µl of the eluate was collected and stored on ice and the remaining eluate was stored at -20°C. The Ni-NTA column was rinsed with filter-sterilized dH_2O and stored in 50% (v/v) ethanol storage solution at 4°C. All the purification steps were conducted on ice.

To perform buffer exchange and remove the imidazole and salts present with the purified protein in the elution buffer, a PD-10 Sephadex^{TM} G-25 M desalting column (GE Healthcare) was equilibrated with 25 ml assay buffer (200 mM Tris, 500 mM NaCl, pH 7.5, pH 7.5) and 2.5 ml protein eluate was applied to the column and allowed to flow through. The protein was eluted with 3.5 ml assay buffer and collected. The concentration of the desalted protein was determined by performing a Bradford assay. The presence of the purified protein was confirmed by SDS- PAGE and the desalted protein was stored in 40% (v/v) glycerol at -20°C.

A Bradford's assay was conducted as described by Bradford (1976) for determining desalted protein concentration. Protein standards were prepared using BSA (Bovine Serum Album Fraction V; Merck) (0.03125-1 mg/ml serial dilution). In a 96-well plate, 5 µl aliquots of the protein standards, equilibration buffer (background) and the collected purification samples were added in duplicates and 250 µl Bradford reagent (Sigma-Aldrich) added. The plate was incubated at room temperature for 10 minutes to allow the reaction to develop and the absorbance was read at 595 nm using the SpectraMax® M3 360 multi-well plate reader (Molecular Devices). A standard curve was constructed using absorbance values obtained by subtracting background samples absorbances from the standard samples absorbances. The curve (Appendix C) was used to determine the concentration of the purified and desalted samples.

2.2.3.3. Refolding of Inclusion Bodies by Dialysis

Large scale protein expression was conducted (Section 2.2.3.1.). The bacterial pellet was resuspended in column equilibration buffer and lysozyme (10 mg/ml) was added, then incubated on ice for 30 minutes. The bacteria were lysed by two cycles (60 Amps) of probe sonication at 60 Hz for 1 minute and centrifuged (JA-14 rotor, 14 000 g, 30 minutes, 4°C) and the pellet was collected. The insoluble pellet was added to 5 ml 1% sarkosyl buffer (1% (w/v) *N*-lauroyl sarcosinate, 50 mM Tris (pH 7.5), 1 mM DTT) and incubated with gentle shaking until the pellet was dissolved. This solution was added to 10 ml of TBS (20 mM Tris, 0.15 mM NaCl, 1 mM DTT, 10% glycerol, pH 7.5) buffer. An appropriate length of dialysis tubing was cut and incubated in water. The dialysis tubing was removed from the water and placed in 250 ml TBS buffer and incubated for 10 minutes. The dissolved pellet in TBS buffer was transferred into the dialysis tubing and the ends of the tubing were sealed. Dialysis was performed against 250 ml of TBS buffer for 4-5 hours, at 4°C. The TBS buffer was replaced with fresh buffer and dialysis was continued overnight at 4°C. A 130 µl aliquot of the buffer exchanged sample was removed and set aside for SDS-PAGE analysis. The remainder of the solution in the dialysis tubing was applied to the Ni-NTA column. Subsequent purification steps were conducted as described above (Section 2.2.3.2) and 130 µl of the purification samples were collected and stored for SDS-PAGE analysis and the Bradford's Assay.

2.2.3.4. Refolding of Inclusion Bodies by Dilution

Large scale protein expression was conducted (Section 2.2.3.1.) followed by cell lysis (Section 2.2.3.2.) and the insoluble pellet was collected. The pellet was added to 5 ml 1% sarkosyl buffer and incubated with gentle shaking until the pellet was dissolved. A 2.5 ml aliquot of the dissolved pellet was slowly added to 50 ml TBS buffer in a beaker with a magnetic stirring bar. The leftover dissolved pellet was slowly added to another beaker with stirring 50 ml TBS buffer. The two resulting solutions were applied to a Ni-NTA column for purification, subsequent column purification steps were carried out as described earlier (Section 2.2.3.2) and 130 µl purification samples were collected and stored for SDS-PAGE analysis and the Bradford assay.

2.2.3.5. Stripping and Re-charging of the Ni-NTA Column

The 50% (v/v) ethanol storage solution was drained from the Ni-NTA fast start kit column. The column was rinsed with filter-sterilized water. Stripping buffer (20 mM sodium phosphate, 500 mM NaCl, 50 mM EDTA, pH 7.4) was run through the column and filter-sterilized water was added to the rinse the column. Recharging buffer (0.1 M $NiSO_4$) was run through the column followed by rinsing with filter-sterilized water. A 50% (v/v) ethanol solution was added to the column to store the resin.

2.2.4. 1-Deoxy-D-xylulose 5-phosphate reductoisomerase (DXR) Assay

2.2.4.1. NADPH-Dependent Enzyme Assay

Final concentrations of 1X TBS (40 mM Tris, 100 mM NaCl, pH 7.5) with $MnCl_2$ (10 mM), NADPH (0.3 mM) and DOXP (0.3 mM) were mixed together from concentrated stocks and distributed into a 96 well plate. To initiate the reaction, the purified recombinant *S. enterica* DXR enzyme (30 µg/ml final concentration) was added. The plate was incubated at 37°C for 1 hour. The absorbance at 340 nm was measured (an end-point measurement) using a SpectraMax® M3 360 multi-well plate reader (Molecular Devices). A reaction without enzyme was included as a control.

2.2.4.2. Resazurin Reduction Assay

As described above, 1X TBS with 10 mM $MnCl_2$, 0.3 mM NADPH and 0.3 mM DOXP were mixed from concentrated stocks, distributed into a 96 well plate, the purified *S. enterica* DXR enzyme (30 µg/ ml) was added to initiate the reaction. The plate was incubated at 37°C for 3o minutes. A 5 µl aliquot of 0.59 mM resazurin in PBS stock was added to the 100 µl reaction mixture and the fluorescence (Exc_{560}/Emm_{590}) was measured in the SpectraMax® M3 360 multi-

well plate reader after an incubation of 30 minutes at 37°C. A reaction without enzyme was included as a control.

2.3. RESULTS

2.3.1. Diagnostic Restriction Enzyme Analysis

To confirm the identity of the plasmid intended for expression of *S. enterica* 1-deoxy-D-xylulose 5-phosphate reductoisomerase (DXR), a diagnostic restriction enzyme digest was conducted. The *S. enterica* DXR coding sequence, codon-optimized for expression in *E. coli*, was inserted into the pET28a(+) expression vector at the *Xho*I and *Nhe*I sites by Genscript (Hong Kong). After transforming the plasmid into XL-10 gold *E. coli* cells, a plasmid miniprep was prepared and it was treated with the *Xho*I and *Nhe*I restriction enzymes and analyzed using agarose gel electrophoresis. The *S. enterica* 1-deoxy-D-xylulose 5-phosphate reductoisomerase (SeDXR) coding sequence was released as a 1413 bp DNA fragment (Fig. 5). Two larger DNA fragments (A and B) which migrated with the calculated values on the agarose gel (DNA fragment A: 6583 bp and DNA fragment B: 5485 bp) were also present. DNA fragment B likely represents the empty pET28a plasmid (5369 bp) and fragment A incompletely digested, linearized plasmid.

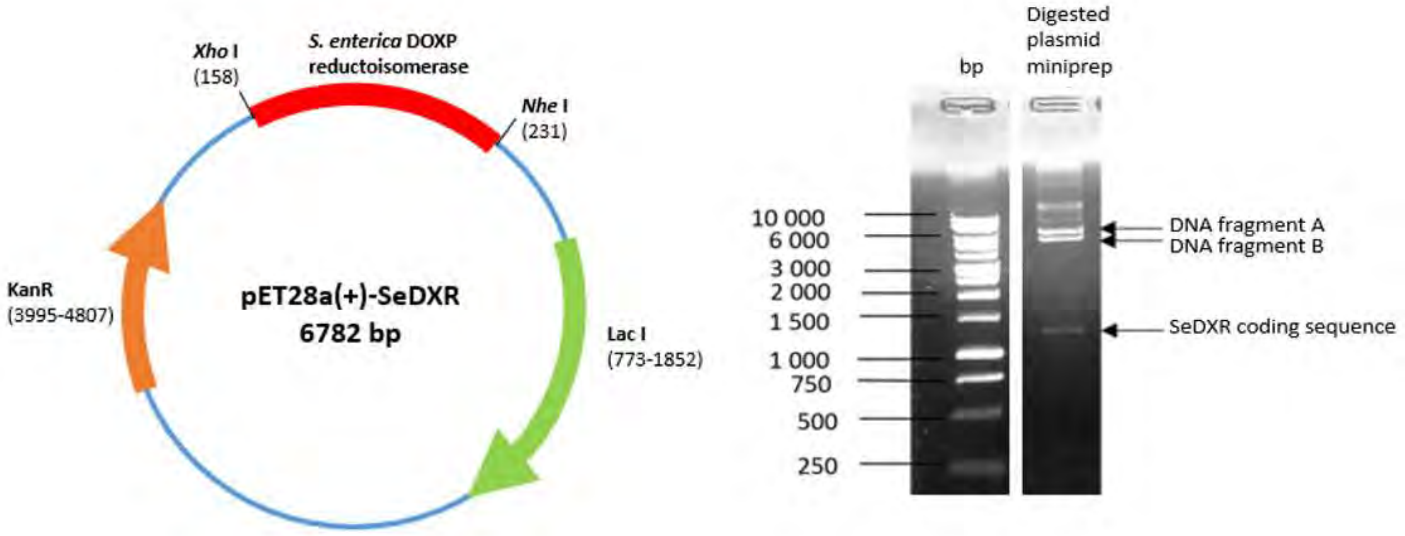

Figure 5: Restriction digest of the pET28a(+)-SeDXR plasmid construct.
The plasmid map of pET28(a)-SeDXR with the kanamycin resistance coding sequence, Lac I gene coding sequence, *Xho*I/*Nhe*I sites and *S. enterica* DXR coding sequence (adapted from Novagen). A 0.8% agarose gel showing the confirmation pET28a-SeDXR plasmid by diagnostic restriction enzyme analysis. A 1 kb DNA ladder (Promega) indicated in bp was run alongside the plasmid miniprep digested with *Xho*I and *Nhe*I restriction enzymes.

2.3.2. Small Scale Protein Expression

E. coli cells are the most commonly used expression host systems. However, their inability to consistently overexpress functional and correctly folded (soluble) proteins is one of the limitations of using them for protein expression. To determine the level of expression and solubility of 1-deoxy-D-xylulose 5-phosphate reductoisomerase (DXR) of *S. enterica* (SeDXR), *M. tuberculosis* (MtDXR) and *P. falciparum* (PfDXR), small scale expression was conducted. Expression cultures inoculated with an overnight culture (containing the transformed T7 Express LysY *E. coli* cells) were prepared. One of the cultures was IPTG induced and the other culture was an uninduced control. The bacterial cells were lysed by sonication and after centrifugation, the soluble and insoluble fractions were collected. This resulted in four samples: induced soluble, induced insoluble, uninduced soluble and uninduced insoluble sample. Protein expression was confirmed by SDS-PAGE analysis. The $(His)_6$ *S. enterica* DXR protein was present in the induced soluble and induced insoluble sample lanes (at the calculated molecular weight of 45.7 kDa) (Fig. 6A). *P. falciparum* DXR and *M. tuberculosis* DXR were present in the induced insoluble samples, represented by prominent dark bands (Fig. 6B, C). However, corresponding bands could not be discerned in the induced vs. uninduced soluble samples, suggesting these proteins were only expressed in insoluble form. In the case of *P. falciparum* DXR, this was confirmed by western blotting with nickel-HRP, which showed a band in the insoluble sample, but not the soluble sample (Fig. 6D).

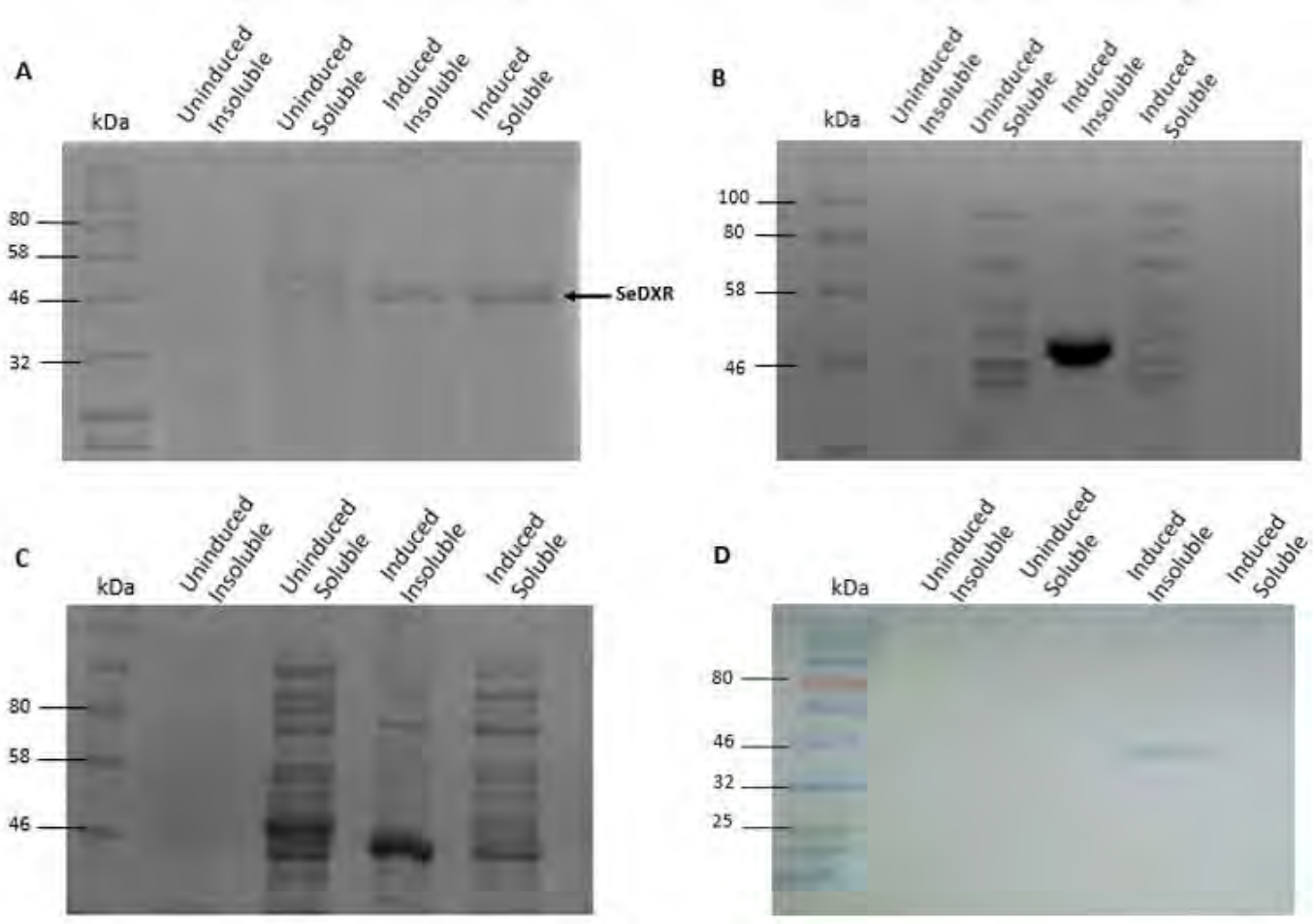

Figure 6: Small scale 1-deoxy-D-xylulose 5-phosphate reductoisomerase expression.
The molecular weight marker (Color Prestained Protein Standard, Broad Range; New England Biolabs) indicated in kDa was run alongside the soluble and insoluble fractions obtained from small scale expression of *S. enterica* DXR (A), *M. tuberculosis* DXR (B) and *P. falciparum* DXR (C) on a 12% SDS-PAGE gel and stained with Coomassie. *P. falciparum* DXR expression was also assessed by western blotting with HisDetector (D).

The SeDXR was expressed as a soluble protein, although prominent bands were present in both the induced soluble and insoluble fractions (Fig. 6A). The PfDXR and MtDXR proteins were found to be insoluble as prominent protein bands were only found in the induced insoluble fraction (Fig. 6B, C, D: Induced Insoluble). An alternative approach in which the bacterial growth conditions were altered was attempted. The temperature, inducer concentration, and length of induction were changed (using lower temperatures, lower IPTG concentrations and decreasing the period of induction). Although this was attempted, these proteins were still found to be insoluble

(Appendix E), therefore other protein solubilization and refolding techniques have to be explored for the expression and purification of the proteins in a native state. An option is to use commercial refolding screens (e.g. the Pierce ProMatrix kit that allows simultaneous evaluation of 96 refolding conditions), or alternative expression hosts (e.g. *Pichia pastoris* yeast or insect cells) used to attempt to increase the soluble expression of the proteins.

2.3.3. Large Scale Protein Purification

The *S. enterica* 1-deoxy-D-xylulose 5-phosphate reductoisomerase (DXR) enzyme was expressed in *E. coli* cultures in a larger volume (large scale) and the IPTG-induced soluble fraction was collected for purification. The enzyme was purified by nickel affinity chromatography (Fig. 7) and yields of up to 229 µg were isolated from a 250 ml culture. Low levels of unbound *S. enterica* DXR protein were present in the wash 1 and wash 2 lanes, but a high concentration of purified protein was present in the column eluate.

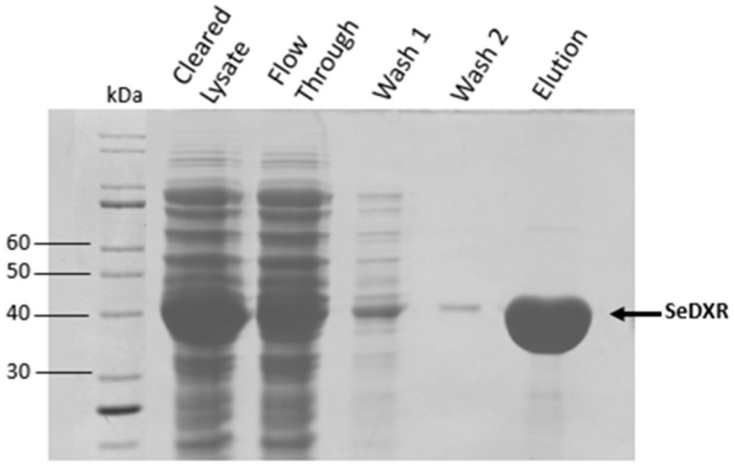

Figure 7: *Salmonella enterica* 1-deoxy-D-xylulose 5-phosphate reductoisomerase purification. The induced soluble *S. enterica* DXR sample was run through the Ni-NTA column followed by subsequent purification steps. The molecular weight markers [Unstained Protein Standard, Broad Range; New England Biolabs)] indicated in kDa were run alongside the *S. enterica* 1-deoxy-D-xylulose 5-phosphate reductoisomerase cleared lysate, flow-through, wash 1, wash 2 and eluate samples on a 12% SDS-PAGE gel stained with Coomassie staining solution.

The nitrilotriacetic acid (NTA; Qiagen) matrix (resin) interacts with four out of the six binding sites in the nickel ion coordination sphere, therefore two binding sites are left free to bind to the $(His)_6$ protein. The resin was saturated with the cleared lysate (Fig. 7: Cleared lysate) containing the $(His)_6$ protein. The presence of high levels of Tris-HCl or sodium chloride (500 mM) and low levels of imidazole (20 mM) in the binding buffer reduces the number of proteins that bind non-specifically to the resin. The presence of protein in the washes is likely due to the weak binding of the protein to the resin because of resin over-saturation (Fig. 7: Wash 1 and 2). The presence of high levels of imidazole (500 mM) in the elution buffer allowed for elution of the protein, whereby the protein was competitively eluted in the presence of 500 mM imidazole (Fig. 7: Elution). The eluates were buffer exchanged, concentrated and stored in aliquots at -80°C. Sufficient amounts of SeDXR were purified for enzyme kinetics analysis and functional analysis.

Due to the problems that arose with the expression of *P. falciparum* DXR and *M. tuberculosis* DXR as soluble proteins (Fig. 6B, C and D), alternative approaches were explored. Possible solubilization and refolding techniques such as slow dilution and dialysis were conducted in attempt to purify these proteins. After inducing expression with IPTG, the bacteria were lysed and the insoluble pellet (inclusion bodies) were retained. The insoluble protein samples were solubilized in a buffer containing 1 % sarkosyl and dialyzed against TBS. Although the pellets appeared to a be dissolved completely in the sarkosyl solution, a prominent white precipitate formed during the dialysis, suggesting that the proteins remained denatured and aggregated as sarkosyl was removed. Low concentrations of *P. falciparum* and *M. tuberculosis* DXR were present in the soluble dialysed samples, but when the samples were applied to nickel-NTA columns to purify them, DXR could not be detected in the eluates (Fig. 8A, B). As a second approach, the sarkosyl solutions were diluted dropwise into a large volume of TBS buffer (1:20 dilution) (Fig. 8C, D). Low levels of *P. falciparum* DXR was present in the diluted sample lane. When the sample was applied to a Ni-NTA column in attempt to purify and concentrate the protein, only a low concentration of *P. falciparum* DXR could be discerned in the eluate (Fig. 8C: Elution). The same approach was applied to the *M. tuberculosis* DXR sarkosyl solution, but no protein could be detected in any of the samples (Fig. 8D).

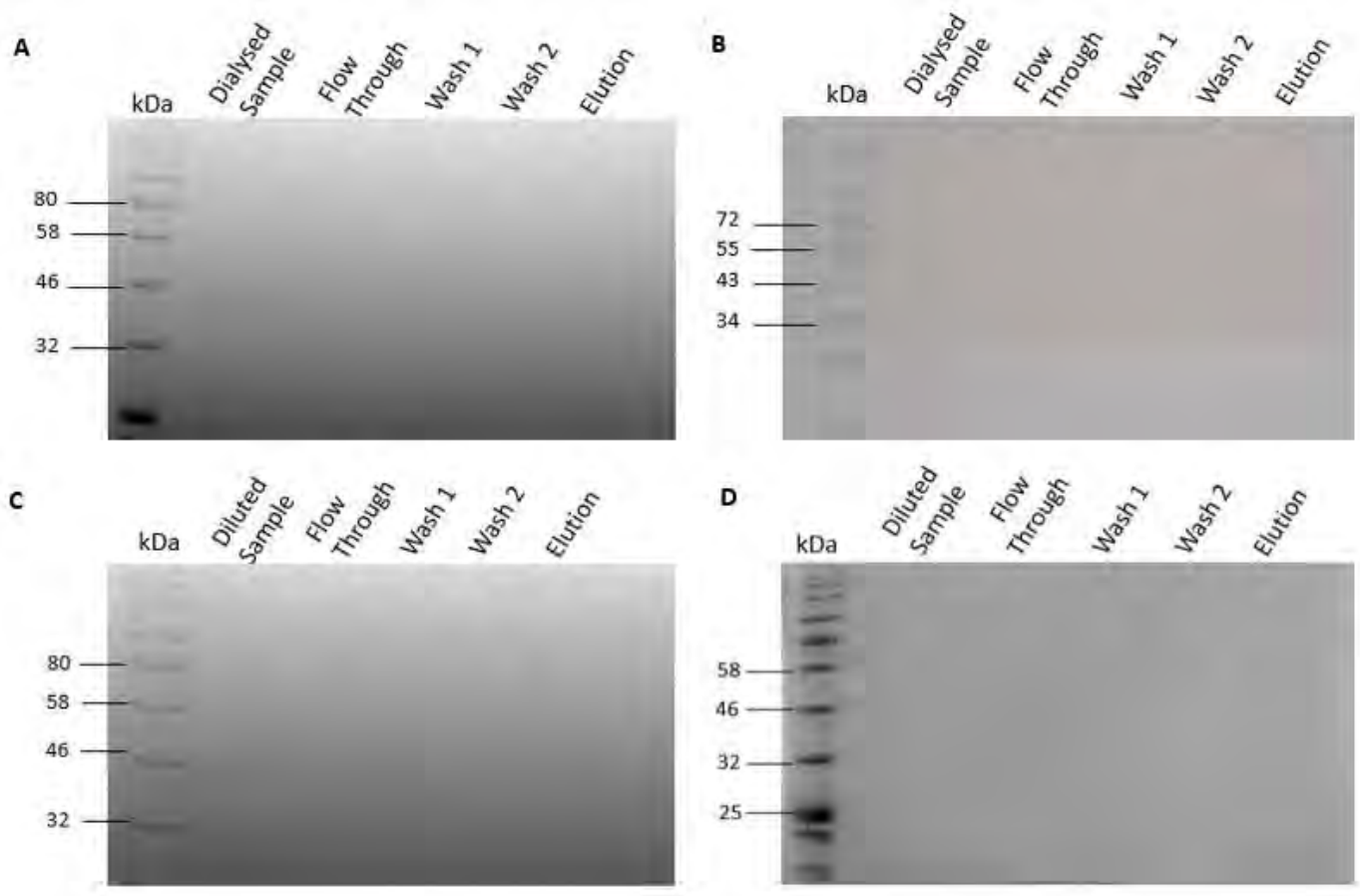

Figure 8: Attempted *Plasmodium falciparum* and *Mycobacterium tuberculosis* 1-deoxy-D-xylulose 5-phosphate reductoisomerase purification.

The induced insoluble *P. falciparum* DXR and *M. tuberculosis* DXR samples were solubilized in 1% sarkosyl, dialyzed and run through the Ni-NTA column (A, B). As an alternative refolding approach, the induced insoluble *P. falciparum* DXR and *M. tuberculosis* DXR samples were also solubilized in 1% sarkosyl, diluted in TBS buffer, and run through the Ni-NTA column (C, D). The molecular weight markers [Color Prestained Protein Standard, Broad Range; New England Biolabs (A, C, D), Blue Prestained Protein Standard; New England Biolabs (B)] indicated in kDa were run alongside the 1-deoxy-D-xylulose 5-phosphate reductoisomerase dialysed/diluted samples, column flow-through, wash 1, wash 2 and eluate samples on a 12% SDS-PAGE gel stained with Coomassie staining solution (A, C and D) or analysed by western blotting with HisDetector (B). The low protein concentration in the soluble dialysed samples is due to the formation of protein precipitates that visibly formed during dialysis.

From large scale protein purification, the SeDXR was successfully purified (Fig. 7). However, initial attempts to refold the PfDXR and MtDXR from insoluble inclusion bodies and purify them

by Ni-NTA chromatography were not as successful (Fig. 8A-D). The purification of the latter two proteins was not further pursued, therefore kinetic and functional analysis was limited to SeDXR.

2.3.4. NADPH-Dependent and Resazurin Reduction Assays

The activity of the purified recombinant *S. enterica* 1-deoxy-D-xylulose 5-phosphate reductoisomerase (DXR) is depicted in Fig. 9. For the NADPH-dependent enzyme assay, the reaction mixture was set up in 96-well plates and contained 1X TBS (40 mM Tris, 100 mM NaCl, pH 7.5), NADPH (0.3 mM) and DOXP (0.3 mM). This was incubated with *S. enterica* DXR for 1 hour at 37°C and the absorbance was measured at 340 nm. For the Resazurin reduction assay, the same reaction conditions were used, followed by addition of 5 µl resazurin into the 100 µl (29.5 µM final resazurin concentration) reaction mixture and incubation for 30 minutes at 37°C. The fluorescence (560/590 nm) was measured, which reflects the concentration of resorufin produced due to the reduction of resazurin by NADPH. Each experiment contained a control (reaction mixture without DXR). These assays were conducted in parallel. Reaction mixtures that were incubated with the *S. enterica* DXR show a decrease in the levels of NADPH (Fig. 9A) and resorufin (Fig. 9B). This suggested that the purified *S. enterica* DXR was enzymatically active, catalyzing the conversion of DOXP to MEP and consuming NADPH in the process.

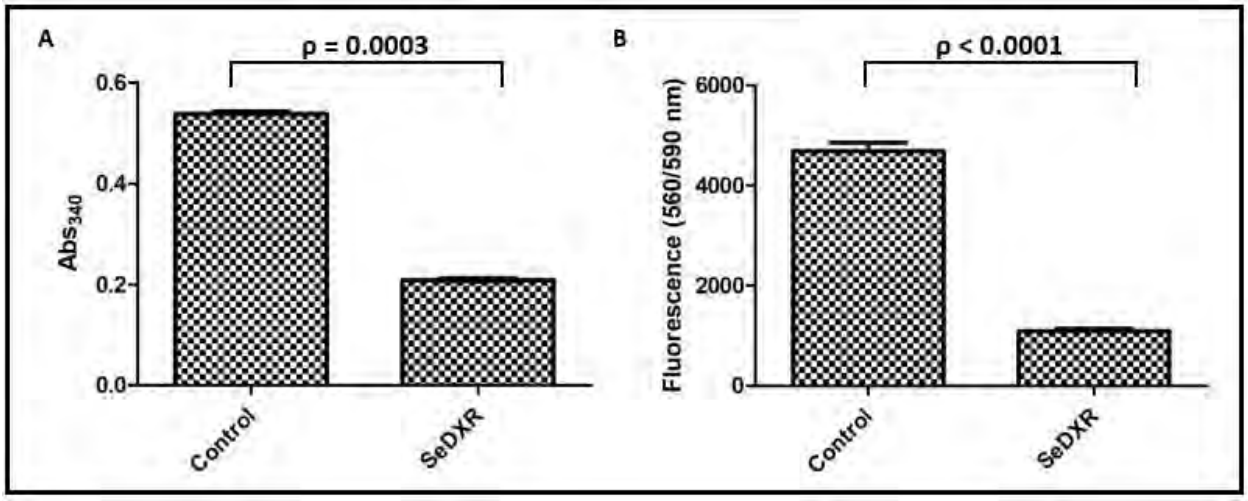

Figure 9: *Salmonella enterica* 1-deoxy-D-xylulose 5-phosphate reductoisomerase activity.

S. enterica DXR was incubated at 37°C in assay buffer containing DOXP and NADPH for 1 hour and the absorbance (340 nm) was measured (A). Alternatively, resazurin was added, incubated for 30 minutes at 37°C and the fluorescence was measured at an excitation and emission wavelength of 560 nm and 590 nm, respectively (B). Each bar represents the mean reading obtained from four technical repeat wells (n=4) and error bars indicate standard deviation.

2.3.5. Kinetic Parameters of *S. enterica* DOXP Reductoisomerase

A characterization of *S. enterica* 1-deoxy-D-xylulose 5-phosphate reductoisomerase (DXR) has not yet been reported in the literature. The kinetic parameters for *S. enterica* DXR were determined using the NADPH-dependent enzyme assay. The kinetic parameters were determined using a final enzyme concentration of 0.66 µM, NADPH concentration of 0.3 mM and a DOXP substrate concentration range of 38 – 900 µM. Reactions were incubated for an hour, this was blanked with a control reaction without enzyme. The absorbance was measured at 340 nm. The Michaelis-Menten and Lineweaver-Burk plots for *S. enterica* DXR are shown in Fig. 10 and were generated using GraphPad Prism (v. 5.02) using the absorbance values obtained. A K_m value of 464.9 µM and a V_{max} value of 0.194 µmol/min/mg. A specific activity of 0.126 µmol/min/mg ± 0.00141 µmol/min/mg was obtained. Specific activity (µmol/min/mg) was calculated by using the average absorbance at 340 over the time of reaction (ΔA/min) multiplied by the volume of reaction and divided by the total protein mass.

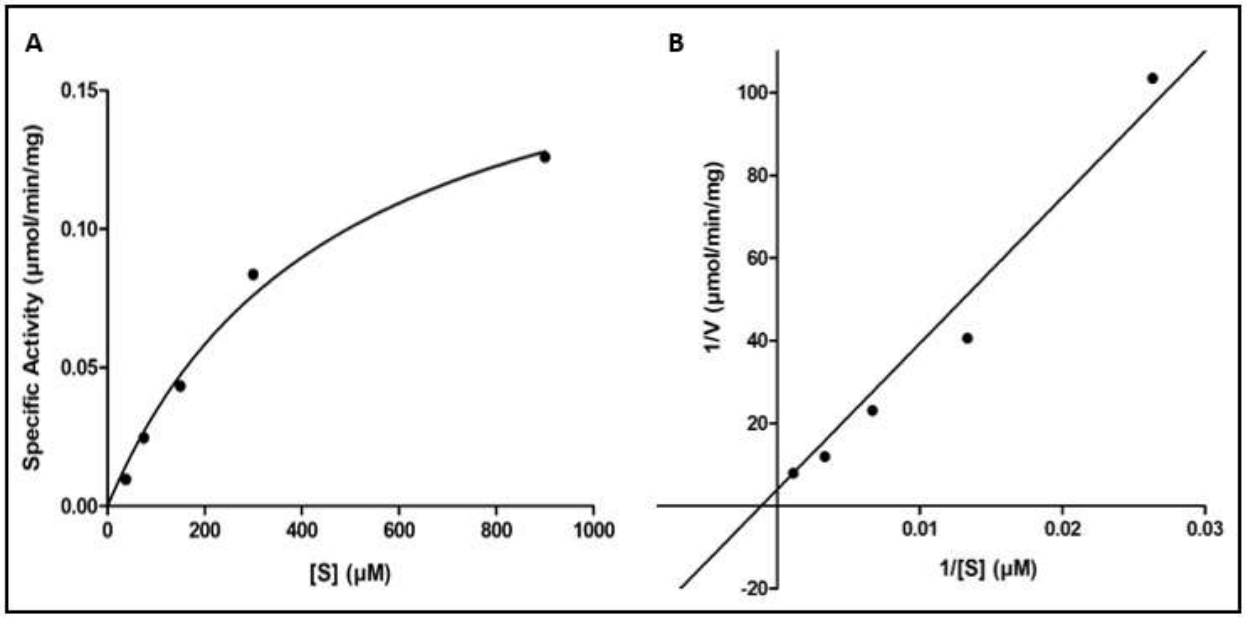

Figure 10: Michaelis-Menten and Lineweaver-Burk Plots for *Salmonella enterica* 1-deoxy-D-xylulose 5-phosphate reductoisomerase.

The oxidation of NADPH was monitored at 340 nm using the NADPH-dependent enzyme assay. The Michaelis-Menten plot (A) for *S. enterica* 1-deoxy-D-xylulose 5-phosphate reductoisomerase and the reciprocal Lineweaver-Burk plot (B). The kinetic parameters were calculated, with a K_m value of 464.9 µM and a V_{max} value of 0.194 µmol/min/mg. The Michaelis-Menten and Lineweaver-Burk plots were generated using GraphPad Prism 5.02.

2.4. CONCLUSION

Heterologous expression and purification of $(His)_6$ *S. enterica* DXR was successful. The native purified *S. enterica* DXR was shown to be active using the NADPH-dependent enzyme assay with a K_m value of 464.9 µM, a V_{max} value of 0.194 µmol/min/mg and a specific activity of 0.126 ± 0.00141 µmol/min/mg. The purification of *P. falciparum* DXR and *M. tuberculosis* DXR was unsuccessful due to expression of the proteins as insoluble inclusion bodies, despite attempts to solubilize and refold the proteins, combined with affinity purification. These enzymes were found to be insoluble when the solubilizing agent (sarkosyl) was removed by dialysis/dilution, and as a result precipitated in the solution during the refolding strategies used. The purification of the

enzymes was not further pursued beyond the dialysis and dilution methods used here and enzyme assays were not possible.

Possible methods that could be used to improve protein solubility in *E. coli* bacteria may include modifying the expression temperature and IPTG concentrations. The use of high expression temperatures, high concentration of inducer and expression under strong promoter systems results in the over-expression of the protein of interest at a high translational rate (Singh *et al.*, 2015). However, this process exhausts the bacterial protein quality control and the misfolded protein molecules aggregate resulting in inclusion bodies (Singh *et al.*, 2015). Initially, there were attempts to over-express these proteins by adjusting protein expression and induction conditions. This was done by using temperature lower than 37°C when inducing protein expression as 37°C was initially used, a lower concentration the inducer, IPTG, was used in attempt to improve the solubility of the protein (Appendix E). From several attempts to over-express these proteins as soluble and fully functional, formation of inclusion bodies was the only result.

Alternative strategies for solubilization and purification of denatured proteins include solubilizing the inclusion bodies using guanidinium hydrochloride or urea, rather than the detergent sarkosyl used here. Alternative refolding protocols may include altering the rate of protein dilution into refolding buffer, using on-column refolding (binding the proteins to affinity columns in a denatured state and washing/eluting in refolding buffers) and/or altering the buffer composition e.g. pH, ionic strength and adding redox buffers (Burgess, 2009). A study by Patra *et al*. (2000) suggests that proteins in inclusion bodies have native-like secondary structures and that bioactive protein can be recovered when these inclusion body proteins are solubilized while retaining their native-like secondary structure, therefore this structure of the inclusion body protein has to be protected. The charge distribution of the protein molecule can be changed by changing the pH which affects protein stability and could potentially unfold the native protein, therefore alkaline pH is best used for solubilizing inclusion bodies without disturbing the native-like secondary structures of the proteins, which prevents pH-induced unfolding of the proteins (Patra *et al*., 2000).

Resazurin conversion is mediated by the reducing environment of cells, therefore, the reducing agent NADPH should also be able to convert resazurin to resorufin. The results in this study suggest that it is equivalent to absorbance at 340 nm in detecting *S. enterica* DXR enzyme activity (although resazurin is more sensitive if there is limited fluorescence quenching). The two assays, NADPH-dependent enzyme and resazurin reduction assay, could be used to find compounds that display inhibitory activity against *S. enterica* DXR.

CHAPTER 3: SCREENING OF NOVEL COMPOUNDS FOR 1-DEOXY-D-XYLULOSE 5-PHOSPHATE REDUCTOISOMERASE INHIBITION ACTIVITY

3.1. INTRODUCTION

The growing resistance in bacterial pathogens to first-line and second-line antibiotics is a great threat to public health (Lewis *et al*., 2004; Jose *et al*., 2017). Therefore, there is a need for new therapies to combat these pathogenic organisms (Jose *et al*., 2017). The discovery of novel bacterial targets will aid in developing new drugs for treatments; the advances in processes in drug discovery aim to identify new small molecules that will play a role in selectively modulating the functions of these bacterial targets (Schenone *et al*., 2013; Jose *et al*., 2017). These small molecules will serve as starting points in the development of potent drugs displaying inhibitory activity against bacterial targets, and potentially be part of therapies for combatting diseases.

Recent advances in organic chemistry and the understanding of many aspects of physiology and biochemistry has evolved rational drug design, and these advances suggest that defined biological sites can be exploited by drugs (Grover, 2015). The concept that a chemical that can bind to the site of a specific pharmacological target that has been identified for a given disease is essential for the development of drugs (Mandal *et al*., 2009). Innovations in biochemical and biophysical techniques include X-ray crystallography, magnetic resonance imaging to identify specific drug targets, development of chemical libraries and technical advances in high-throughput screening, has aided this concept (Grover, 2015). The drug discovery process has also been revolutionized by advances in bioinformatics, whereby the high costs and time-consuming processes associated with drug discovery have been reduced (Jiang and Zhou, 2005; Saha *et al*., 2013).

The subsequent step in the drug discovery process, once a drug target has been validated, is the identification of small molecules that modulate the functions of the drug target (Carnero, 2006; Schenone *et al*., 2013). These small molecules can be agonists or antagonists for receptors, activate

or inhibit enzyme activity and open or close ion channels (Carnero, 2006). Molecules that display favourable results in modulating drug targets can potentially become clinical candidates with enough biological activity, providing safety and possessing drug-like properties so that they can reach human testing (Mohs and Greig, 2017).

A variety of screening technologies can be applied for identifying hit molecules, referred to as compounds that exhibit the desired activity in the screening process Among these is high-throughput screening (HTS) (Bleicher *et al*., 2003; Hughes *et al*., 2011). High-throughput screening (HTS) is a process whereby a large number of biological modulators and effectors are screened and assayed against known and selected drug targets (Szymański *et al*., 2012). At present, HTS is the most widely applicable technology for drug discovery programmes and has emerged as one of the most important strategies in identifying novel drug targets. Compounds identified using this technology are not always suitable for further medicinal chemistry exploration (Bleicher *et al*., 2003; Visser *et al*., 2011). However, a variety of drug candidates and marketed drugs have resulted from hits that were generated by HTS technology and this demonstrates the potential success of using HTS technology for developing drugs (Bleicher *et al*., 2003).

An entire compound library developed using chemometric analysis software and molecular binding modelling is screened directly against the drug target in HTS technology (Fox *et al*., 2006). Different types of libraries, such as combinatorial chemistry, genomics, protein and peptide libraries can be screened using HTS (Szymański *et al*., 2012). The use of target-focused compound libraries is increasingly popular in drug discovery. These compounds are designed to interact with protein targets such as kinases, G-protein coupled receptors (GPCRs), nuclear hormone receptors and ion channels (Harris *et al*., 2011; Dandapani *et al*., 2012). Such libraries allow for the screening of fewer compounds to obtain hit compounds and higher hit rates are observed in the screening compared to the screening of diverse compound collections (Harris *et al*., 2011).

The Pathogen Box, used here in this study, is a collection of 400 drug-like compounds that have been discovered to have activity against a number of pathogenic organisms (Duffy *et al*., 2017; Nugraha *et al*., 2019; Veal, 2019). These organisms cause diseases such as trypanosomiasis, filariasis, leishmaniosis, dengue virus, sleeping sickness, malaria and tuberculosis (Nugraha *et al*.,

2019; Veal, 2019). The Medicines for Malaria Venture (MMV) foundation (Geneva, Switzerland) has provided the Pathogen Box, offering researchers worldwide free access to the compounds (Nugraha *et al*., 2019). The collection contains 26 reference compounds that have well-characterised antimicrobial activity and/or are available on the market as drugs for microbial diseases (Maccesi *et al*., 2019). The fact that the compounds are bioactive – have previously been found to have activity against organisms – means that the compounds have privileged structures, i.e. are capable of binding to and inhibiting target proteins. The compounds display low toxicity for mammalian cells and reasonable levels of cytotoxicity for drug discovery programs (Mayer and Kronstad, 2017). The Pathogen Box is provided with each compound's details including its structure, trivial name, salt form and cLogP (this supporting information is found in an Excel spreadsheet) (Spalenka *et al*., 2018).

Alternatively, compounds can be screened against the drug target in a more complex assay system, for example a cell-based assay in which the activity of the compounds depends on the target. Secondary assays would be required for confirmation of the compounds' site of action (Fox *et al*., 2006). The hit molecules generated from HTS undergo a comprehensive assessment so that they could be progressed into lead series. This includes chemical integrity, synthetic accessibility, functional behavior, structural-activity-relationships (SAR), bio-physicochemical and absorption, distribution, metabolism and excretion (ADME) properties (Bleicher *et al*., 2003). Firstly, the compounds are tested in a primary screen, this is less quantitative than biological assays (Szymański *et al*., 2012). Secondly, the hits from the primary screen will be tested in a secondary screen and calculations of their half-maximal inhibitory concentration (IC_{50}) will be performed.

To compare different inhibitors of a single enzyme, the IC_{50} is used as a measure of the efficacy of the compounds (Caldwell *et al*., 2012). It indicates the concentration of a specific inhibitor that is required so that a given biological activity or process can be inhibited by half (Aykul and Martinez-Hackert, 2016). Approaches that are used for IC_{50} determination of pharmacological compounds include assays that use whole cell systems (Aykul and Martinez-Hackert, 2016). Inhibitors that have small IC_{50} values interact more effectively compared to inhibitors with large IC_{50} values (Caldwell *et al*., 2012). The data obtained during the testing for IC_{50} determination involves dose-response assays, whereby the enzyme is incubated with serial dilutions of test

compounds, dose-response plots of enzyme activity (or inhibition) vs. log of the compound concentrations are prepared and IC_{50} values derived from the resulting sigmoidal curves by non-linear regression analysis (Sebaugh, 2010). It may require manual calculation, usually with the use of spreadsheet programs, however, as an alternative commercially available statistical software (e.g. GraphPad Prism from GraphPad Software) or the drift package for the R statistical environment can be used for performing the same calculations (Nevozhay, 2014).

This section aimed to:

- Screen novel compounds (from the Pathogen Box library) using FR900098 as a positive control compound to find compounds that can inhibit *S. enterica* DXR
- Confirm the enzyme inhibition activity of possible hit compounds
- Determine the IC_{50} of the hit compounds along with FR900098

3.2. EXPERIMENTAL PROCEDURE

3.2.1. 1-Deoxy-D-xylulose 5-phosphate Reductoisomerase Inhibition Assay with FR900098

The DXR reaction was prepared in a 96-well plate as described in Section 2.2.4.1., except that 50 µM FR900098 was included. The FR900098 (Sigma-Aldrich) was added from a 2.5 mM stock in DMSO, prior to the addition of the enzyme to initiate the reaction. Controls included a reaction without the inhibitor and one without enzyme. The plate was incubated at 37°C for 1 hour. The decrease in absorbance at 340 nm was measured in the plate reader at 37°C. Alternatively, 5 µl resazurin from a 0.59 mM stock in PBS was added to the 100 µl reaction mix, followed by a 30 minute incubation 37°C and fluorescence (Exc_{560}/Emm_{590}) was measured in the plate reader. For IC_{50} determination, the same procedure was followed, except that the reactions included five-fold serial dilutions (0.016 - 10 µM) of FR900098. The IC_{50} values were determined by non-linear regression analysis of % enzyme activity vs. log (inhibitor concentration) plots using GraphPad Prism (v. 5.02). Refer to Appendix F for % enzyme activity calculations.

3.2.2. Screening of Novel Compounds

Compounds (50 µM final concentration) from the Pathogen Box (10 mM stocks in DMSO) were incubated with 1X TBS (40 mM Tris, 100 mM NaCl, pH 7.5) with $MnCl_2$ (10 mM), NADPH (0.3 mM), DOXP (0.3 mM) and DXR enzyme (0.126 µmol/min/mg) in a 96 well plate at 37°C for 1 hour. The decrease in absorbance at 340 nm was measured in the SpectraMax® M3 360 multi-well plate reader. Hit compounds displaying ≥ 70% enzyme inhibition (Refer to Appendix F for calculations) were subjected to confirmatory assays using the same procedure, except that incubations were carried out in triplicate wells per compound, rather than single wells as was done in the initial screen. IC_{50} values for the two best confirmed hits (diethylcarbamazine and MMV228911) were carried out by dose-response assays as described above, except that the reactions included two-fold serial dilutions of the compounds.

3.3. RESULTS

3.3.1. The 1-Deoxy-D-xylulose 5-phosphate Reductoisomerase Inhibition Assay with FR900098

Studies have shown that the FR900098 inhibitor has antibacterial and antimalarial activity by inhibiting 1-deoxy-D-xylulose 5-phosphate reductoisomerase (DXR) of the isoprenoid synthesis pathway of various organisms (Wiesner *et al*., 2016). However, the sensitivity of *S. enterica* or its DXR enzyme to this compound has not been reported. To assess the inhibition of the enzyme by FR900098, the NADPH-dependent enzyme assay and the resazurin reduction assay were both used. Reaction mixtures containing the *S. enterica* DXR enzyme with/without FR900098 inhibitor (50 µM final concentration) were incubated in a 96-well plate for 1 hour at 37°C and the absorbance (340 nm) was measured. Other reaction mixtures containing the same components followed by the addition of 5 µl resazurin stock to a 100 µl reaction (29.5 µM final resazurin concentration) were incubated in a 96-well plate for 30 minutes at 37°C and the fluorescence (560/590 nm) was measured. Higher levels of NADPH were obtained in the presence of FR900098, suggesting that FR900098 was successful at inhibiting *S. enterica* DXR (Fig. 11). To confirm the inhibition of SeDXR by FR900098, both assays were repeated with additional controls. Control reactions (incubations without SeDXR and FR900098, as well as incubations without SeDXR) contained high levels of NADPH (Fig. 12). By comparison, much lower levels of NADPH were obtained in the presence of *S. enterica* DXR (SeDXR) in the absence of FR900098. Higher NADPH levels remained in the presence of both *S. enterica* DXR and FR900098.

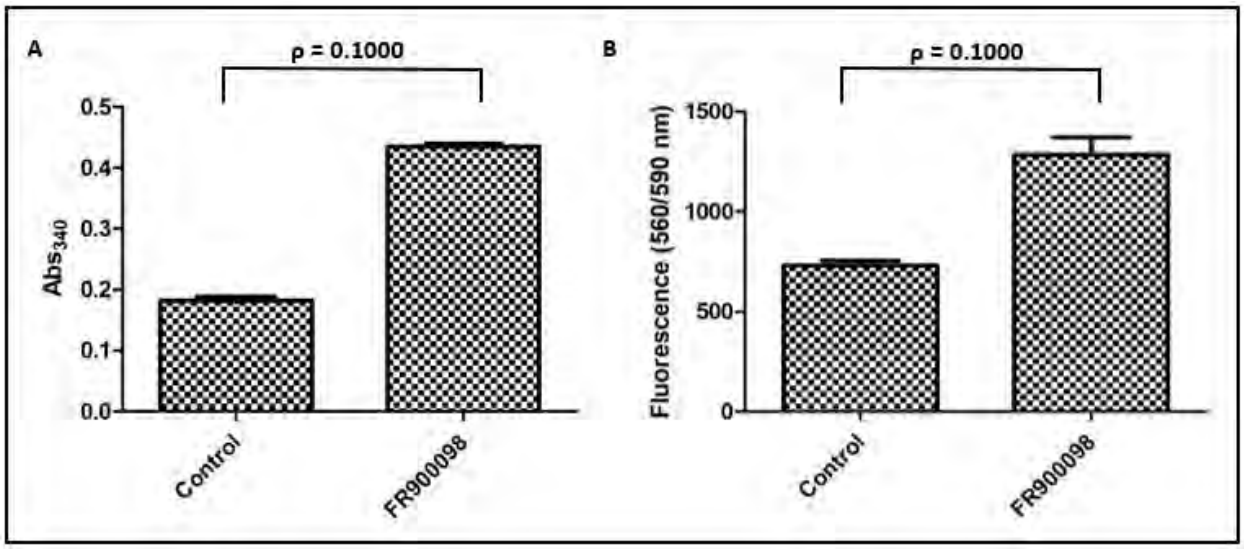

Figure 11: FR900098 inhibits *Salmonella enterica* 1-deoxy-D-xylulose 5-phosphate reductoisomerase.

Reactions containing *S. enterica* DXR were incubated with the FR900098 inhibitor (50 μM) and without FR900098 (control) for 1 hour and the absorbance was measured at 340 nm (A), or resazurin was added to the reaction after a 30 minute incubation and the fluorescence (560 nm/590 nm) was measured (B). Each bar represents the mean and standard deviation of readings obtained from 3 replicate wells (n = 3). The p-values derived by a non-parametric t-test indicating the statistical significance of the difference between the enzyme reactions with and without FR900098 are indicated above the relevant bars.

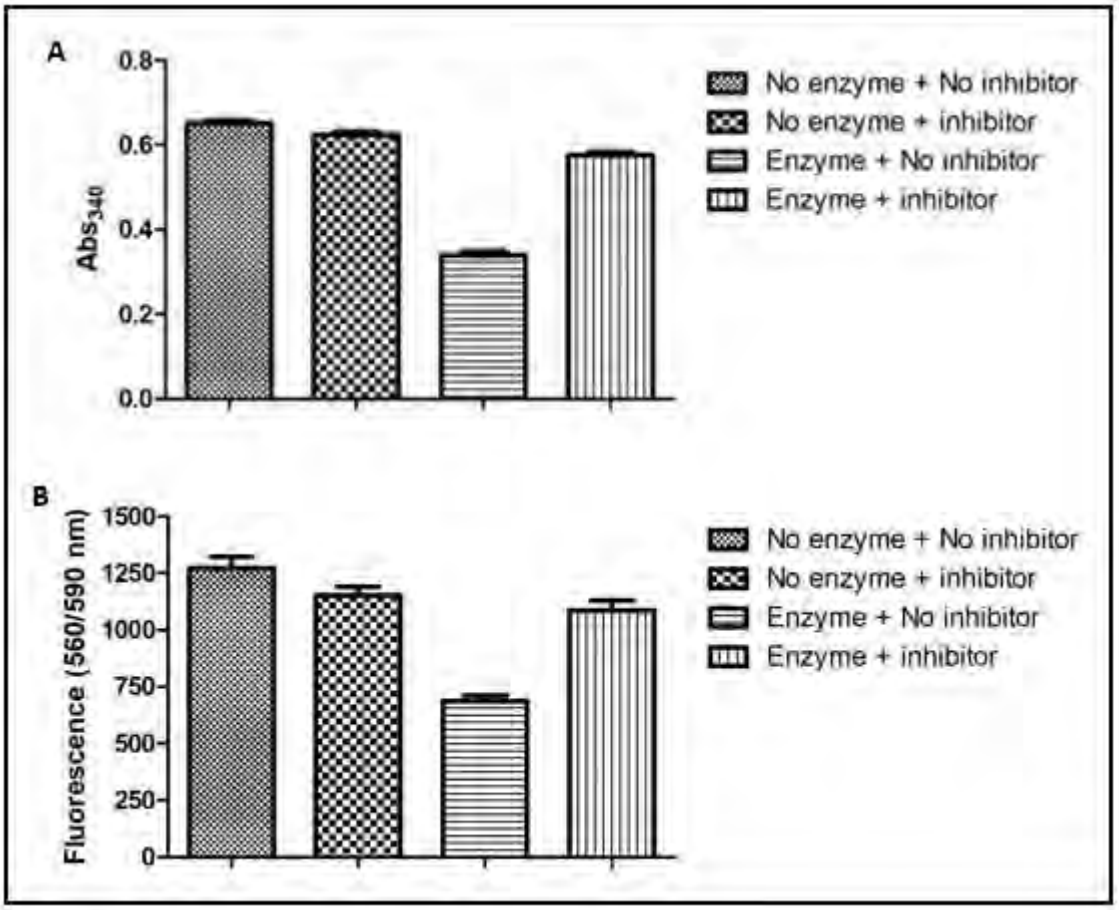

Figure 12:The inhibitory effect of FR900098 on *Salmonella enterica* 1-deoxy-D-xylulose 5-phosphate reductoisomerase.

The NADPH-dependent enzyme assay (A) and resazurin reduction assay (B) were performed with/without the *S. enterica* DXR enzyme and with/without 50 μM FR900098 inhibitor. The reactions were incubated for 1 hour at 37°C and the absorbance was measured at 340 nm (A), or resazurin was added to the reaction after a 30 minute incubation at 37°C and the fluorescence (560 nm/590 nm) was measured (B).

3.3.2. Compound Screening

Studies show that compounds from the Pathogen Box library have activity against neglected tropical diseases and their activity against *S. enterica* 1-deoxy-D-xylulose 5-phosphate reductoisomerase (DXR) have not yet been reported. To assess the inhibitory activity of these drug-like compounds against *S. enterica* DXR (SeDXR), the NADPH-dependent enzyme assay was performed. Reaction mixtures with the *S. enterica* DXR enzyme and Pathogen Box

compounds (50 μM final concentration) were incubated in a 96-well plate for 1 hour at 37°C and the absorbance was measured at 340 nm. Control reactions included a positive control (with enzyme, without compounds), a negative control (without either compounds or enzyme) and an FR900098 control (with enzyme and FR900098). The % enzyme inhibition displayed by each compound was calculated using the absorbance readings that were obtained (Refer to Appendix F for calculations). A cut-off of 70% inhibition and above was chosen to select compounds that are likely to have low micromolar IC_{50} values, without disregarding compounds that have moderate activities but could be useful scaffolds for further optimization, particularly given the relatively small size of the Pathogen Box library. A significant number of compounds were found to be active against *S. enterica* DOXP reductoisomerase, with a wide range of % inhibition (0 – 174 % inhibition). The presence of compounds displaying >100% inhibition suggests that there may have been a disparity between the NADPH concentrations in the negative control (incubations without enzyme) used to establish the baseline of 100% inhibition, and the reaction mixtures that were used to assess the compounds. Nonetheless, it still allowed the identification of the most prominent inhibitors in the Pathogen Box collection and comparison of the relative inhibitory activity of the compounds.

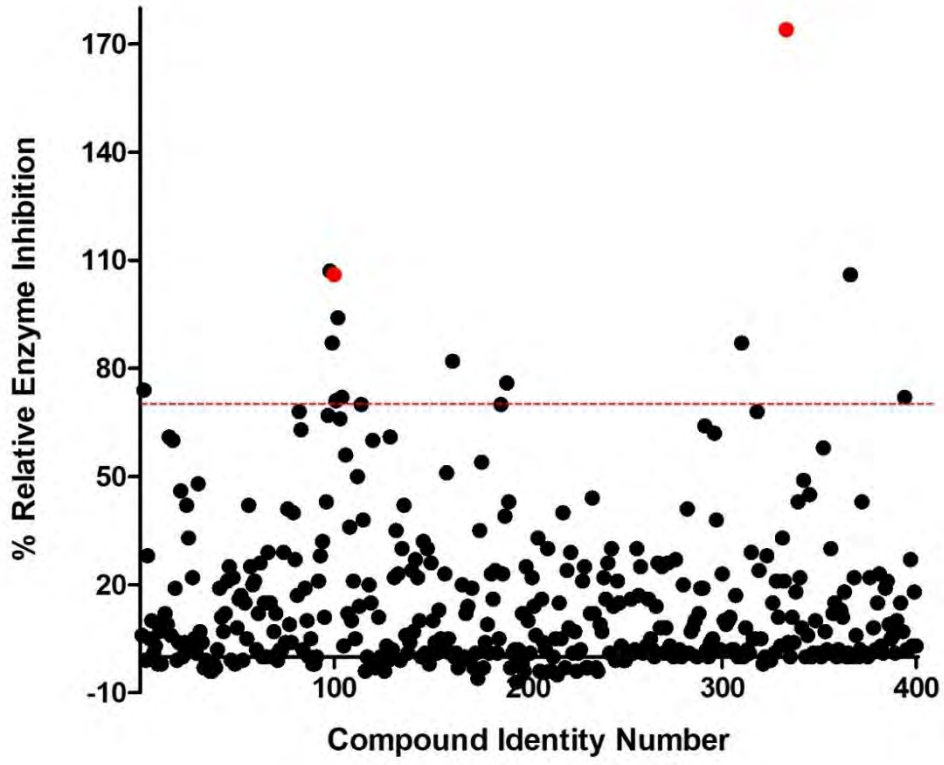

Figure 13: % Relative Enzyme Inhibition exhibited by the Pathogen Box compounds screened against *Salmonella enterica* 1-deoxy-D-xylulose 5-phosphate reductoisomerase.
Compounds (400) from Pathogen Box library were incubated with *S. enterica* DXR and the absorbance (340 nm) was measured. The % inhibition exhibited by each compound was determined. Compound relative enzyme inhibition activities are indicated by the dots, the cut-off for selecting compounds for subsequent confirmation assays is 70% inhibition shown by the red dotted line. The two compounds that emerged as the best hits in subsequent confirmation assays are indicated by the red dots.

3.3.3. 1-Deoxy-D-xylulose 5-phosphate Reductoisomerase Assay: Hit Confirmation

To further asses the inhibitory activities of the hit compounds obtained in the initial screen, they were retested in order to confirm this desired activity, while FR900098 was used as a control compound (not shown). The compounds (50 µM) were incubated with *S. enterica* DXR for an hour and the NADPH absorbance (340 nm) determined, while a control without compounds was

included. Two compounds, diethylcarbamazine and MMV228911, exhibited the best inhibitory activity against *S. enterica* DOXP reductoisomerase (Appendix H), emerging as the best hits. High levels of NADPH were present in reactions containing the two compounds compared to reactions without the compounds, suggesting strong inhibition of *S. enterica* DXR activity (Fig. 14).

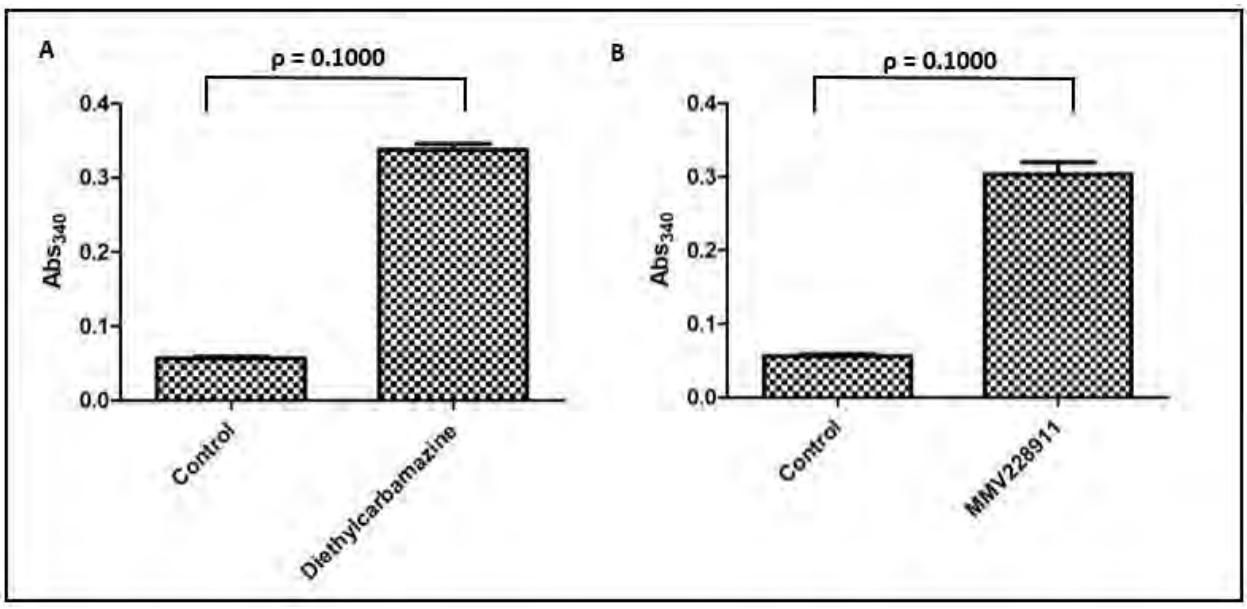

Figure 14: Novel inhibitors of *Salmonella enterica* 1-deoxy-D-xylulose 5-phosphate reductoisomerase.

S. enterica DXR was incubated with 50 µM diethylcarbamazine and MMV228911, compounds from the Pathogen Box library, for 1 hour at 37°C and the absorbance was measured at 340 nm. The compound relative enzyme inhibition activities are indicated above. A control without the compounds was included. The p-values derived by a non-parametric t-test indicating the statistical significance of the difference between the control and reaction with the compounds are indicated above the relevant bars.

3.3.4. 1-Deoxy-D-xylulose 5-phosphate Reductoisomerase Inhibition Assay: IC_{50} Determination

To obtain a more accurate indication of the inhibitory activity of a compound, dose-response assays should be conducted. In this study, dose-response assays were conducted for FR900098, diethylcarbamazine and MMV228911 (compound structures shown in Fig. 15). Reaction mixtures containing *S. enterica* DXR were incubated with serial dilutions of FR900098 (0.016 – 10 µM) and the two compounds (0.390625 – 100 µM) in 96-well plates for 1 hour and the absorbance (340 nm) was measured. To compensate for the effect of FR900098 and compounds described above, wells not containing NADPH were used as background controls and subtracted from readings obtained in wells containing FR900098/compounds and enzyme. These absorbance values were converted to percentage DXR activity. Dose-response graphs (% SeDXR activity against log [Compound]) were generated using GraphPad Prism 5.02 software (Fig. 16A, B, C). Using non-linear regression, the IC_{50} (concentration of the inhibitor required to reduce the rate of the enzymatic reaction by 50%) values were determined by GraphPad Prism 5.02. The IC_{50} values of FR900098, diethylcarbamazine and MMV228911 were 1.23 µM, 2.17 µM and 6.86 µM respectively.

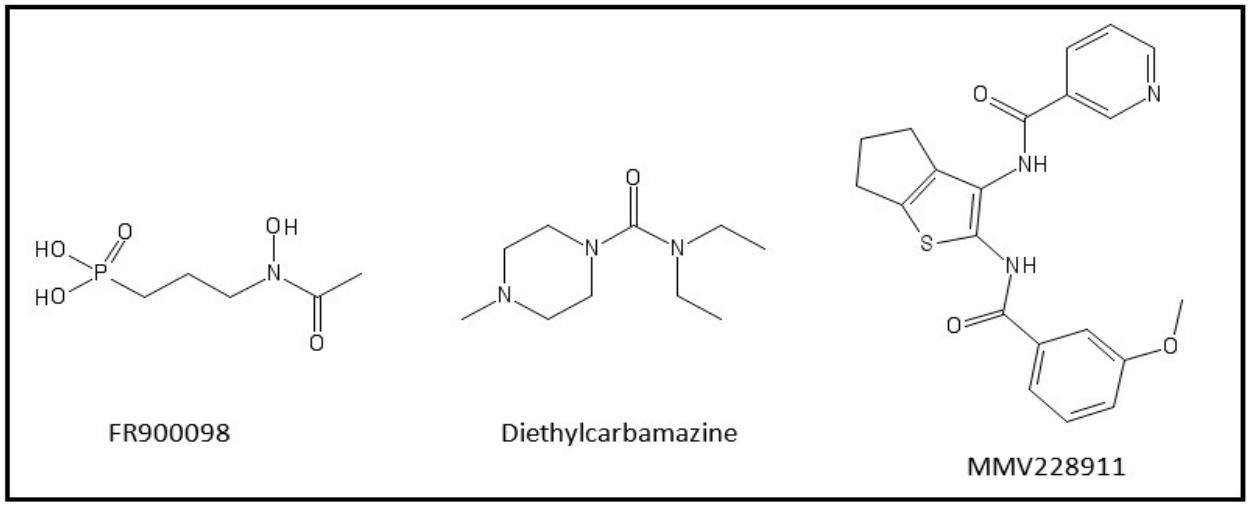

Figure 15: Structures of the Compounds.
The chemical structures of FR900098 (adapted from Wiesner *et al*., 2016), diethylcarbamazine and MMV228911 (adapted from Veale, 2019) compounds which display strong inhibitory activity against *S. enterica* DXR

FR900098 binds to the catalytic domain of DXR, preventing the binding of the DOXP substrate from binding to the enzyme (Umeda *et al*., 2011). FR900098 contains a hydroxamate moiety, (bearing functional group RCNR') that chelates with the divalent metal cation and a phosphonate group (negatively charged), which are important in the binding efficacy and inhibition of DXR by FR900098. Diethylcarbamazine and MMV228911 may probably bind away from the catalytic pocket. However, MMV228911 may bind to the NADPH-binding domain suggesting that it would more than likely be very non-selective in where it blocks, resulting in other non-targetted enzymes also being affected.

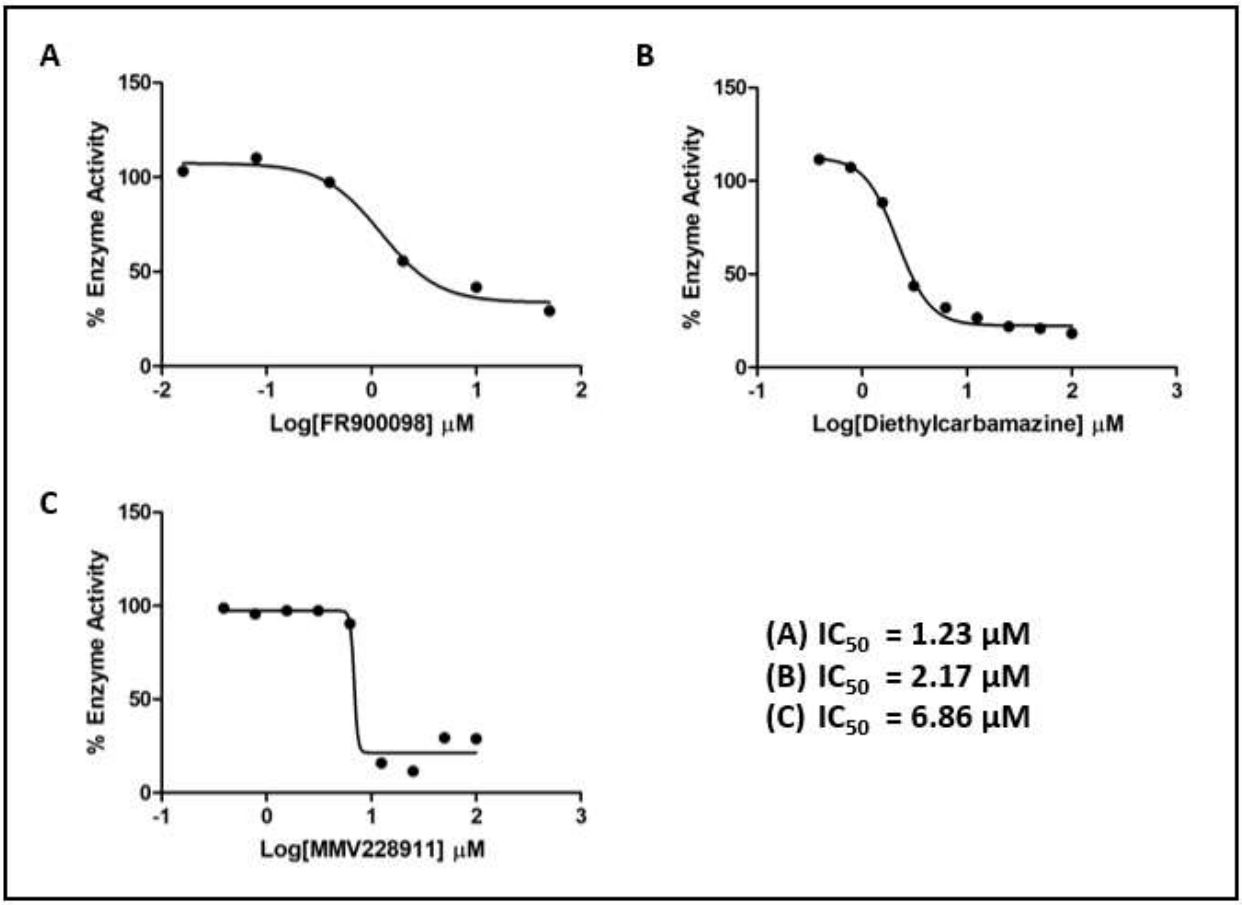

Figure 16: Dose-Response graphs for FR900098, diethylcarbamazine and MMV228911. Serial dilutions of FR900098, diethylcarbamazine and MMV228911 were incubated with a reaction mixture containing *S. enterica* DXR, and the absorbance (340 nm) was measured. The absorbance readings were converted to % enzyme activity and plotted against Log [Compound]. The IC_{50} values were determined by non-linear regression using GraphPad Prism 5.02 software.

3.4. CONCLUSION

To identify inhibitors, *S. enterica* DXR activity was assayed by monitoring the decrease in NADPH, whereby a decrease in NADPH levels (measured as a decrease in Abs_{340}) indicated that the enzyme is catalyzing the conversion of DOXP to MEP. The inhibitory activity of FR900098, the acetyl derivative of the antimicrobial compound fosmidomycin, was tested against *S. enterica* DXR. FR900098 was found to inhibit *S. enterica* DXR with an IC_{50} value of 1.23 µM. In comparison, the reported IC_{50} values of FR900098 in studies using DXR from other organsisms include: 62 nM for *E. coli* DXR (Haemers *et al*., 2006), 18 nM for *P. falciparum* DXR (Giessmann *et al*., 2008), 160 nM for *M. tuberculosis* DXR (Jansson *et al*., 2013), 230 nM for *F. tularensis* DXR (McKenney *et al*., 2012) and 231 nM for *Y. pestis* DXR (Haymond *et al*, 2014). Both fosmidomycin and FR900098 exhibit potent *in vitro* antimalarial activity, however, it has been discovered that FR900098 inhibits malarial growth with twice the efficacy of fosmidomycin due to FR900098's higher affinity for the target enzyme DXR (Wiesner *et al*., 2016). The assay was used for screening the Pathogen Box library in order to identify possible 'hit' compounds, while FR900098 was used as a control compound.

The Pathogen Box, containing 400 compounds which have been found to have inhibitory activity against neglected tropical diseases including trypanosomiasis (African sleeping sickness and Chaga's disease), leishmaniasis, cryptosporidiosis, toxoplasmosis, tuberculosis, malaria, filariasis, schistosomiasis, dengue virus and trichuriasis (Veale, 2019). Provided free of charge on request by the Medicines for Malaria Venture (MMV), it provides a convenient starting point for assessing a small collection of drug-like compounds against new indications/targets. These compounds were screened against the activity of *S. enterica* DXR. Twelve of these compounds displayed the desired activity and were considered as hit compounds. However, upon confirmation of these hit compounds, only two hit compounds namely diethylcarbamazine and MMV228911 demonstrated inhibitory activity against *S. enterica* DXR. With these two compounds displaying a desirable activity, their potency was determined using dose response analysis. The IC_{50} values of diethylcarbamazine and MMV228911 were 2.17 µM and 6.86 µM respectively.

CHAPTER 4: DISCUSSION

1-Deoxy-D-xylulose 5-phosphate reductoisomerase (DXR) is a well-established drug target known for catalyzing the NADPH-dependent reduction of 1-deoxy-D-xylulose 5-phosphate (DOXP) yielding 2-C-methyl-$_D$-erythritol 4-phosphate (MEP) in the second step of the non-mevalonate (MEP) pathway (Murkin *et al*., 2014). This drug target plays a vital role in the production of isoprenoid precursors, required for organism growth and survival, via the non-mevalonate pathway. Despite the non-mevalonate pathway being regarded as an attractive drug target for antimicrobial drug discovery, there are no published reports describing the properties of *Salmonella enterica* DXR. This drug target can be exploited by establishing an assay that can be used for screening large compound libraries for novel inhibitors of *S. enterica* DXR. These compounds could potentially be used for developing anti-Salmonellosis drugs.

The expression and nickel-chelate affinity purification of soluble active *S. enterica* DXR was successfully achieved. The recombinant *S. enterica* DXR had a specific activity of 0.126 ± 0.0014 µmol/min/mg and a K_m and V_{max} of 464.9 µM and 0.194 µmol/min/mg respectively. The K_m and V_{max} values determined deviated from the published *P. falciparum* DXR K_m and V_{max} values which were 67 µM and 1.33 µmol/min/mg respectively (Goble *et al*., 2013), those of *M. tuberculosis* DXR were 47.1 µM and 463.8 pmol/min respectively (Dhiman *et al*., 2005), and those of *E. coli* DXR were 249 µM and 11.04 µmol/min/mg respectively (Goble *et al*., 2013). The K_m values of other organisms including *Zymomonas mobilis*, *Yersinia pestis* and *Francisella tularensis* were 300 µM (Grolle *et al*., 2000), 252 µM (Haymond *et al*., 2014) and 104 µM (Jawaid *et al*., 2009) respectively. Published K_m values therefore range from 47 – 300 µM and V_{max} for the *M. tuberculosis*, *P. falciparum* and *E. coli* DXR enzymes were 0.463, 1.33 and 11.04 µmol/min/mg respectively. The results suggest that the *S. enterica* DXR preparation used in this study had a lower affinity for DOXP and Vmax compared to reported enzymes from other species. Therefore, it would be useful to repeat the kinetic measurements on different batches of purified *S. enterica* DXR to determine whether the kinetic characteristics were peculiar to the particular sample or are reproducible. This would also have to be compared to the wild type enzyme to validate the model established with recombinant His-tagged DXR.

The difficulties of producing soluble *P. falciparum* DXR and *M. tuberculosis* DXR and consequent problems in purifying the recombinant proteins made functional analysis of these proteins not possible. Although the solubilization and refolding of the misfolded recombinant proteins by dialysis and dilution was attempted, *P. falciparum* DXR and *M. tuberculosis* DXR still remained insoluble. The problems encountered with regards to the insolubility of proteins are not uncommon, as it has been reported that the generation of poor quality and misfolded recombinant proteins is one of the challenges of using *E. coli* as a host for protein overexpression (Makhoba *et al*., 2016).

A common problem with the production of some *P. falciparum* proteins in the *E. coli* expression host is due to the mRNA of *P. falciparum* being characterized by high A/T content and multiple lysine and arginine repeats (Baca and Hol, 2000; Birkholtz *et al*., 2008). This tends to result in the early termination of the mRNA translation process, therefore the recombinant *P. falciparum* aggregates, forming insoluble inclusion bodies (Flick *et al*., 2004). A problem with the production of some *M. tuberculosis* proteins in the *E. coli* expression host, mycobacterial genes have a GC content of 65 to 70% while the GC content of *E. coli* genes is 50% (Lakey *et al*., 2000). This has resulted in the production of poor yields of *M. tuberculosis* proteins, even when strong *E. coli* promoters are used, due to the presence of low-usage *E. coli* codons (Lakey *et al*., 2000).

A study by Goble *et al*. (2013) demonstrated the successful overexpression and purification of soluble active *P. falciparum* DXR using codon harmonization, including co-expression with molecular chaperones. Therefore, the coding region of *P. falciparum* DXR was recoded for heterologous expression in *E. coli* by replacing native codons with synonymous codons that have similar usage frequencies in *E. coli* (Angov *et al*., 2008; Goble *et al*., 2013). By using this strategy, the coding region of *P. falciparum* DXR would be designed in such a way that the most frequently used codons in the *E. coli* expression host are included as a way of avoiding problems that occur due to codon bias. Alternatively, codon optimization (using the most frequently used *E. coli* codon for every *P. falciparum* amino acid) has also been used as a strategy for overcoming such problems, however, codon harmonization was found to produce better results, as it permits translation in the heterologous host the same way as the native host, potentially enhancing protein folding, unlike the product of a codon optimized gene (Angov *et al.*, 2008).

Goble *et al*. (2013) also showed that the co-expression of the *E. coli* molecular chaperone, GroEL, with *P. falciparum* DXR enhanced the solubility of the DXR protein. Molecular chaperones have emerged as key players in most cellular processes, which includes facilitating the unfolding, disaggregation, refolding and degradation of existing proteins under physiological and stress conditions, as well as assisting newly synthesized proteins to fold into their stable, globular structure (Pavithra *et al*., 2007; Saibil, 2013). Bacterial molecular chaperones include GroEL, DnaK, HptG, ClpA and ClpB, and these chaperones act in a complex network as a main defence against protein aggregation (Carrió and Villaverde, 2003; Saibil, 2013). A study by Mehlin and co-workers involved the analysis of 1000 genes from *P. falciparum* parasites produced in the *E. coli* expression host system, where only 337 were successfully expressed of which only 63 were reported to be produced as soluble proteins, suggesting that coexpression of proteins of interest with molecular chaperones could enhance production of proteins (Mehlin *et al.*, 2006; Makhoba *et al*., 2016). It would be useful to co-express *E. coli* molecular chaperones with *P. falciparum* DXR as a strategy to enhance the protein's solubility.

A study by Dhiman *et al*. (2005) reported the successful over-expression and purification of *M. tuberculosis* DXR. The *E. coli* expression host BL21(DE3)pLysS was transformed with the pET28a(+) plasmid containing the coding sequence of *M. tuberculosis* DXR (Dhiman *et al*., 2005). The cells were harvested, and the cell debris was removed and the supernatant containing the recombinant protein was loaded onto a Talon Co^{2+} immobilized metal affinity (IMAC) resin (Dhiman *et al*., 2005). Although Ni^{2+} is the most commonly used metal ion in IMAC, interestingly the Co^{2+} ion has been found to be useful in the purification of low expressed histidine-tagged target proteins, also resulting in high purity with good yields of these proteins (Hornsten *et al*., 2012). Henriksson and members cloned, expressed and purified *M. tuberculosis* DXR by use of a pET101D-TOPO vector (Henriksson *et al*., 2007). This plasmid was transfected into *E. coli* TOP10F' cells and Ni^{2+} IMAC was used for purification (Henriksson *et al*., 2007).

The activity of *S. enterica* DXR was detected using the NADPH-dependent enzyme assay and the resazurin reduction assay. The NADPH-dependent enzyme assay is widely used for detecting the activity of enzymes that either consume or produce NADPH. Most studies that have been done on

determining the activity of the DXR enzyme from a number of organisms such as *E. coli*, *P. falciparum*, *M. tuberculosis*, *F. tularensis*, *Y. pestis* and *Z. mobilis*, used this enzyme assay, however, in this study, endpoint measurements of the absorbance (340 nm) of NADPH instead were taken instead kinetic reads (Grolle *et al*., 2000; McKenney *et al*., 2012; Goble *et al*., 2013; Jansson *et al*., 2013; Haymond *et al*., 2014; Armstrong *et al*., 2015). The use of the resazurin reduction assay for *S. enterica* DXR activity has not been reported. Hall *et al*. (2016) suggests that resazurin reduction assay can be used for detecting the activity of enzymes that consume or produce NADPH or NADH and could be a useful substitute method if the reaction contains additional components or compounds that absorb at 340 nm. Resazurin reduction has been used for detecting the dehydrogenase activity of different enzymes including: cellobiose dehydrogenase (CDH) (Blažić *et al*., 2019); Glucose 6-phosphate (G6P) dehydrogenase (Zhu *et al*., 2009); lactate dehydrogenase (LDH) (Bopp and Letteri, 2008).

In this study, FR900098 displayed inhibitory activity against the recombinant *S. enterica* DXR, with an IC_{50} value of 1.23 µM. FR900098 and fosmidomycin have demonstrated inhibition against several Gram-negative bacteria, Gram-positive bacteria and malaria parasites (Haymond *et al*., 2014). These inhibitors bind to the catalytic domain of DXR preventing binding of DOXP substrate (Umeda *et al*., 2011). FR900098 has also been reported to display DXR inhibition in most bacteria and parasites, with reported IC_{50} values including: 62 nM for *E. coli* (Haemers *et al*., 2006); 18 nM for *P. falciparum* (Giessmann *et al*., 2008); 230 nM for *F. tularensis* (McKenney *et al*., 2012); 160 nM for *M. tuberculosis* (Jansson *et al*., 2013); 231 nM for *Y. pestis* (Haymond *et al*, 2014). The IC_{50} values of fosmidomycin against DXRs from pathogens include: 30 nM for *E. coli* (Haemers *et al*., 2006); 32 nM for *P. falciparum* (Giessmann *et al*., 2008); 247 nM for *F. tularensis* (McKenney *et al*., 2012); 80 nM for *M. tuberculosis* (Jansson *et al*., 2013); 710 nM for *Y. pestis* (Haymond *et al*, 2014). Interestingly, the IC_{50} of FR900098 or fosmidomycin against *S. enterica* or its DXR enzyme has not been reported.

Almost all original work on DXR implied that the phosphonate group was essential for proper binding to the active site, as approaches towards the development of DXR inhibitors are based on analogues or derivatives of fosmidomycin/FR900098 that target the substrate binding site and the NADPH binding site (San Jose *et al*., 2013). Studies on the development of DXR inhibitors have

attempted to bridge the substrate and NADPH binding sites for yielding high affinity bisubstrate ligands, while also considering that increased lipophilicity is needed (Deng *et al*., 2011_1; Deng *et al*., 2011_2; McKenney *et al*., 2012; Jansson *et al*., 2013; San Jose *et al*., 2013). Although both fosmidomycin and FR900098 have antimalarial activity, they are limited in their effect as there have been cases in which active infection re-emerged after completion of treatment and low bioavailability as a result of low lipophilicity (McKenney *et al*., 2012). There have been attempts to improve the bioavailability of FR900098 by masking the dianionic charge found on the phosphate moiety, resulting in the production of ester prodrugs which are known for enhancing oral absorption of compounds that have low lipophilicity (Deng *et al*., 2011_1; Cobb *et al*., 2015).

The development of new compounds, from the initial target validation to final validation, is a very costly and time-consuming process (Hughes *et al*., 2011). An alternative approach is therefore drug repurposing, where compounds that have known drug-like properties and bioactivity (e.g. the Pathogen Box used in this study) or that are already marketed for clinical use are used as a starting point for screening campaigns. Unlike developing new drugs, is cost effective and time effective, and as a result has increased over the years (Hughes *et al*., 2011; Pantziarka and André, 2019). It was explored whether the Pathogen Box contains promising compounds for potent inhibition of *S. enterica* DXR. Two compounds, diethylcarbamazine and MMV228911, were found to have activity against *S. enterica* DXR. Diethylcarbamazine is an antiparasitic drug that is used in the primary treatment strategy for filariasis in humans, caused by three species of nematodes namely *Wuchereria bancrofti*, *Brugia malayi*, and *Brugia timori*, and is one of the drugs used in the Global Programme for the Elimination of Lymphatic Filariasis (McGarry *et al*., 2005; Adinarayanan *et al*., 2007; Veale, 2019). This compound is a piperazine derivative. Piperazine is known for being an agonist of GABA receptors, however, the mode of action of diethylcarbamazine is different from that of piperazine and is not fully understood (Wolstenholme, 2011). Diethylcarbamazine interferes with the metabolism of arachidonic acid via the 5-lipoxygenase pathway by inhibiting the production of leukotrienes, prostaglandins, prostacyclins and thromboxanes, which play important roles in regulating immune and inflammatory responses, and clot formation (McGarry *et al*., 2005; Ribeiro *et al*., 2014; Yui *et al*., 2015). This drug blocks bronchial vasoconstrictor substances, and as a result, has been found to be effective in treating the symptoms of bronchial

asthma (Ribeiro *et al*., 2014). Diethylcarbamazine displayed inhibitory activity against *S. enterica* DXR at an IC_{50} value of 2.17 µM.

The Medicines for Malaria Venture (MMV) has reported MMV228911 as a potential antituberculosis compound. This compound was reported to have a minimum inhibitory concentration (MIC) of 4.7 – 12.5 µM for *M. tuberculosis* and no cytotoxicity was observed against HepG2 cells (CC50 > 50 µM). This compound displayed inhibitory activity against *S. enterica* DXR at an IC_{50} value of 6. 86 µM. Diethylcarbamazine and MMV228911 displayed 1 µM> IC_{50} <10 µM, therefore these compounds are worth pursuing further for *S. enterica* drug development. However, it should be borne in mind that these IC_{50} values were determined against a batch of His-tagged recombinant DXR produced in *E. coli*, which may not correlate with the inhibitory activity of the compounds against wild type DXR collected directly from *Salmonella enterica* bacteria.

The screen in this study has enabled the identification of two compounds, diethylcarbamazine (a reference compound) and MMV228911, involved in the inhibition of *S. enterica* DXR. The inhibitory effect of FR900098 against *S. enterica* DXR was also assessed. These compounds can be investigated for the development of drugs that can potentially treat *Salmonella* infections. Fosmidomycin and FR900098 compete with the DOXP substrate for binding to DXR. Interestingly, the structures of diethylcarbamazine and MMV228911 differ significantly from each other and from fosmidomycin/FR900098, which suggests that they may bind away from catalytic pocket of DXR. X-ray crystallographic studies can be conducted in order to find out how diethylcarbamazine and MMV228911 bind to DXR which in turn could lead to identifying novel druggable sites on the DXR enzyme. Enzyme kinetics experiments can be conducted as a way of determining whether diethylcarbamazine and MMV228911 compete with DOXP or NADPH or whether they have other binding sites on the DXR enzyme.

Expression and purification of DXR enzymes from other organisms can be attempted to determined how specific diethylcarbamazine and MMV228911 are for *S. enterica* DXR. The inhibitory effect of diethylcarbamazine and MMV228911 on *S. enterica* bacteria can be assessed by measuring bacterial growth using turbidimetry assays or by using resazurin to indicate cell viability. If these compounds are found to inhibit *S. enterica* bacterial growth, experiments can be

done to confirm if they are inhibiting *S. enterica* DXR. To do this, one could generate *S. enterica* bacteria that are resistant to the compounds and do whole genome sequencing to determine whether sensitivity to the compounds is due to mutations in DXR, leading to validation of DXR as a drug target in *Salmonella*.

In this study, the NADPH-dependent enzyme assay was used for high-throughput screening of compounds that inhibit *S. enterica* DXR. FR900098, a well known antimalarial agent, and diethylcarbamazine and MMV228911, compounds from the Pathogen Box, displayed *in vitro* inhibitory activity against *S. enterica* DXR. These compounds could potentially form basis for developing new broad-spectrum antibiotics that could be used in the treatment of Salmonellosis. The hypothesis set up for this study was approved, as the results of this study implied that the inhibition screening of the *S. enterica* DXR enzyme can be used in high-throughput screening assays to identify potential drug compounds that can be used in anti-salmonellosis drug discovery.

REFERENCES

Abdel-Magid A. F. (2015). Allosteric Modulators: An Emerging Concept in Drug Discovery. *ACS Med Chem Lett*. 6, 104–107.

Adinarayanan S., Critchley J., Das P. K., and Gelband H. (2007). Diethylcarbamazine (DEC)-medicated salt for community-based control of lymphatic filariasis. *Cochrane database Syst. Rev*. 2007 (1).

Aitken M., Berndt E.R., Cutler D.M. (2009) Prescription Drug Spending Trends in The United States: Looking Beyond The Turning Point. *Health Aff*. 28, 151-160.

Akullian A., Montgomery J. M., John-Stewart G., Miller S. I., H. S., Radey M. C., Hager K. R., Verani J. R., Ochieng J. B., Juma J., Katieno J., Fields B., Bigogo G., Audi A. and Judd Walson J. (2018). Multi-drug resistant non-typhoidal Salmonella associated with invasive disease in western Kenya. *PLoS Negl Trop Dis*. 12, 1-16.

Al kraiem A. A., Yang G., Al kraiem F. and Chen T. (2018). Challenges associated with ceftriaxone resistance in *Salmonella*. *Front Life Sci*. 11, 26-34.

Al-Nasiry S., Geusens N., Hanssens M., Luyten C., Pijnenborg R. (2007). The use of Alamar Blue assay for quantitative analysis of viability, migration and invasion of choriocarcinoma cells. *Hum Reprod*. 22, 1304–1309.

Ao T.T., Feasey N.A., Gordon M.A., Keddy K.H., Angulo F.J. and Crump J.A. (2015). Global Burden of Invasive Nontyphoidal *Salmonella* Disease, 2010. *Emerg Infect Dis*. 21, 941-948.

Armstrong C. M., Meyers D. J., Imlay L. S., Freel Meyers C. and Odom A. R. (2015). Resistance to the antimicrobial agent fosmidomycin and an FR900098 prodrug through mutations in the deoxyxylulose phosphate reductoisomerase gene (dxr). *Antimicrob Agents Chemother*. 59, 5511-5519

Aykul S. and Martinez-Hackert E. (2016). Determination of Half-Maximal Inhibitory Concentration Using Biosensor-Based Protein Interaction Analysis. *Anal Biochem*. 508, 97-103.

Baca A. M. and Hol W. G. J. (2000). Overcoming codon bias: A method for high–level overexpression of Plasmodium and other AT–rich parasite genes in Escherichia coli. *Int. J. Parasitol*. 30, 113–118.

Batas B. and Chaudhuri J. B. (1996). Protein Refolding at High Concentration Using Size-Exclusion Chromatography. *Biotechnol and Bioengin*. 50, 16-23.

Bertacine Dias M. V., Santos J. C., Libreros-Zúñiga G. A., Ribeiro J. A., Chavez-Pacheco S. M. (2018). Folate biosynthesis pathway: mechanisms and insights into drug design for infectious diseases. *Future Med Chem*. 10, 935-95.

Birkholtz L.-M., Blatch G., Coetzer T. L., Hoppe H. C., Human E., Morris J., Ngcete Z., Oldfield L., Roth R., Shonhai A., Stephens L. and Louw A. L. (2008). Heterologous expression of plasmodial proteins for structural studies and functional annotation. *Malaria J*. 7, 197.

Blažić M., Balaž A. M., Prodanović O., Popović N., Ostafe R., Fischer R. and Prodanović R. (2019). Directed Evolution of Cellobiose Dehydrogenase on the Surface of Yeast Cells Using Resazurin-Based Fluorescent Assay. *Appl. Sci*. 9, 1413.

Blázquez J. (2003). Hypermutation as a Factor Contributing to the Acquisition of Antimicrobial Resistance. *Clin Infect Dis*. 37, 1201–1209.

Bleicher K. H., Böhm H. J., Müller K., Alanine A. I. (2003). Hit and lead generation: beyond high-throughput screening. *Nat Rev Drug Discov*. 2, 369-378.

Bopp S. K. and Lettieri T. (2008). Comparison of four different colorimetric and fluorometric cytotoxicity assays in a zebrafish liver cell line. *BMC Pharmacol*. 8, 8.

Borra R. C., Lotufo M. A., Gagioti S. M., de Mesquita Barros F. and Andrade P. M. (2009). A simple method to measure cell viability in proliferation and cytotoxicity assays. *SciELO*. 23, 55-62.

Bornhorst J. A. and Falke J. J. (2000). Purification of Proteins using Polyhistidine Affinity Tags. *Methods Enzym*. 326, 245-254.

Boshoff H. I. M., Xu X., Tahlan K., Dowd C. S., Pethe K., Camacho L. R., Park T., Yun C., Schnappinger D., Ehrt S. William K. J. and Barry C. E. (2008). Biosynthesis and Recycling of Nicotinamide Cofactors in *Mycobacterium tuberculosis* an essential role for NAD in nonreplicating bacili. *J. Biol. Chem*. 283, 19329-19341.

Bradford M. M. (1976). A rapid and sensitive method for the quantitation of microgram quantities of protein utilizing the principle of protein-dye binding. *Anal Biochem*. 72, 248-54.

Bromke M. A. (2013). Amino Acid Biosynthesis Pathways in Diatoms. *Metabol*. 3, 294–311.

Brown S. A., Palmer K. L. and Whiteley M. (2008). Revisiting the host as a growth medium. *Nat Rev Microbiol*. 6, 657–666.

Brown A.C. and Parish T. (2008). Dxr is essential in *Mycobacterium tuberculosis* and fosmidomycin resistance is due to a lack of uptake. *BMC Microbiol*. 8, 78.

Bukau B., Deuerling E., Pfund C. and Craig E. A. (2000). Getting Newly Synthesized Proteins into Shape. *Cell*. 101, 119–122.

Bull S. C. and Doig A. J. (2015). Properties of Protein Drug Target Classes. *PLoS ONE*. 10, 1-44.

Burgess R. R. (2009). Refolding Solubilized Inclusion Body Proteins. *Methods in Enzymol*. 463, 259-282.

Cabrita L. D. and Bottomley S. P. (2004). Protein Expression and Refolding – a practical guide to getting the most out of inclusion bodies. *Biotechnol Ann Rev*. 10, 31-50.

Caldwell G. W., Yan Z., Lang W. and Masucci J. A. (2012). The IC_{50} Concept Revisited. *Cur Top in Med Chem*. 12, 1282-1290.

Carnero H. (2006). High Throughput Screening in drug discovery. *Clin. Transl Oncol*. 8, 482-90.

Carrió M. M. and Villaverde A. (2003). Role of molecular chaperones in inclusion body formation. *FEBS Letters*. 537, 215-221.

Chang, A., Scheer, M., Grote, A., Schomburg, I., Schomburg, D. BRENDA, AMENDA and FRENDA the enzyme information system: new content and tools in 2009. *Nucl. Acids Res*. 37, 588–592.

Chen R. (2012). Bacterial expression systems for recombinant protein production: *E. coli* and beyond. *Biotechnol Adv*. 30, 1102-1107.

Cinquin O., Christopherson R. I. and Menz R. I. (2001). A hybrid plasmid for expression of toxic malarial proteins in *Escherichia coli*. *Mol. Biochem. Parasitol*. 117, 245-247.

Clem A. S. (2011). Fundamentals of Vaccine Immunology. *J Glob Infect Dis*. 3, 73–78.

Cobb R. E., Bae B., Li Z., DeSieno M. A., Nair S. K. and Zhao H. Structure-guided design and biosynthesis of a novel FR-900098 analogue as a potent *Plasmodium falciparum* 1-deoxy-$_D$-xylulose-5-phosphate reductoisomerase (Dxr) inhibitor. *Chem Commun (Camb)*. 51, 2526-2528.

Collignon P., Beggs J. J., Walsh T. R., Gandra S., Laxminarayan R. (2018). Anthropological and socioeconomic factors contributing to global antimicrobial resistance: a univariate and multivariable analysis. *Lancet Plan Hea*. 2, 398–405.

Crowther G. J., Shanmugam D., Carmona S. J., Doyle M. A., Hertz-Fowler C., Berriman M., Nwaka S., Ralph S. A., Roos D. S., Van Voorhis W. C. and Agüero F. (2010). Identification of Attractive Drug Targets in Neglected Disease Pathogens Using an *In Silico* Approach. *PLoS Negl Trop Dis*. 4, e804.

Crump J. A., Sjölund-Karlsson M., Gordon M. A. and Parry C. M. (2015). Epidemiology, Clinical Presentation, Laboratory Diagnosis, Antimicrobial Resistance, and Antimicrobial Management of Invasive Salmonella Infections. *Clin Microb Rev*. 28, 901-937.

Cuypers W. L., Jacobs J., Wong V., Klemm E. J., Deborggraeve1 S. and Van Puyvelde S. (2018). Fluoroquinolone resistance in Salmonella: insights by wholegenome sequencing. *Microb Gen*. 4, 1-9.

Dale J. W.and Patki A. (1990). Mycobacterial gene expression and regulation. In: McFadden J, editor. Molecular biology of the mycobacteria. London, United Kingdom: Surrey University Press. 173–198.

Dandapani, S., Rosse, G., Southall, N., Salvino, J. M., & Thomas, C. J. (2012). Selecting, Acquiring, and Using Small Molecule Libraries for High-Throughput Screening. *Curr Protoc Chem biol*. 4, 177–191.

De Bernadez Clark E. (2001). Protein refolding for industrial processes. *Curr. Opin. Biotechnol*. 12, 202-207.

Deng L., Diao J., Chen P., Pujari V., Yao Y., Cheng G., Crick D. C., Prasad B. V. and Song Y. (2011_1). Inhibition of 1-deoxy-D-xylulose-5-phosphate reductoisomerase by lipophilic phosphonates: SAR, QSAR, and crystallographic studies. *J Med Chem*. 54, 4721–4734.

Deng L., Endo K., Kato M., Cheng G., Yajima S. and Song Y. (2011_2). Structures of 1-Deoxy-$_D$-Xylulose-5-Phosphate Reductoisomerase/Lipophilic Phosphonate Complexes. *ACS Med Chem Lett*. 2, 165-170

Dhiman R. K., Schaeffer M. L., Bailey A. M., Testa C. A., Scherman H. and Crick D. C. (2005). 1-Deoxy-D-Xylulose 5-Phosphate Reductoisomerase (IspC) from *Mycobacterium tuberculosis*: towards Understanding Mycobacterial Resistance to Fosmidomycin. *J. of Bacter*. 187, 8395-8402.

Dölle C., Skoge R. H., Van Linden M. R. and Mathias Ziegler M. (2013). NAD Biosynthesis in Humans - Enzymes, Metabolites and Therapeutic Aspects. *Cur Top Med Chem*. 13, 2907-2917.

Duffy S., Sykes M. L., Jones A. J., Shelper T. B., Simpson M., Lang R., Poulsen S-A., Sleebs B. E. and Avery V. M. (2017). Screening the Medicines for Malaria Venture Pathogen Box across multiple pathogens reclassifies starting points for opensource drug discovery. *Antimicrob Agents Chemother*. 61, e00379-17.

Eng S., Pusparajah P., Ab Mutalib N., Ser H., Chan K. and Lee L. (2015). Salmonella: A review on pathogenesis, epidemiology and antibiotic resistance. *Front Life Sci*. 8, 284-293.

Feasey N.A., Dougan G., Kingsley R.A., Heyderman R.S. and Gordon M.A. (2012). Invasive non-typhoidal salmonella disease: an emerging and neglected tropical disease in Africa. *Lancet*. 379, 2489–2499.

Fernández M., Conde S., de la Torre J., Molina-Santiago C., Ramos J., Duque E. (2012). Mechanisms of Resistance to Chloramphenicol in *Pseudomonas putida* KT2440. *Antimicrob Ag Chemo.* 56, 1001–1009.

Flick K., Ahuja S., Chene A., Bejarano M. T. and Chen O. (2004). Optimized expression of *Plasmodium falciparum* erythrocyte membrane protein 1 domains in *Escherichia coli*. *Malar J*. 3, 50.

Fox S., Farr-Jones S., Sopchak L., Boggs A., Nicely A. W., Khoury R. and Biros M. (2006). High-throughput screening; Update on practices and success. *J Biol Screen*. 11, 864–869.

Fuller J. C., Burgoyne N. J., Jackson R. M. (2009). Predicting druggable binding sites at the protein-protein interface. *Drug Discov Today*. 14, 155-161.

Gaberc-Porekar V. and Menart V. (2001). Perspectives of immobilized-metal affinity chromatography. *J. Biochem. Biophys. Methods*. 49, 335–360.

Gerdes S. Y., Scholle M. D., D'Souza M., Bernal A., Baev M. V., Farrell M., Kurnasov O. V., Daugherty M. D., Mseeh F., Polanuyer B. M., Campbell J. W., Anantha S., Y. Shatalin K. Y., Chowdhury S. A. K., Fonstein M. Y., and Osterman A. L. (2002). From Genetic Footprinting to Antimicrobial Drug Targets: Examples in Cofactor Biosynthetic Pathways. *J Bacteriol*. 184, 4555–4572.

Gieβmann D., Heidler P., Haemers T., Van Calenbergh S., Reichenberg A., Jomaa H., Weidemeyerd C., Sanderbrand S., Wiesner J. and Link A. (2008). Towards new antimalarial drugs: synthesis of non–hydrolyzable phosphate mimics as feed for a predictive QSAR study on 1–deoxy–D–xylulose–5–phosphate reductoisomerase inhibitors. *Chem. Biodiv*. 5, 643– 656.

Goble J.L., H. Johnson, J. de Ridder, L. L. Stephens, A. Louw, G. L. Blatch, A. Boshoff. (2013). The druggable antimalarial target PfDXR: overproduction strategies and kinetic characterization. *Protein Pept. Lett*. 20: 115-124.

Grolle S., Bringer-Meyer S. and Sahm H. (2000). Isolation of the dxr gene of *Zymomonas mobilis* and characterization of the 1-deoxy-D-xylulose 5-phosphate reductoisomerase. *FEMS Microbiol Lett.* 191, 131-137.

Grover A. K. (2013). Use of Allosteric Targets in the Discovery of Safer Drugs . *Med. Prin. Pract*. 22, 418-426.

Gustafsson C., Govindarajan S. and Minshull J. (2004). Codon bias and heterologous protein expression. *TRENDS in Biotechnol*. 22, 346-353.

Haemers, T., Wiesner, J., Van Poecke, S., Goeman, J., Henschker, D., Beck, E., Jomaa, H., Van Calenbergh, S., (2006). Synthesis of alpha-substituted fosmidomycin analogues as highly potent *Plasmodium falciparum* growth inhibitors. *Bioorg. Med. Chem. Lett*. 16, 1888–1891.

Hall M. D., Simeonov A. and Davis M. I. (2016). Avoiding Fluorescence Assay Interference - The Case for Diaphorase. *Assay Drug Dev Technol*. 14, 175–179.

Hansen-Wester I., Stecher B. and Hensel M. (2002). Type III Secretion of Salmonella enterica Serovar Typhimurium Translocated Effectors and SseFG. *Infect Imm*. 70, 1403–1409.

Harris C. J., Hill R. D., Sheppard D. W., Slater M. J., & Stouten P. F. (2011). The design and application of target-focused compound libraries. *Comb Chem & High Throughput Screen*. 14, 521–531.

Haymond A., Johny C., Dowdy T., Schweibenz B., Villarroel K., Young R., Mantooth C. J., Patel M., Bases J., San Jose G., Jackson E. R., Dowd C. S. and Couch R. D. (2014). Kinetic Characterization and Allosteric Inhibition of the *Yersinia pestis* 1-Deoxy-D-Xylulose 5-Phosphate Reductoisomerase (MEP Synthase). *PLoS ONE*. 9, e106243.

Henriksson L. M., Unge T., Carlsson J., Åqvist J., Mowbray S. L. and Jones T. A. (2007). Structures of Mycobacterium tuberculosis 1-Deoxy-D-xylulose-5-phosphate Reductoisomerase. *J Biolog Chem*. 282, 19905–19916.

Heuston S., Begley M., Gahan C.G.M and Hill C. (2012). Isoprenoid biosynthesis in bacterial pathogens. *Microbiol*. 158, 1389-1401.

Hobernik D. and Bros M. (2018). DNA Vaccines—How Far From Clinical Use? *Int J Mol Sci*. 19, 1-28.

Hornsten L., Carlsson M., Lundqvist J., Grane´r T. and Andersson L. Column Purification of Histidine-Tagged Proteins from Unclarified Samples. *J Biomolec Tech*. 23, S41-S42.

Hughes J. P., Rees S., Kalindjian S. B. and Philpott K. L. (2011). Principles of early drug discovery. *Br J Pharmacol*. 162, 1239-1249.

Hunter W. N. (2007). The Non-mevalonate Pathway of Isoprenoid Precursor Biosynthesis. *J. of Biol. Chem.* 282, 21573–21577.

Inouye S., Sahara-Miura Y., Sato J. and Suzuki T. (2015). Codon Optimization of Genes for Efficient Protein Expression in Mammalian Cells by Selection of Only Preferred Human Codons. *Prot Express Pur*. 109, 47–54.

Jansson A. M., Więckowska A., Bjorkelid C., Yahiaoui S., Sooriyaarachchi S., Lindh M., Bergfors T., Dharavath S., Desroses M., Suresh S., Andaloussi M., Nikhil R., Sreevalli S.and Srinivasa B.S. Larhed M., Jones T.A., Karlen A., and Mowbray S.L. (2013). DXR Inhibiton by Potent Mono- and Disubstituted Fosmidomycin Analogues. *J Med Chem*. 56, 6190-6199.

Jawaid S., Seidle H., Zhou W., Abdirahman H., Abadeer M., Hix J. H., van Hoek M. L. and Couch R. D. (2009). Kinetic Characterization and Phosphoregulation of the *Francisella tularensis* 1-Deoxy-D-Xylulose 5-Phosphate Reductoisomerase (MEP Synthase). *PLoS ONE*. 4, e8288.

Jiang Z. and Zhou Y. (2005). Using bioinformatics for drug target identification from the genome. *Am J Pharmacogenomics*. 5, 387-96.

Jomaa H., Wiesner J., Sanderbrand S., Altincicek B., Weidemeyer C., Hintz M., Turbachova I., Eberl M., Zeidler J., Lichtenthaler H.K., Soldati D. and Beck E. (1999). Inhibitors of the nonmevalonate pathway of isoprenoid biosynthesis as antimalarial drugs. *Sci*. 285, 1573-1536.

Kantele A., Pakkanen S. H., Siitonen A., Karttunen R. and Kantele J. M. (2012). Live oral typhoid vaccine Salmonella Typhi Ty21a - a surrogate vaccine against non-typhoid salmonella? *Vacc*. 30, 7238-7245.

Kariuki S. and Dougan G. (2014). Antibacterial resistance in sub-Saharan Africa: an underestimated emergency. *Ann N Y Acad Sci.*1323, 43-55.

Kaur J., Kumar A. and Kaur J. (2018). Strategies for Optimization of Heterologous Protein Expression in *E. coli*: Roadblocks and Reinforcements. *Int J Bio Macromol*. 106, 803–822.

Kingsley R. A., Msefula C. L., Thomson N. R., Kariuki S., Holt K. E., Gordon M. A., Harris D., Clarke L., Whitehead S., Sangal V., Marsh K., Achtman M., Molyneux M. E., Cormican M., Parkhill J., MacLennan C. A., Heyderman R. S. and Gordon Dougan G. (2009). Epidemic multiple drug resistant *Salmonella Typhimurium* causing invasive disease in sub-Saharan Africa have a distinct genotype. *Gen Res*. 19, 2279–2287.

Kuzuyama T., Takahashi S., Takagi M. and Seto H. (2000). Characterization of 1-deoxy-D-xylulose 5-phosphate reductoisomerase, an Enzyme Involved in Isopentenyl Diphosphate Biosynthesis, and Identification of Its Catalytic Amino Acid Residues. *J Bio Chem*. 30, 19928-19932.

Kuzuyama, T., Shimizu, T., Takahashi, S. and Seto, H. (1998) Fosmidomycin, a Specific Inhibitor of 1-Deoxy-Dxylulose 5-Phosphate Reductoisomerase in the Nonmevalonate Pathway for Terpenoid Biosynthesis. *Tetrahedron Letters*. 39, 7913-7916.

Lakey D. L., Voladri R. K. R., Edwards K. M., Hager C., Samten B., Wallis R. S., Barnes P. F. and Kernodle D. S. (2000). Enhanced Production of Recombinant Mycobacterium tuberculosis Antigens in Escherichia coli by Replacement of Low-Usage Codons. *Infect Immun*. 68, 233–238.

Laemmli U.K. (1970). Cleavage of structural proteins during the assembly of the head of bacteriophage T4. *Nature*. 227, 680-685.

Lell B. and Kremsner P. G. (2002). Clindamycin as an Antimalarial Drug: Review of Clinical Trials. *Antimicrob Agents Chemother*. 46, 2315–2320.

Lell B., Ruangweerayut R., Wiesner J., Missinou M. A., Schindler A., Baranek T., Hintz M., Hutchinson D., Jomaa H. and Kremsner P. G. (2003). Fosmidomycin, a novel chemotherapeutic agent for malaria. *Antimicrob Agents Chemother*. 47, 735-738.

Lewis L. M., Engle L. J., Pierceall W. E., Hughes D. E. and Shaw K. J. (2004). Affinity capillary electrophoresis for the screening of novel antimicrobial targets. *J Biomol Screen*. 9, 303-308.

Li J., Liu Y., Wang F., Ma G. and Su Z. (2004). Hydrophobic interaction chromatography correctly refolding proteins assisted by glycerol and urea gradients. *J Chromatogr A*. 1061, 193-199.

Lunguya O., Lejon V., Phoba1 M.F., Bertrand S., Vanhoof R., Glupczynski Y., Verhaegen J., Muyembe-Tamfum J.J. and Jacobs J. (2013). Antimicrobial Resistance in Invasive Non-typhoid *Salmonella* from the Democratic Republic of the Congo: Emergence of Decreased Fluoroquinolone Susceptibility and Extended-spectrum Beta Lactamases. *PLOS Negl Trop Dis*.7, e2103.

Maccesi M., Aguiar P. H. N., Pasche V., Padilla M., Suzuki B. M., Montefusco S., Abagyan R., Keiser J., Mourão M. M. and Caffrey C. R. (2019). Multi-center screening of the Pathogen Box collection for schistosomiasis drug discovery. Parasites & Vectors. 12,1-10.

Macheboeuf P., Contreras-Martel C., Job V., Dideberg O. and Dessen A. (2006). Penicillin Binding Proteins: key players in bacterial cell cycle and drug resistance processes. *FEMS Microbiol Rev*. 30, 673–691.

Mac Sweeney A., Lange R., Fernandes R.P.M., Schulz H., Dale G.E., Douangamath A., Proteau P.J. and Oefner C. (2005). The Crystal Structure of *E. coli* 1-Deoxy-D-xylulose 5-phosphate Reductoisomerase in a Ternary Complex with the Antimalarial Compound Fosmidomycin and NADPH Reveals a Tight-Binding Closed Enzyme Conformation. *J. Mol. Biol.* 345, 115-127.

MacLennan C. A., Martin L. B. and Micoli F. (2014). Vaccines against invasive *Salmonella* disease Current status and future directions. *Hum Vaccin Immunother*. 10, 1478–1493.

MacLennan C.A. and Levine M.M. (2013). Invasive nontyphoidal *Salmonella* disease in Africa: current status. *Expert Rev. Anti Infect Ther*. 11, 443-446.

Makhoba X. H., Burger A., Coertzen D., Zininga T., Birkholtz L. and Shonhai A. (2016). Use of a Chimeric Hsp70 to Enhance the Quality of Recombinant *Plasmodium falciparum* S-Adenosylmethionine Decarboxylase Protein Produced in *Escherichia coli*. *PLoS ONE*. 11, 1-21.

Mandal S., Moudgi M. and Mandal S. K. (2009). Rational drug design. *Eur J Pharmacol*. 625, 90-100.

Manore C., Graham T., Carr A., Feryn A., Jakhar S., Mukundan H. and Callender Highlander H. (2019). Modeling and Cost Benefit Analysis to Guide Deployment of POC Diagnostics for Non-typhoidal Salmonella Infections with Antimicrobial Resistance. *Sci Rep*. 9, 1-17.

Martin A., Camacho M., Portaels F. and Palomino J. C. (2003). Resazurin Microtiter Assay Plate Testing of *Mycobacterium tuberculosis* Susceptibilities to Second-Line Drugs: Rapid, Simple, and Inexpensive Method. *Antimicrob Agents Chemother*. 47, 3616–3619.

Matambo T. S., Odunuga O. O., Boshoff A. and Blatch G. L. (2004). Overproduction, purification, and characterization of the Plasmodium falciparum heat shock protein 70. *Protein Expr. Purif*. 33, 214–222.

Matsuo K., Yamaguchi R., Yamazaki A., Tasaka H. and Yamada Y. (1988). Cloning and expression of the Mycobacterium bovis BCG gene for extracellular alpha antigen. *J Bacteriol*. 170, 3847–3854.

Mayer F. L. and Kronstad J. W. (2017). Discovery of a novel antifungal agent in the Pathogen Box. *mSphere*. 2, e00120-17.

McGarry H. F., Plant L. D. and Taylor M. J. (2005). Diethylcarbamazine activity against *Brugia malayi* microfilariae is dependent on inducible nitric-oxide synthase and the cyclooxygenase pathway. *Filaria J.* 4, 4.

McKenney E.S., Sargent M., Khan H., Uh E., Jackson E.R., San Jose G., Robin D. Couch R.D., Dowd C.S., and van Hoek L.M. (2012). Lipophilic Prodrugs of FR900098 Are Antimicrobial against *Francisella novicida* In Vivo and In Vitro and Show GlpT Independent Efficacy. *PLoS One*. 7, e.38167.

Mehlin C., Boni E., Buckner F. S., Engel L., Feis T, Gelb M. H., Haji L., Kim D., Liu C., Mueller N., Myler P. J., Reddy J. T., Sampson J. N., Subramanian E., Van Voorhis W. C., Worthey E., Zucker F. and Hol, W. G. J. (2006). Heterologous expression of proteins from *Plasmodium falciparum*: Results from 1000 genes. *Mol. Biochem. Parasitol.* 148, 144–160.

Menzella H. G. (2011). Comparison of two codon optimization strategies to enhance recombinant protein production in *Escherichia coli*. *Microb Cell Fact*. 10, 1-8.

Micoli F., Rondini S., Alfini R., Lanzilao L., Necchi F., Negrea A., Rossia O., Brandt C., Clare S., Mastroenic P., Rappuoli R., Saula A. and MacLennan C. A. (2018). Comparative immunogenicity and efficacy of equivalent outer membrane vesicle and glycoconjugate vaccines against nontyphoidal Salmonella. *PNAS*.115, 10428–10433.

Missinou M. A., Borrmann S., Schindler A., Issifou S., Adegnika A. A., Matsiegui P. B., Binder R., Lell B., Wiesner J., Baranek T., Jomaa H., Kremsner P. G. (2002). Fosmidomycin for malaria. *Lancet*. 360, 1941-1942.

Miziorko H. M. (2011). Enzymes of the Mevalonate Pathway of Isoprenoid Biosynthesis. *Arch Biochem Biophys*. 505, 131–143.

Mohs R. C. and Greig N. H. (2017). Drug discovery and development: Role of basic biological research. *Alzheimers Dement (N Y)*. 3, 651-657.

Mondal K. and Gupta M. N. (2006). Affinity-Based Strategies for Protein Purification. *Analyt Chem*. 3499-3504.

Munos J. W., Pu X., Mansoorabadi S. O., Kim H. and Liu H. (2009). A Secondary Kinetic Isotope Effect Study of the 1-Deoxy-Dxylulose-5-phosphate Reductoisomerase-catalyzed Reaction: Evidence for a Retroaldol-Aldol Rearrangement. *J Am Chem Soc*. 131, 2048–2049.

Murima P., McKinney J. D. and Pethe K. (2014). Targeting Bacterial Central Metabolism for Drug Development. *Chem & Bio*. 21, 1423-1432.

Murkin A.S., Manning K.A. and Kholodar S.A. (2014). Mechanism and Inhibition of 1- deoxy-D- xylulose-5-phosphate reductoismerase. *Bioorg Chem*. 57, 171-185.

Na-Bangchang K., Ruengweerayut R., Karbwang J., Chauemung A. and Hutchinson D. (2007). Pharmacokinetics and pharmacodynamics of fosmidomycin monotherapy and combination therapy with clindamycin in the treatment of multidrug resistant falciparum malaria. *Malar J*. 6, 70.

Narum D. L., Kumar S., Rogers W. O., Fuhrmann S. R., Liang H., Oakley M., Taye A., Sim B. K. L., Hoffman S. L. (2001). Codon optimization of gene fragments encoding *Plasmodium falciparum* merzoite proteins enhances DNA vaccine protein expression and immunogenicity in Mice. *Infect. Immun*. 69, 7250–7253.

Neelapu N. R. R., Srimath-Tirumala-Peddinti R. C. P. K., Nammi D. and Pasupuleti A. C. M. (2013). New Strategies and Paradigm for Drug Target Discovery: A Special Focus on Infectious Diseases Tuberculosis, Malaria, Leishmaniasis, Trypanosomiasis and Gastritis. *Infect Disord Drug Targ*. 13, 352-364.

Nevozhay D. (2014). Cheburator Software for Automatically Calculating Drug Inhibitory Concentrations from *In Vitro* Screening Assays. *PLoS ONE*. 9, 1-10.

Nugraha A. B., Tuvshintulga B., Guswanto A., Tayebwa D. S., Rizk M. A., Gantuya S., Batiha G. E., Beshbishy A. M., Sivakumar T., Yokoyama N. and Igarashi, I. (2019). Screening the Medicines for Malaria Venture Pathogen Box against piroplasm parasites. *Int J Parasitol Drugs Drug Resist*. 10, 84–90.

Oany A. R., Mia M., Pervin T., Hasan N. and Hirashima A. (2018). Identification of potential drug targets and inhibitor of the pathogenic bacteria *Shigella flexneri* 2a through the subtractive genomic approach. *In Silico Pharmacol*. 6, 1-16.

Onwuezobe I. A., Oshun P. O. and Odigwe C. C. (2012). Antimicrobials for treating symptomatic non-typhoidal Salmonella infection. *Cochrane Database Syst Rev*. 2012, 1-49.

Osaka I. and Hefty P. S. (2013)Simple resazurin-based microplate assay for measuring *Chlamydia* infections. *Antimicrob Agents Chemother*. 57, 2838-2840.

Pantziarka P., & André N. (2019). Editorial: Drug Repurposing. *Front Med (Lausanne)*. 6, 154.

Parsons J. B. and Rock C. O. (2011). Is Bacterial Fatty Acid Synthesis a Valid Target for Antibacterial Drug Discovery? *Curr Opin Microbiol*. 14, 544–549.

Partridge S. R., Kwong S. M., Firth N., Jensen S. O. (2018). Mobile Genetic Elements Associated with Antimicrobial Resistance. *Clin Microbiol Rev*. 31, e00088-17.

Passalacqua K. D., Charbonneau M. E. and O'Riordan M. X. (2016). Bacterial Metabolism Shapes the Host-Pathogen Interface. *Microbiol Spectr*. 4, 1-31.

Patra A. K., Mukhopadhyay R., Mukhija R., Krishnan A., Garg L. C, Panda A. K. (2000). Optimization of Inclusion Body Solubilization and Renaturation of Recombinant Human Growth Hormone from *Escherichia coli*. *Prot Express Pur*. 18, 182–92.

Pavithra S. R., Kumar R. and Tatu U. (2007). Systems Analysis of Chaperone Networks in the Malarial Parasite *Plasmodium falciparum*. *PLoS Comput Bio*. 9, 1701-1715.

Punde N., Kooken J., Leary D., Legler P. M. and Angov E. (2019). Codon harmonization reduces amino acid misincorporation in bacterially expressed *P. falciparum* proteins and improves their immunogenicity. *AMB Expr*. 167, 1-14.

Qidwai T., Jamal F., Khan M.Y. and Sharma B. (2014). Exploring Drug Targets in Isoprenoid Biosynthetic Pathway for *Plasmodium falciparum*. *Biochem Res Int*. 2014, 657189.

Redgrave L. S., Sutton S. B., Webber M. A. and Piddock L. J. (2014). Fluoroquinolone resistance: mechanisms, impact on bacteria, and role in evolutionary success. *Trends Microbiol*. 22, 438-445.

Repp K. K., Menor S. A. and Pettit R. K.(2007). Microplate Alamar blue assay for susceptibility testing of *Candida albicans* biofilms. *Med Mycol*. 45, 603–607.

Reuter K., Sanderbrand S., Jomaa H., Wiesner J., Steinbrecher I., Beck E., Hintz M., Klebe G. and Stubbs M. T. (2002). Crystal Structure of 1-Deoxy-D-xylulose-5-phosphate Reductoisomerase, a Crucial Enzyme in the Non-mevalonate Pathway of Isoprenoid Biosynthesis. *J. Biol. Chem*. 277, 5378–5384.

Ribeiro E. L., de Souza Barbosa K. P., Fragoso I. T., Donato M. A. M., dos Santos Gomes F. O., da Silva B. S., e Silva A. K. S., Santos Rocha S. W., da Silva Junior V. A. and Alves Peixoto C. (2014). Diethylcarbamazine Attenuates the Development of Carrageenan-Induced Lung Injury in Mice. *Mediat of Inflamm*. 2014, 1-12.

Ricagno S., Grolle S., Bringer-Meyer S., Sahm H., Lindqvista Y. and Schneidera G. (2004). Crystal structure of 1-deoxy-D-xylulose-5-phosphate reductoisomerase from *Zymomonas mobilis* at 1.9-Å resolution. *Biochem. Biophys. Act.* 1698, 37-44.

Robinson P. K. (2015). Enzymes: principles and biotechnological applications. *Essays Biochem*. 59, 1–41.

Rosano G. L. and Ceccarelli E. A. (2014). Recombinant protein expression in Escherichia coli: advances and challenges. *Front Micro*. 5, 1-17.

Roy S., Ghosh P., Ahmed I., Chakraborty M., Naiya G. and Ghosh B. (2018). Constrained α-Helical Peptides as Inhibitors of Protein-Protein and Protein-DNA Interactions. *Biomeds*. 6, 118.

Ruangweerayut R., Looareesuwan S., Hutchinson D., Chauemung A., Banmairuroi V. and Na-Bangchang K. (2008). Assessment of the pharmacokinetics and dynamics of two combination regimens of fosmidomycin-clindamycin in patients with acute uncomplicated falciparum malaria. *Malar J*. 7, 225.

Saibil H. (2013). Chaperone machines for protein folding, unfolding and disaggregation. *Nat Rev Mol Cell Biol*. 14, 630-642.

Saha D., Emran T. B. and Paul S. (2013). Bioinformatics: The effects on the cost of drug discovery. *Gal. Med. J*. 18, 44-50.

Sakharkar K. R., Sakharkar M. K. and Chow Y. T. (2004). A novel genomics approach for the identification of drug targets in pathogens, with special reference to *pseudomonas aeruginosa*. *In silico biol*. 4, 355–360.

San Jose G., Jackson E. R., Uh E., Johny C., Haymond A., Lundberg L., Pinkham C., Kehn-Hall K., Boshoff H. I., Couch R. D. and Dowd C. S. (2013). Design of potential bisubstrate inhibitors against *Mycobacterium tuberculosis* (Mtb) 1-deoxy-D-xylulose 5-phosphate reductoisomerase (Dxr)-evidence of a novel binding mode. *Med Chem Commun*. 4, 1099-1104.

Schager A. E., Dominguez-Medina C., Necchi F., Micoli F., Goh Y., Margaret Goodall M., Flores-Langarica A., Bobat S., Cook C. N. L., Melissa Arcuri M., Marini A., King L. D. W., Morris F. C., Graham Anderson G., Toellner K., Henderson I. R., López-Macías C., MacLennan C. A. and Cunningham A. F. (2018). IgG Responses to Porins and Lipopolysaccharide within an Outer Membrane-Based Vaccine against Nontyphoidal Salmonella Develop at Discordant Rates. *mBio*. 9, e02379-17.

Schenone M. Dančík V., Wagner B. K. and Clemons P. A. (2013). Target identification and mechanism of action in chemical biology and drug discovery. *Nat Chem Biol*. 9, 232–240.

Sebaugh J. L. (2011). Guidelines for accurate EC50/IC50 estimation. *Pharm Stat*. 10, 128-134.

Singh A., Upadhyay V., Upadhyay A.K., Singh S.M. and Panda A. K. (2015). Protein Recovery from Inclusion Bodies of *Escherichia coli* Using Mild Solubilization Process. *Microb Cell Fact*. 41, 1-10.

Shahbaz K. (2017). Cephalosporins: pharmacology and chemistry. *Pharm. Biolog. Eval*. 4, 234-238.

Shanmugham B. and Pan A. (2013). Identification and Characterization of Potential Therapeutic Candidates in Emerging Human Pathogen *Mycobacterium abscessus*: A Novel Hierarchical *In Silico* Approach.

Sköld O. (2000). Sulfonamide resistance: mechanisms and trends. *Drug Resist Updat*. 3, 155-160.

Speer B. S., Shoemaker N. and Salyers A. (1992). Bacterial Resistance to Tetracycline: Mechanisms, Transfer, and Clinical Significance. *Clin Microbiol Rev*. 5, 387-399.

Sirinavin S. and Garner P. (1999). Antibiotics for treating salmonella gut infections. *Cochrane Database Syst. Rev*. Issue 1.

Steinbacher, S., Kaiser, J., Eisenreich, W., Huber, R., Bacher, A. & Rohdich, F. (2003). Structural basis of fosmidomycin action revealed by the complex with 2-C-methyl-D-erythritol 4-phosphate synthase (IspC). Implications for the catalytic mechanism and anti-malaria drug development. *J Biol Chem*. 278, 18401–18407.

Stentz R., Carvalho A. L., Jones E. J. and Carding R. S. (2018). Fantastic voyage: the journey of intestinal microbiota-derived microvesicles through the body. *Biochemical Society Transactions*. 46, 1021–1027.

Szymański P., Markowicz M. and Mikiciuk-Olasik E. (2012). Adaptation of High-Throughput Screening in Drug Discovery - Toxicological Screening Tests. *Int. J. Mol. Sci*. 13, 427-452.

Takahashi S., Kuzuyama T. and Seto H. (1998). A 1-deoxy-D-xylulose 5-phosphate reductoisomerase catalyzing the formation of 2-C-methyl-D-erythritol 4-phosphate in an alternative nonmevalonate pathway for terpenoid biosynthesis. *Proc. Natl. Acad. Sci. USA*. 95, 9879–9884.

Takenoya M., Ohtaki A., Noguchi K., Endo K., Sasaki Y., Ohsawa K., Yajima S., Yohda M. (2010). Crystal structure of 1-deoxy-D-xylulose 5-phosphate reductoisomerase from the hyperthermophile *Thermotoga maritima* for insights into the coordination of conformational changes and an inhibitor binding. *J. Struct Biol*. 170, 532–539.

Taneja N. K. and Tyagi J. S. (2007). Resazurin Reduction Assays for Screening of Anti-Tubercular Compounds Against Dormant and Actively Growing *Mycobacterium tuberculosis*, *Mycobacterium bovis* BCG and *Mycobacterium smegmatis*. *J Antimicrob Chem*. 60, 288-293.

Tennant S. M., MacLennan C. A., Raphael Simon R., Martin L. B. and Khan M. I. (2016). Nontyphoidal Salmonella Disease: Current Status of Vaccine Research and Development. *Vacc*. 34, 2907–2910.

Umeda T., Tanaka N., Kusakabe Y., Nakanishi M., Kitade Y. and Nakamura K. T. (2010). Crystallization and preliminary X-ray crystallographic study of 1-deoxy-D-xylulose 5-phosphate reductoisomerase from *Plasmodium falciparum*. *Acta Cryst*. 66, 330–332

Umeda T., Tanaka N., Kusakabe Y., Nakanishi M., Kitade Y. and Nakamura K. T. (2011). Molecular basis of fosmidomycin's action on the human malaria parasite *Plasmodium falciparum*. *Sci. Rep*. 1, 1-8.

Vallejo L. F. and Ursula Rinas U. (2004). Strategies for the recovery of active proteins through refolding of bacterial inclusion body proteins. *Microb Cell Fact*. 11, 1-12.

Vartak A. and Sucheck S. J. (2016). Recent Advances in Subunit Vaccine Carriers. *Vacc*. 4, 1-18.

Veale C.G.L. (2019). Unpacking the Pathogen Box—An Open Source Tool for Fighting Neglected Tropical Disease. *ChemMedChem*. 14, 386-453.

Veale C. G. L. and Hoppe H. C. (2018). Screening of the Pathogen Box reveals new starting points for anti-trypanosomal drug discovery. *Med Chem Commun*. 9, 2037-2044.

Veale C.G.L., Laming D., Swart T., Chibale K. and Hoppe H. C. (2019). Exploring the anti-plasmodial 2-aminopyridines as potential anti-trypanosomal agents. *ChemMedChem*. 14, 1-9.

Velge P., Wiedemann A., Rosselin M., Abed N., Boumart Z., Chaussé A. M., Grépinet O., Namdari F., Roche S. M., Rossignol A., Virlogeux-Payant I. (2012). Multiplicity of Salmonella entry mechanisms, a new paradigm for Salmonella pathogenesis. *Microbiol open*. 1, 243-258.

Villaverde A. and Carrió M. M. (2003). Protein aggregation in recombinant bacteria: biological role of inclusion bodies. *Biotechnol Lett*. 25, 1385-1395.

Visser U., Abeyruwan S., Vempati U., Smith R. P., Lemmon V. and Schürer S. C. (2011). BioAssay Ontology (BAO): a semantic description of bioassays and high-throughput screening results. *BMC Bioinform*. 12, 1-16.

Wang F., Liu Y., Chen J. and Su Z. (2005). Chromatographic Refolding of Proteins: Molecular Action and Column Control. *China Partic*. 3, 337-342.

WHO (2015) World Health Organization. Global action plan on antimicrobial resistance, Geneva (available online at http://www.who.int/antimicrobialresistance/ global-action-plan/en/)

WHO (2019) World Health Organization. Biologicals, DNA Vaccines (available online at https://www.who.int/biologicals/areas/vaccines/dna/en/)

Wiesner J., Ziemann C., Hintz M., Reichenberg A., Ortmann R., Schlitzer M., Fuhst R., Timmesfeld N., Vilcinskas A. and Jomaa H. (2016). FR-900098, an antimalarial development candidate that inhibits the non-mevalonate isoprenoid biosynthesis pathway, shows no evidence of acute toxicity and genotoxicity. *Viru*. 7, 718-728.

Williams S. L. and McCammon J. A. (2009). Conformational dynamics of the flexible catalytic loop in *Mycobacterium tuberculosis* 1-deoxy-D-xylulose 5-phosphate reductoisomerase. *Chem Biol Drug Des.* 73 , 26–38.

Wolstenholme AJ (2011). Ion channels and receptor as targets for the control of parasitic nematodes. *Int J Parasitol Drugs Drug Resist*. 14; 1, 2-13.

Wright H. T. and Reynolds K. A. (2007). Antibacterial Targets in Fatty Acid Biosynthesis. *Curr Opin Microbiol*. 10, 447–453.

Yajima S., Nonaka T., Kuzuyama T., Seto H. and Ohsawa K. (2002). Crystal Structure of 1-Deoxy-D-xylulose 5-phosphate Reductoisomerase Complexed with Cofactors: Implications of a Flexible Loop Movement upon Substrate Binding. *J. Biochem*. 131, 313-317.

Yajima S., Hara K., Iino D., Sasaki Y., Kuzuyama T., Ohsawa K. and Seto H. (2007). Structure of 1-deoxy-D-xylulose 5-phosphate reductoisomerase in a quaternary complex with a magnesium ion, NADPH and the antimalarial drug fosmidomycin. *Acta Cryst*. 63, 466–470.

Yamaguchi H. and Miyazaki M. (2014). Refolding Techniques for Recovering Biologically Active Recombinant Proteins from Inclusion Bodies. *Biomol*. 4, 235-251.

Yeh I., Hanekamp T., Tsoka S., Karp P. D. and Altman R. B. (2004). Computational analysis of *Plasmodium falciparum* metabolism: organizing genomic information to facilitate drug discovery. *Gen Res*. 14, 917-24.

Yui K., Imataka G., Nakamura H., Ohara N., Naito Y. (2015). Eicosanoids Derived From Arachidonic Acid and Their Family Prostaglandins and Cyclooxygenase in Psychiatric Disorders. *Curr Neuropharmacol*. 13, 776-785.

Zhao L., Chang W., Xiao Y., Liu H., and Liu P. (2013). Methylerythritol Phosphate Pathway of Isoprenoid Biosynthesis. *Annu Rev Biochem*. 82, 497–530.

Zhi Y., Lin S. M., Jang A., Ahn K. B., Ji H. J., Guo H., Lim S. and Seo H. S.(2019). Effective mucosal live attenuated Salmonella vaccine by deleting phosphotransferase system component genes ptsI and crr. *J Microbiol*. 57, 64-73.

Zhu A., Romero R. and Petty H. R. (2009). An enzymatic fluorimetric assay for glucose-6-phosphate: application in an in vitro Warburg-like effect. *Anal Biochem*. 388, 97–101.

APPENDICES

Appendix A: pET28a(+) Plasmid Map

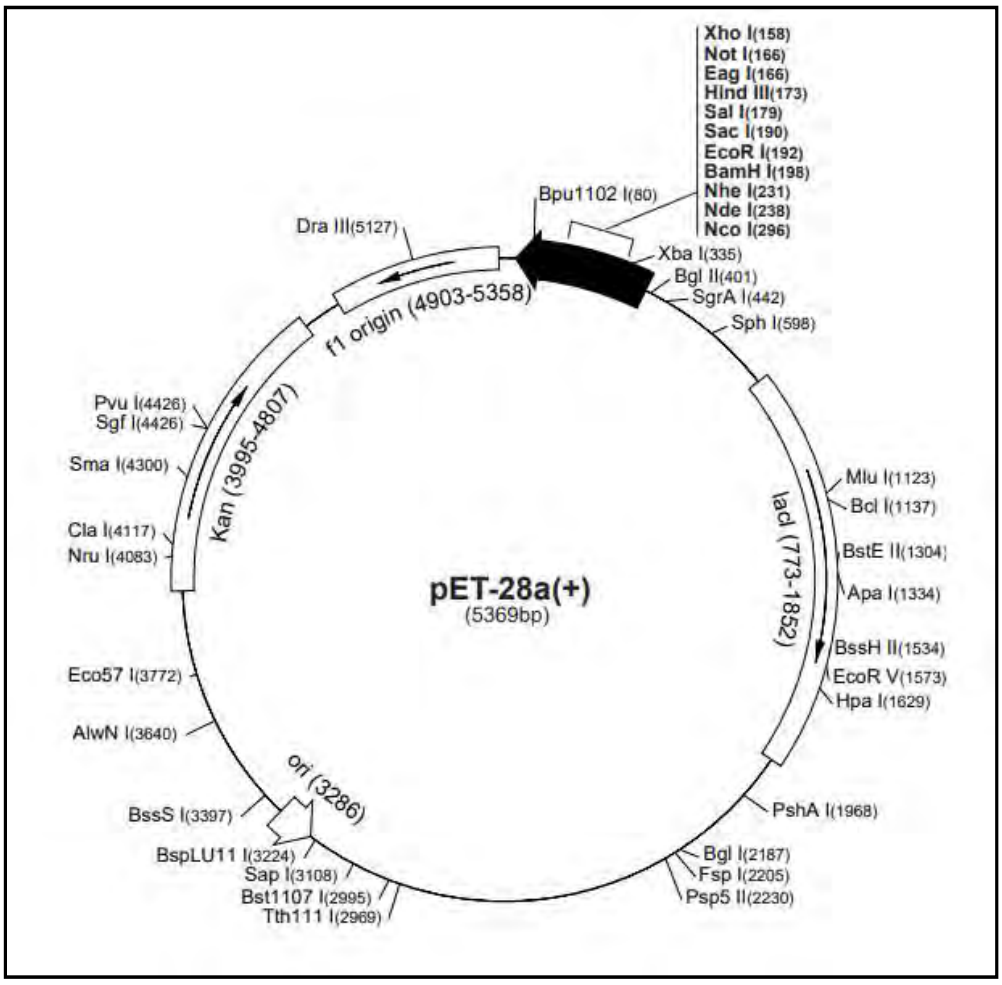

The plasmid map of the pET28(+) plasmid (Obtained from Novagen).

Appendix B: Molecular Size Determination for Restriction Digestion Products

Example using the agarose gel presented below:

Migration Distance (mm)	Rf Value	DNA Ladder Bands (bp)	Log MW
4	0.095238	10000	4
7	0.166667	6000	3.778151
12	0.285714	3000	3.477121
16	0.380952	2000	3.30103
19	0.452381	1500	3.176091
25	0.595238	1000	3
29	0.690476	750	2.875061
34	0.809524	500	2.69897
43	1.02381	250	2.39794

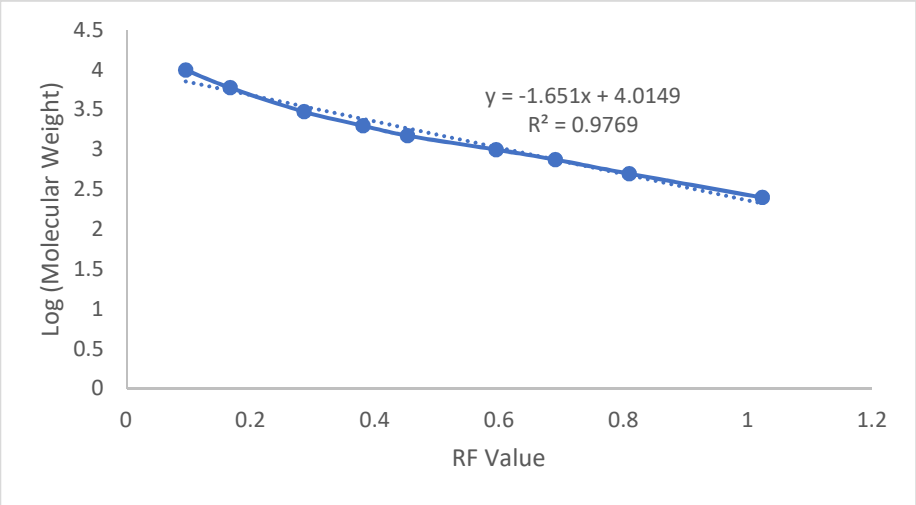

Calculation:

Rf Value of DNA Fragment A band = 5/42 = 0.119

y = -1.651(0.119) + 4.0149

y = 3.8184

$10^{3.8184}$ = 6583 bp

Appendix C: Molecular Size Determination for Protein Band Sizes

Example using the polyacrylamide gel presented below:

Migration Distance (mm)	Rf Value	Protein Ladder Bands (kDa)	Log MW
10	0.313	85	1.929418926
18	0.563	60	1.77815125
23	0.719	50	1.698970004
26	0.813	40	1.602059991
32	1	30	1.477121255

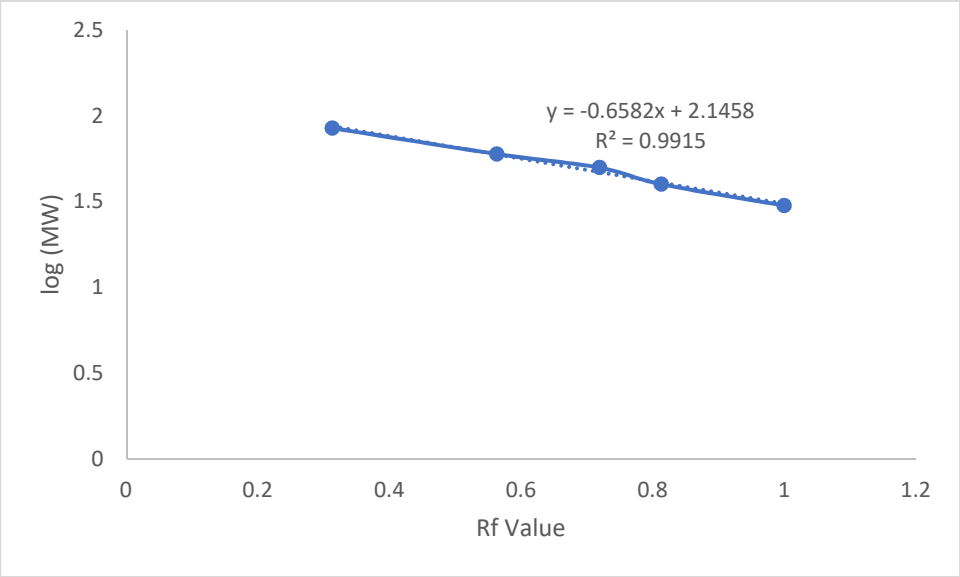

Calculation:

Rf Value of protein band = 19/32 = 0.594

y = -0.6582(0.594) + 2.1458

y = 1.7548

$10^{1.7548}$ = 56.86 kDa

Appendix D: Bradford Assay Standard Curve

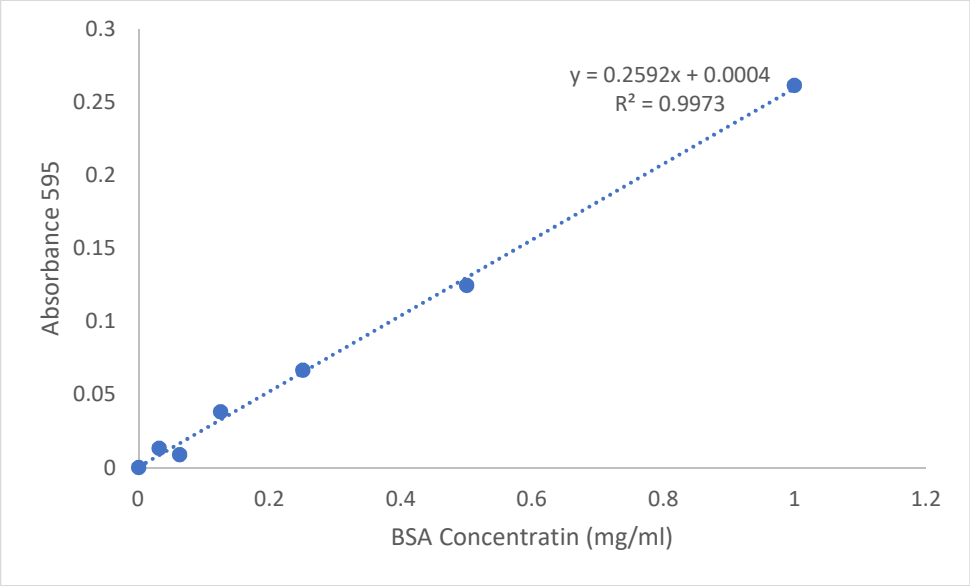

The Bradford protein assay was performed at 0.03, 0,06, 0.13, 0.25, 0.5 and 1 mg/ml BSA concentrations. Absorbance of the Bradford reagent was measured at 595 nm after 5 minutes.

Appendix E: Small Scale Protein Expression

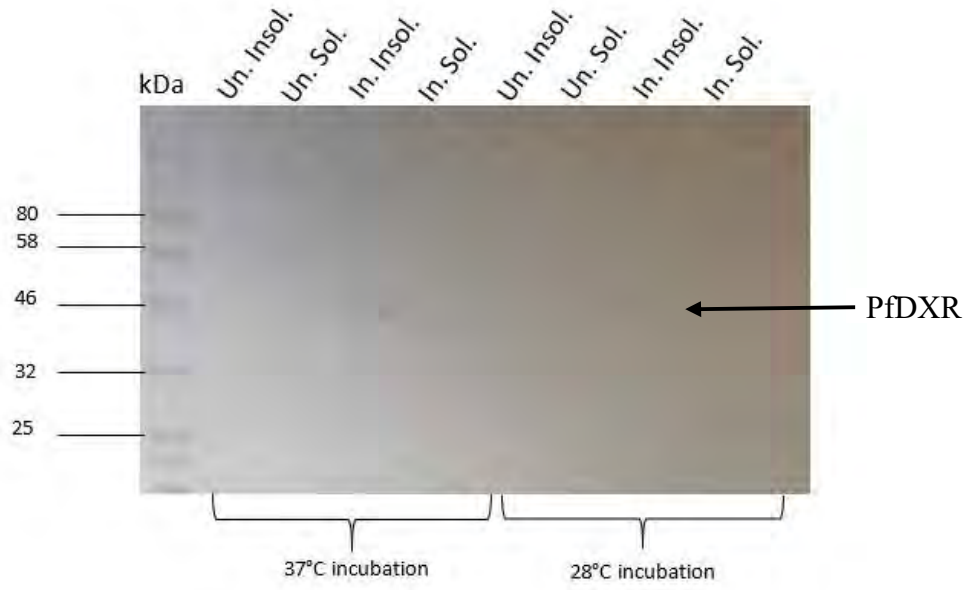

PfDXR expression at 28°C and 37°C using 0.1 mM IPTG for induction. The PfDXR protein is found in the induced insoluble lanes.

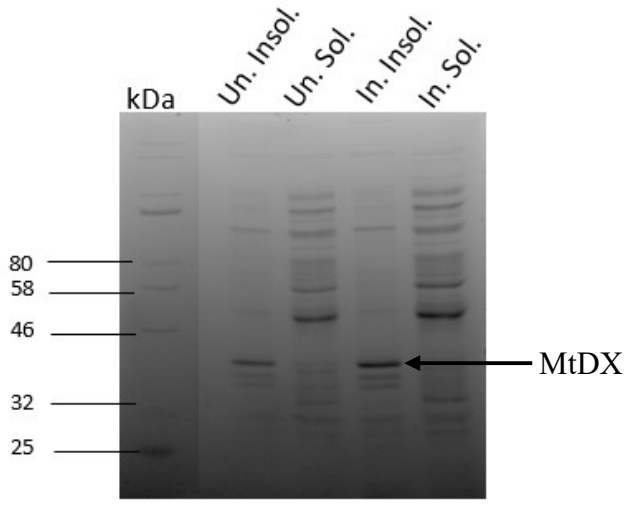

DXR expression at 37°C using 0.1 mM IPTG for induction. The MtDXR protein is found in both the induced and uninduced insoluble lanes.

Appendix F: % Enzyme Activity and Inhibition Determination

$$\% \text{ Enzyme Activity} = \frac{Abs\,(negative\ control) - Abs\,(sample)}{negative\ control - positive\ control} \times 100$$

$$\% \text{ Enzyme Inhibition} = \frac{Abs\,(positive\ control) - Abs\,(sample)}{negative\ control - positive\ control} \times 100$$

Positive Control - reaction with enzyme and without compound

Negative Control - reaction without enzyme and compound

Appendix G: Heat Map for Pathogen Box Compound Screening

Pathogen Box Plate A

	1	2	3	4	5	6	7	8	9	10	11	12
A	0.1522	0.1789	0.1513	0.355	0.2673	0.1487	0.2198	0.1521	0.2414	0.1579	0.1641	0.4139
B	0.1603	0.4033	0.1801	0.2209	0.1631	0.1558	0.1932	0.1846	0.2248	0.2534	0.2536	0.4179
C	0.1596	0.155	0.1519	0.1542	0.2296	0.1521	0.1797	0.2115	0.2285	0.2077	0.1693	0.4216
D	0.1587	0.2489	0.1895	0.17	0.1758	0.1431	0.1988	0.2141	0.1633	0.1563	0.2941	0.4187
E	0.4891	0.1755	0.1979	0.3111	0.1596	0.1446	0.2279	0.1547	0.1967	0.1814	0.1859	
F	0.4881	0.1894	0.1876	0.159	0.3164	0.1519	0.2412	0.2059	0.2442	0.1988	0.1696	
G	0.4841	0.1624	0.3599	0.1717	0.1792	0.1478	0.1549	0.1736	0.1581	0.1556	0.2901	
H	0.4895	0.1668	0.1761	0.2974	0.1695	0.1643	0.2305	0.2974	0.2058	0.1641	0.2453	

6	-2	60	33	-3	19	-2	25	0	2
74	7	19	2	-1	11	8	20	29	29
-1	-2	-1	22	-2	7	16	21	15	4
28	10	4	5	-4	12	17	2	0	41
5	12	46	1	-4	21	-1	12	7	9
10	9	0	48	-2	25	15	26	12	4
1	61	4	7	-3	-1	5	0	-1	40
3	6	42	4	2	22	42	15	2	27

Pathogen Box Plate B

	1	2	3	4	5	6	7	8	9	10	11	12
A	0.1546	0.2075	0.1523	0.3481	0.167	0.1982	0.1504	0.3326	0.1739	0.1589	0.1597	0.4153
B	0.1583	0.3507	0.1526	0.4615	0.3172	0.3569	0.1518	0.1645	0.1596	0.2477	0.195	0.4081
C	0.1607	0.3376	0.159	0.4064	0.193	0.2669	0.189	0.2201	0.1681	0.1616	0.1734	0.4128
D	0.1579	0.1646	0.2167	0.4601	0.2609	0.1455	0.1565	0.2583	0.2265	0.2433	0.1679	0.411
E	0.4461	0.2128	0.2388	0.3591	0.1854	0.1581	0.1541	0.2221	0.178	0.151	0.2232	
F	0.4423	0.187	0.2493	0.4252	0.2183	0.2152	0.1479	0.1557	0.2344	0.2316	0.302	
G	0.4363	0.1591	0.1893	0.3446	0.1731	0.2004	0.1652	0.2441	0.2196	0.1855	0.1714	
H	0.4446	0.1711	0.2795	0.3615	0.2987	0.3283	0.155	0.2767	0.1867	0.1683	0.1616	

17	-2	67	3	14	-3	61	6	0	1
68	-2	107	56	70	-2	2	1	32	13
63	0	87	12	38	11	22	4	1	5
2	21	106	36	-4	0	35	24	30	4
19	28	71	10	0	-1	23	7	-2	23
10	32	94	21	20	-4	-1	27	26	51
0	11	66	5	15	3	30	22	10	5
5	43	72	50	60	-1	42	10	4	1

Pathogen Box Plate C

	1	2	3	4	5	6	7	8	9	10	11	12
A	0.1882	0.4451	0.2271	0.1732	0.199	0.1898	0.1878	0.1904	0.1986	0.1716	0.3243	0.4245
B	0.1905	0.183	0.1811	0.1966	0.4058	0.1621	0.2524	0.2802	0.3122	0.1862	0.2213	0.4254
C	0.172	0.1878	0.2451	0.2113	0.2552	0.1896	0.2293	0.1712	0.1728	0.19	0.1732	0.4251
D	0.1816	0.1745	0.1723	0.1855	0.3094	0.1763	0.2008	0.1706	0.2609	0.2517	0.1694	0.4077
E	0.4965	0.1839	0.1871	0.256	0.4252	0.2214	0.2881	0.1816	0.2076	0.2645	0.2128	
F	0.5033	0.2475	0.1647	0.2338	0.32	0.1699	0.1716	0.2003	0.2768	0.1739	0.2065	
G	0.5039	0.1823	0.2954	0.2613	0.1725	0.2635	0.2339	0.1679	0.1849	0.1721	0.2548	
H	0.5102	0.2212	0.3545	0.1847	0.1877	0.2152	0.1946	0.2302	0.2061	0.2227	0.2331	

82	14	-3	5	2	1	2	5	-4	44
0	-1	4	70	-7	22	30	40	1	12
1	19	9	23	2	14	-4	-3	2	-3
-3	-3	1	39	-2	6	-4	24	21	-4
0	1	23	76	12	33	0	8	25	9
20	-6	16	43	-4	-4	5	29	-3	7
0	35	24	-3	25	16	-5	1	-3	22
12	54	1	1	10	4	15	7	12	16

Pathogen Box Plate D

	1	2	3	4	5	6	7	8	9	10	11	12
A	0.1545	0.2545	0.1532	0.2195	0.1556	0.1699	0.1616	0.2277	0.2975	0.165	0.1651	0.4473
B	0.1602	0.1606	0.1547	0.2475	0.2082	0.1602	0.3079	0.2275	0.1637	0.1634	0.1623	0.4495
C	0.159	0.2662	0.1562	0.1596	0.2515	0.1565	0.1604	0.3934	0.1642	0.218	0.2649	0.4567
D	0.1544	0.2088	0.1596	0.1634	0.1857	0.2575	0.1829	0.1629	0.241	0.156	0.1762	0.4458
E	0.5179	0.1551	0.2155	0.1699	0.25	0.1594	0.1874	0.1553	0.1945	0.1575	0.1739	
F	0.5212	0.2362	0.159	0.2159	0.1591	0.1653	0.1949	0.1724	0.1918	0.4786	0.4077	
G	0.5479	0.2131	0.1656	0.1746	0.1878	0.156	0.1553	0.1754	0.1929	0.1564	0.2448	
H	0.517	0.1666	0.2673	0.1645	0.2539	0.2309	0.2004	0.3844	0.1972	0.1879	0.1746	

26	-1	17	0	3	1	19	38	2	2
1	-1	25	14	1	41	19	2	2	1
30	0	1	26	0	1	64	2	17	29
14	1	2	8	27	7	2	23	0	5
-1	16	3	25	1	8	0	10	0	5
21	1	16	1	2	10	4	9	87	68
15	2	5	8	0	0	5	10	0	24
3	30	2	26	20	12	62	11	8	5

Pathogen Box Plate E

	1	2	3	4	5	6	7	8	9	10	11	12
A	0.1628	0.1618	0.2109	0.1828	0.3395	0.1934	0.2189	0.1892	0.1708	0.2492	0.1948	0.4265
B	0.1696	0.166	0.1786	0.2381	0.1668	0.1738	0.2106	0.1686	0.1976	0.2007	0.4464	0.4505
C	0.1703	0.2765	0.2944	0.3328	0.1699	0.1711	0.2372	0.1751	0.1774	0.1888	0.1769	0.4447
D	0.1687	0.1644	0.248	0.2521	0.2054	0.2821	0.1673	0.3323	0.2258	0.1898	0.1752	0.4413
E	0.5556	0.163	0.8351	0.1983	0.1708	0.2152	0.1702	0.1717	0.2566	0.1728	0.27	
F	0.5544	0.2258	0.1824	0.3575	0.1702	0.2266	0.5735	0.1698	0.1804	0.2063	0.1792	
G	0.5514	0.1708	0.1677	0.1674	0.1681	0.1682	0.1686	0.1672	0.1716	0.1954	0.2369	
H	0.5471	0.247	0.2098	0.1915	0.3911	0.175	0.2536	0.2512	0.241	0.2265	0.1802	

-2	11	4	45	7	13	6	1	21	7
0	3	18	0	2	11	0	8	9	72
28	33	43	1	1	18	2	2	5	2
-1	21	22	10	30	0	43	15	6	2
-1	174	8	1	12	1	1	23	1	27
15	4	49	1	15	106	1	3	10	3
1	0	0	0	0	0	0	1	7	18
21	11	6	58	2	22	22	19	15	3

Heat Map of the Pathogen Box compounds screened against the activity of *S. enterica* DXR enzyme. The Positive control without compounds is showed in yellow, the negative control without compounds and enzyme is showed in green and the FR900098 control with both FR900098 inhibitor and enzyme is showed in blue. Below are the % inhibition for each compound, compounds exhibiting a % inhibition and above are shaded pink.

Appendix H: Confirmation of the Pathogen Box hit compounds

Profiles and percentage inhibition of the hit compounds (≥ 70% inhibition at 50 μM) in the MMV pathogen box. The hit compounds that exhibited ≥ 70% inhibition (from screening) were selected and retested to confirm their inhibitory activity against *S. enterica* DXR. The barcode of the plate, position of compound on the plate, compounds ID and the % inhibition of the compounds are shown in the table below:

Plate barcode	Well Position	Compound ID	Inhibition (%) at 50 μM concentration
PathogenBox_PlateA	B02	MMV1110498	-8
PathogenBox_PlateB	B04	MMV002529	-4
PathogenBox_PlateB	C04	MMV676382	-1
PathogenBox_PlateB	D04	MMV676536	-2
PathogenBox_PlateB	F04	MMV003270	0
PathogenBox_PlateC	A02	MMV675997	-2
PathogenBox_PlateC	B05	MMV687749	2
PathogenBox_PlateC	E05	MMV687146	-2
PathogenBox_PlateD	F10	MMV688474	55
PathogenBox_PlateE	B11	MMV688352	4
PathogenBox_PlateE	E03	MMV002816	89
PathogenBox_PlateE	F07	MMV228911	78